

SOME PROBLEMS ASSOCIATED WITH
INTERPLANETARY FLIGHT

HOWARD AUSTIN SHARTEL
ROBERT HOLDERMANN SMALL
ROBERT BRUCE ROBINSON

DUDLEY KNOX LIBRARY
NAVAL POSTGRADUATE SCHOOL
MONTEREY CA 93943-5101

SOME PROBLEMS ASSOCIATED WITH
INTERPLANETARY FLIGHT

by

HOWARD AUSTIN SHARTEL, LT, USN

B.S. U.S. Naval Academy - 1950

B.S. U.S. Naval Postgraduate School - 1957

ROBERT HOLDERMANN SMALL, LT, USN

B.S. U.S. Naval Academy - 1951

B.S. U.S. Naval Postgraduate School - 1957

ROBERT BRUCE ROBINSON, LT, USN

B.S. Pennsylvania State University - 1951

B.S. U.S. Naval Postgraduate School - 1957

54

SUBMITTED IN PARTIAL FULFILLMENT OF THE
REQUIREMENTS FOR THE DEGREE OF
MASTER OF SCIENCE

at the

MASSACHUSETTS INSTITUTE OF TECHNOLOGY

May, 1958

SOME PROBLEMS ASSOCIATED WITH
INTERPLANETARY FLIGHT

by

Howard Austin Shartel

Robert Holdermann Small

Robert Bruce Robinson

Submitted to the Department of Aeronautical Engineering
on May 26, 1958, in partial fulfillment of the requirements for
the degree of Master of Science.

ABSTRACT

The general problem chosen for consideration concerns the establishment of a payload in orbit about the planet Mars. Emphasis in this study has been placed upon a comparison of the various paths available for a free-fall, space stabilized rocket, the requirements necessary to achieve such paths, and the selection of the optimum path. The optimum path has been compared with other trajectories and conclusions have been drawn as to the requirements for deviations from the optimum path. The study is primarily concerned with the midcourse portion of the trip, which has been defined by the authors as that part of the overall trajectory extending from a desired circular orbit about Earth to a desired circular orbit about Mars. A firm basis for the selection of the orbit has been established. Treatment has also been given in this report to the continuous determination of present position in space and the initiation of corrective action

when deviation from a desired path exists. The study also includes generalized instrumentation and guidance requirements. Extensive quantitative information has been compiled which will serve as a basis for the determination of instrumentation requirements as well as create a proper background for an appreciation of flight within the solar system.

Thesis Supervisor: Winston R. Markey

Title: Assistant Professor
of Aeronautical
Engineering

ACKNOWLEDGEMENT

The authors gratefully acknowledge the assistance of Dr. Winston R. Markey and Dr. Walter Wrigley, whose classroom presentations have created the interest and motivation for this study.

Appreciation is expressed to the personnel of the Instrumentation Laboratory, Massachusetts Institute of Technology, for their help and counsel.

The graduate work for which this thesis is a partial requirement was performed while the authors were assigned to the U.S. Naval Administrative Unit, Massachusetts Institute of Technology.

TABLE OF CONTENTS

CHAPTER	Page
1 INTRODUCTION	15
2 THE SOLAR SYSTEM	17
2.1 The Sun and its Planets	17
2.2 Solar Radiation and Temperature in Space. .	19
2.3 Approximate Orbital Paths of Planets.	19
2.4 Perturbations of Planetary Orbits	23
2.5 The Invariable Plane	24
2.6 Cislunar Motion	24
2.7 Solar Motion.	24
2.8 Fixed Stars	26
2.9 Gravitations Effects	26
3 THE PROBLEM SIMPLIFIED	31
3.1 Introduction	31
3.2 Differential Equation of Motion of the Rocket	32
3.3 Inertial Points within the Solar System	34
3.4 Simplified Differential Equations of Rocket Motion	35
3.5 The Lunar Gravity Field Effect	37
3.6 The Flight-Phase Concept.	38
4 THE TRAJECTORY.	41
A. SOME POSSIBLE TRAJECTORIES	41
4.1 Basic Criterion for Selection	41
4.2 Classifications of Trajectories	41
4.3 Powered Trajectories	41
4.4 Unpowered Trajectories.	42
4.5 Combination Trajectories	43
4.6 Trajectory selected for Further Study	43
B. THE UNPOWERED TRAJECTORY	45
4.7 Introduction	45
4.8 Basic Relations	46
4.9 Some Simplified Trajectory Parameters . . .	47

4.10	Rocket Velocity Vectors with respect to Earth and Mars	51
4.11	Time of Flight	55
4.12	Angular Separation of Earth and Mars . . .	58
4.13	$V_{\oplus\Delta}$ and $V_{O\Delta}$ as Functions of $(\theta_o - \theta_s)$. . .	65
4.14	The Rocket Plane (Δ plane) Concept	65
5	DEPARTURE AND ARRIVAL ORBITS	79
5.1	Introduction	79
5.2	Optimum Orbit Radii	80
5.3	Use of Optimum Orbit Concept	85
5.4	The Least Orbit Concept	85
6	THRUST AND ENERGY CONSIDERATIONS	91
A.	THRUST REQUIREMENTS	91
6.1	Introduction.	91
6.2	The Optimal Payload Ratio	91
6.3	An Interpretation of Optimum Altitude . . .	94
6.4	The Assumption of Impulsive Thrust	94
B.	ENERGY CONSIDERATIONS	99
6.5	Introduction	99
6.6	General Theory	99
6.7	Rocket Thrust Direction	102
7	NAVIGATION IN SPACE	105
A.	POSITION IN SPACE	105
7.1	General Discussion of Problem	105
7.2	Factors indicating Necessity for "On Board" Automatic Solution	105
7.3	Selection of a Reference Coordinate System	106
7.4	Establishing the Reference Coordinate System	109
7.5	Determining Celestial Latitude and Longitude of the Vehicle	110
7.6	Determining the Radius Vector to the Sun .	110
7.7	Some Additional Methods for Position Determination	115
7.8	Determination of the Shape of Actual Transfer Ellipse	116
7.9	Determination of Orientation of Actual Transfer Ellipse	121

B. In-Flight Corrections	125
7.10 Introduction	125
7.11 Analytical Development.	126
7.12 Corrective Action	129
7.13 Interception at Newly Calculated Time . .	130
7.14 Summary	133
8 GUIDANCE AND CONTROL	135
8.1 General.	135
8.2 The Basic System	136
8.3 The Tracking Section	138
8.4 The Computing Section	144
8.5 Thrust and Stabilization	153
8.6 Errors and Effects	154
9 CONCLUSIONS AND RECOMMENDATIONS FOR FURTHER STUDY	161
9.1 Introduction	161
9.2 Conclusions	161
9.3 Recommendations	163
SYMBOLS	165
BIBLIOGRAPHY	175

LIST OF FIGURES, TABLES, AND SUMMARIES

FIGURES

Figure		Page
2.1	Angular Motion of Major Planets from 1965 to 1970.	18
2.2	Incident Solar Energy as a Function of Distance from Sun	20
2.3	Black Body Temperature as a Function of Distance from Sun	21
2.4	Basic Ellipse	22
2.5	Basic Ellipse Oriented to Reference Plane.	22
2.6	Motion of the Earth in the Ecliptic Plane	25
2.7	Cislunar Motion	25
2.8	Gravitational Field Effects	30
3.1	Reference Frames	33
3.2	Planetary Configurations for Table 3.1	33
3.3	Illustration of Rocket - Moon Separation	37
4.1	The Hohmann Ellipse	47
4.2	General Trajectory Configuration	48
4.3	Some Vector-Angle Relations for the General Trajectory	48
4.4	Velocities Relative to Earth	50
4.5	Velocities Relative to Mars	50
4.6	Ellipticity as a Function of θ_o and θ_A	52
4.7	Rocket Velocity Magnitude with Respect to the Sun as a Function of θ_o and θ_A	53
4.8	Rocket Velocity Magnitude with Respect to Earth as a Function of θ_o and θ_A	56
4.9	Rocket Velocity Magnitude with Respect to Mars as a Function of θ_o and θ_A	57
4.10	Time of Flight as a Function of θ_o and θ_A	59
4.11	Mars Angular Position Measured from Earth Aphelion as a Function of Time	61
4.12	Earth Angular Position Measured from Earth Aphelion as a Function of Time (Overlay #1)	62
4.13	Rocket Velocity Magnitude with Respect to Earth as a Function of θ_o and $\theta_o - \theta_s$	66

4.14	Rocket Velocity Magnitude with Respect to Mars as a Function of $\theta_o - \theta_s$	67
4.15	Angular Quantities of a Representative Trajectory Discussed in Section 4.14	69
4.16	A Typical Trajectory Showing the Effect of Tilt to Account for Non-Co-Planarity of Earth and Mars Motion	70
4.17	Assisting Supplementary View to Figure 4.16 . . .	71
4.18	Plan View of Body Motions for Trajectory Discussed in Section 4.14	72
4.19	Cumulative Rocket Displacement from the Δ Plane as a Function of Time	73
5.1	Pertinent Velocity Relations	79
5.2	Velocity of "Escape" from the Sun and some Planets as a Function of Distance	81
5.3	Optimal Relationships between V_{inc} and r_{js} for Earth and Mars	82
5.4	Non-Dimensional Relationships for $\frac{V_{inc}}{(V_{inc})_{opt}}$ and $\frac{r_{js}}{(r_{js})_{opt}}$	83
6.1	Payload Ratios VS. Orbit Altitude for the Hohmann Ellipse	95
6.2	Payload Ratios VS. Orbit Altitude for a Repre- sentative Trajectory	96
6.3	Orbit Period as a Function of Altitude Above Planet Center	97
6.4	The Theoretical Mode of Transfer	102
7.1	Reference Coordinate Systems	107
7.2	Determination of Heliocentric Latitude and Longitude	111
7.3	Geometrical Relationships Determining Radial Distance from the Sun	112
7.4	Geometrical Relationships Determining Radial Distance from the Sun with Earth as the Reference Planet	114
7.5	The Rocket Ellipse in Space	118
7.6	Orientation of Transfer Ellipse	122
7.7	Interception at Originally Predicted Time, t_2 . .	127
7.8	Interception at Newly Calculated Time	131

8.1	Line Functional Information Flow Diagram of a Proposed Guidance and Control System	137
8.2	Illustrative Schematic of Tracking System with Gyro Assist.	139
8.3	Line Functional Information Flow Diagram of Tracking System I	140
8.4	Illustrative Schematic Diagram of Tracking System with Stellar Assisted Gyro Space Reference	142
8.5	Line Functional Information Flow Diagram, Tracking Section II	143
8.6	Line Functional Information Flow Diagram for Tracking Line Computer (System One)	146
8.7	Line Functional Information Flow Diagram for Tracking Line Computer (System Two)	147
8.8	Line Functional Information Flow Diagram for Prediction Computer	148
8.9	Line Functional Information Flow Diagram for Comparator Section	151
8.10	Line Functional Information Flow Diagram for Corrector Section	152
8.11	Line Functional Information Flow Diagram for Thrust and Stabilization Section	155

TABLES

Table		Page
2.1	Principal Elements of Solar System	28
2.2	Principal Elements of Solar System	29
3.1	Planetary Gravitational Effects.	39
3.2	Sample Calculations for Table 3.1	40
6.1	Some Representative Trajectories with Corresponding Payload Requirements.	93
6.2	A Comparison of Orbital Period and Burning Time .	98
7.1	Reference Coordinate Systems	108

INFORMATION SUMMARIES

Information Summary

4.1	Construction and Use of Overlay Number 1	63
-----	--	----

DERIVATION SUMMARIES

Derivation Summary

4.1	Derivation of the Equation for the Determination of the Displacement of the Rocket Normal to the Rocket Plane.	74
5.1	Departure and Arrival Orbits	86
7.1	Determination of Three Basic Elements of Actual Elliptical Trajectory from Observed Data	117

DEFINITION SUMMARIES

Definition Summary

1.	Symbols	165
----	-------------------	-----

OBJECT

The object of this paper is to investigate the mid-course guidance requirements to place a payload in orbit about Mars.

CHAPTER I

INTRODUCTION

The authors have undertaken this study in order to bring together, in proper context, some considerations which may be anticipated in interplanetary flight. A journey to the planet Mars has been chosen as the basis for the presentation. However, many of the ideas and methods set forth here can be considered applicable to flight to other bodies within the solar system. It is felt that no loss of generality will result if attention is focused upon this particular choice.

This paper has evolved as a study of several problems associated with interplanetary flight. The objective to be pursued is concerned with placing a payload in orbit about the planet Mars. Departure is assumed to originate from orbit about Earth. The attainment or possibility of flight is not questioned. Rather, this is a broad study of some preferred methods, minimum requirements, and ideas concerned with fulfillment of the general objective.

Recent developments have justified studies of interplanetary flight. It is realized, however, that the topic is hopefully optimistic in many respects. For this reason the study is necessarily broad and is not designed to give an intricate, detailed account of methodology.

A flight to the moon will logically precede planetary flight, but its close proximity causes this problem to become quite specialized as contrasted to the Mars flight. Piloting a boat in an inland waterway as compared to navigating a ship on the open sea is an appropriate analogy. The two problems are independent

in a large sense.

This study has been preceded by an extensive search through the literature for information regarding this comparatively new field. Treatments have generally varied from the popularized texts to the highly specialized mathematical developments. There appears to be a paucity of practical approaches to the problem which can be interpreted by the systems designer or engineer.

The authors generally envisage an unmanned vehicle with small payload, unpowered except for terminal and corrective thrust requirements. It is believed instrumentation can be handled with components whose performances do not differ too radically from slight extensions of present day development.

A practical simplified view has been taken as a rule due to the lack of an available high speed digital computer. Such a device would of necessity be required if accurate trajectory studies were in order. However, it is felt that little departure from reality exists under the assumptions imposed. In fact, the simplifications add to the comprehension of the material.

Solutions are sought in answer to the following questions:

- (1) What are the major influences of the solar system upon the rocket in flight?
- (2) What simplifying assumptions can be made?
- (3) What routes may be taken?
- (4) What criteria are available for the selection of one trajectory or route in preference to another?
- (5) How may position in space be continuously determined for navigational purposes?
- (6) How may the rocket be assured of arriving in the target area if errors do occur?

CHAPTER 2

THE SOLAR SYSTEM

A summary of currently accepted data concerning the universe, which is pertinent to this study, is needed for formulation of assumptions and as basis for computation. This is presented below as discussion and in tabular form and figures, ^{2, 4, 9, 44, 53, 54, 59*} and has been derived from references.

2.1 The Sun and its Planets

The solar system consists of the sun, nine conspicuous planets, and numerous smaller planets. The conspicuous planets are placed in two groups. The major planets, Jupiter, Saturn, Uranus, and Neptune, are large, have low density, and are surrounded by high atmospheres. The terrestrial or minor planets, Mercury, Venus, Earth, Mars, and Pluto are similar to the earth in many respects. The so called navigational planets are Venus, Mars, Jupiter, and Saturn, deriving this classification from their nautical use for position determination.⁹

For the period of 1956-1970, the angular motion of the major planets in the solar system will be as shown in Fig. 2.1. The minor planets, Mars, Earth, and Venus, are shown in their positions as of 1 January 1970, and in their respective orbits, drawn as circles.

A generalization which serves to illustrate the area occupied by the planets and sun is to picture a piece of 1/4 inch plywood cut in a circle of 5 feet diameter. This would contain all the planets in their orbits around the sun (except Pluto) if drawn to a scale such that Neptune's major planetary axis was 5 feet.

* Superscript numbers refer to bibliography.

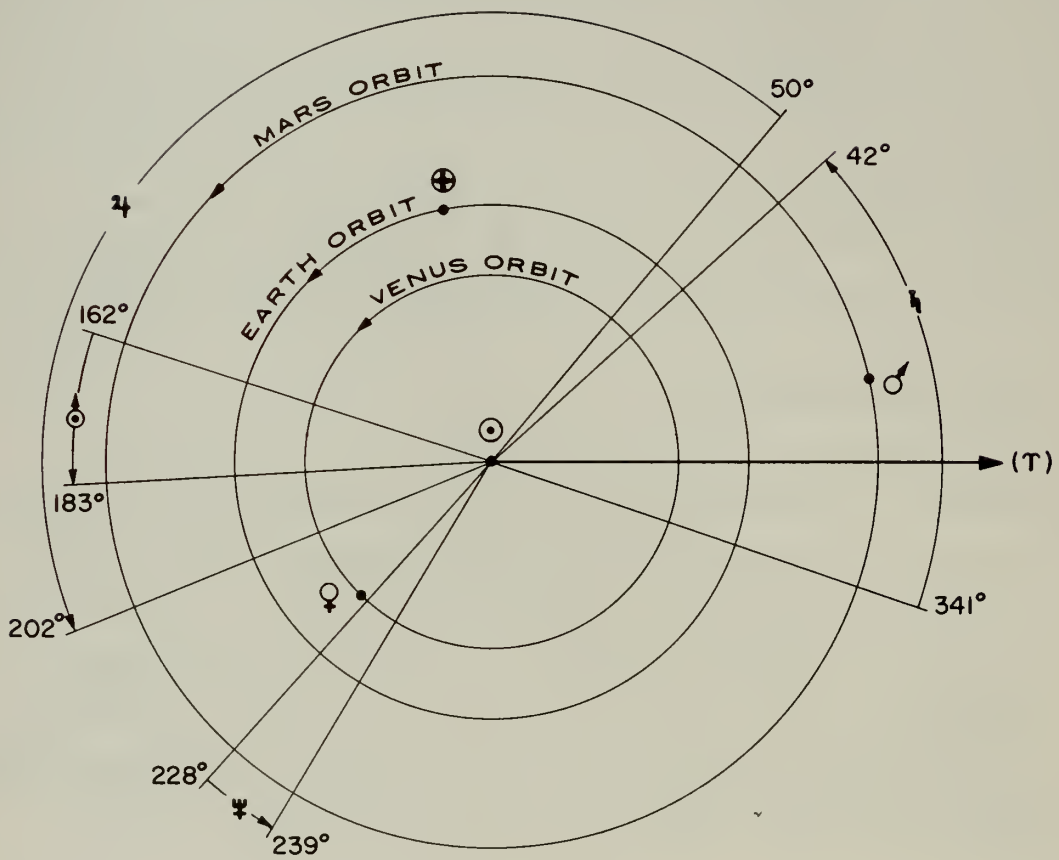


Fig. 2.1 Angular motion of major planets from 1965 to 1970

2.2 Solar Radiation and Temperature in Space

The solar constant of sun's radiation is 1.938 calories per minute per square centimeter, $\pm .05^{54}$. This value is equivalent to 1.35×10^6 ergs per second per centimeter square or 87.1×10^6 ergs per second per inch square at a distance of 1 AU from the sun. This incident energy varies as the reciprocal of the range squared, as shown in Fig. 2.2.

The maximum temperature of the surface of a black body planet with no atmosphere varies as the reciprocal of the square root of the distance of the body from the sun, as shown in fig. 2.3. At a distance of 1 AU from the sun this temperature is 392°K .

2.3 Approximate Orbital Paths of Planets

The path of a planet or body in orbit about the sun can be completely described by seven elements, in so far as the body depends only upon the sun's attractive force. These are:

1. Semi major axis (a)
2. Eccentricity (e)
3. Inclination (i)
4. Longitude of ascending node (Ω_i)
5. Longitude of perihelion (π)
6. Period (T)
7. Epoch

These are shown in Fig. 2.4 and 2.5.

Kepler's Three Laws of Planetary Motion are also applicable and are:

1. The planets move in ellipses, with sun at one of the focuses
2. The radius vector sweeps out equal areas in equal time

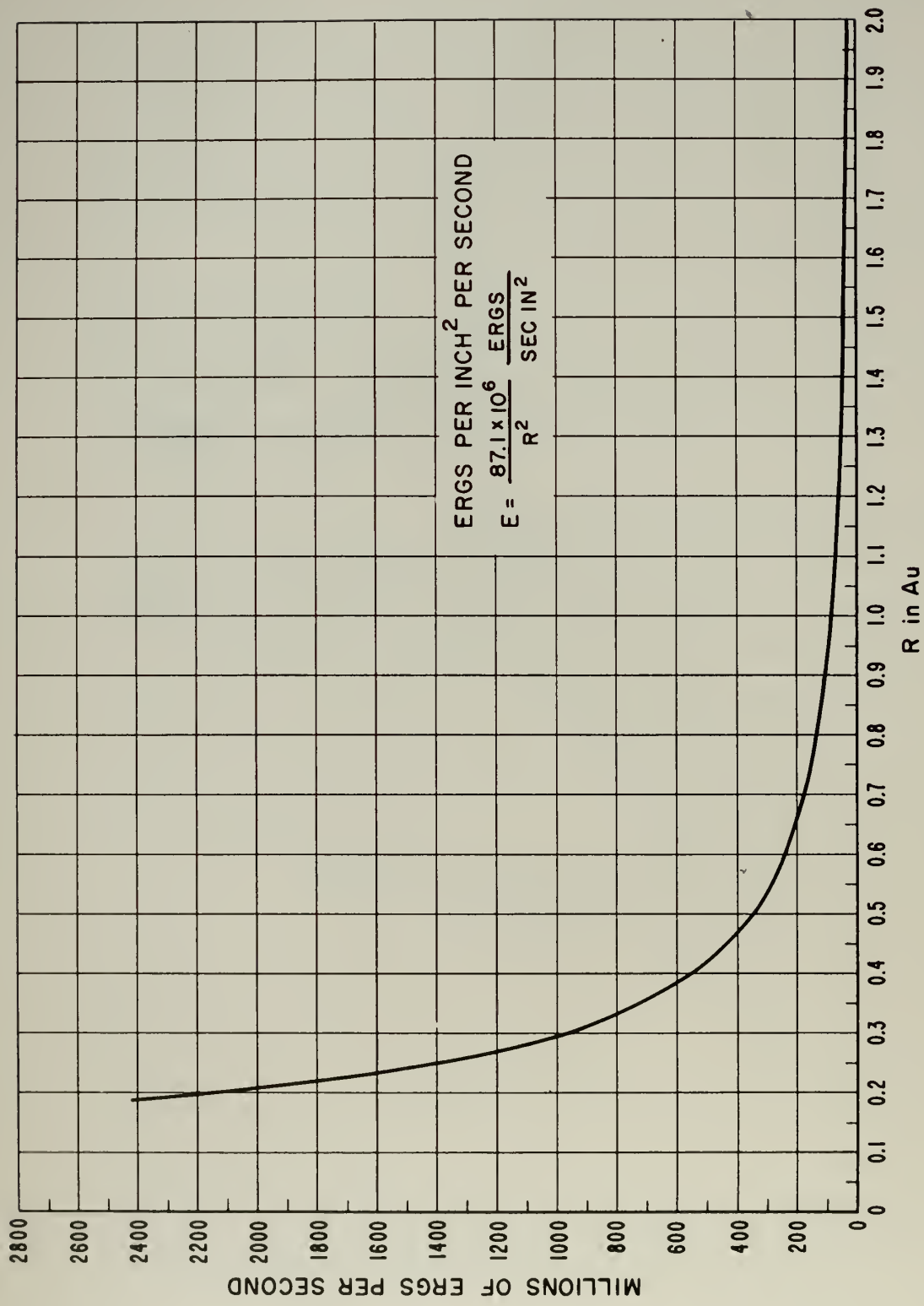


Fig. 2.2 Incident solar energy as a function of distance from Sun

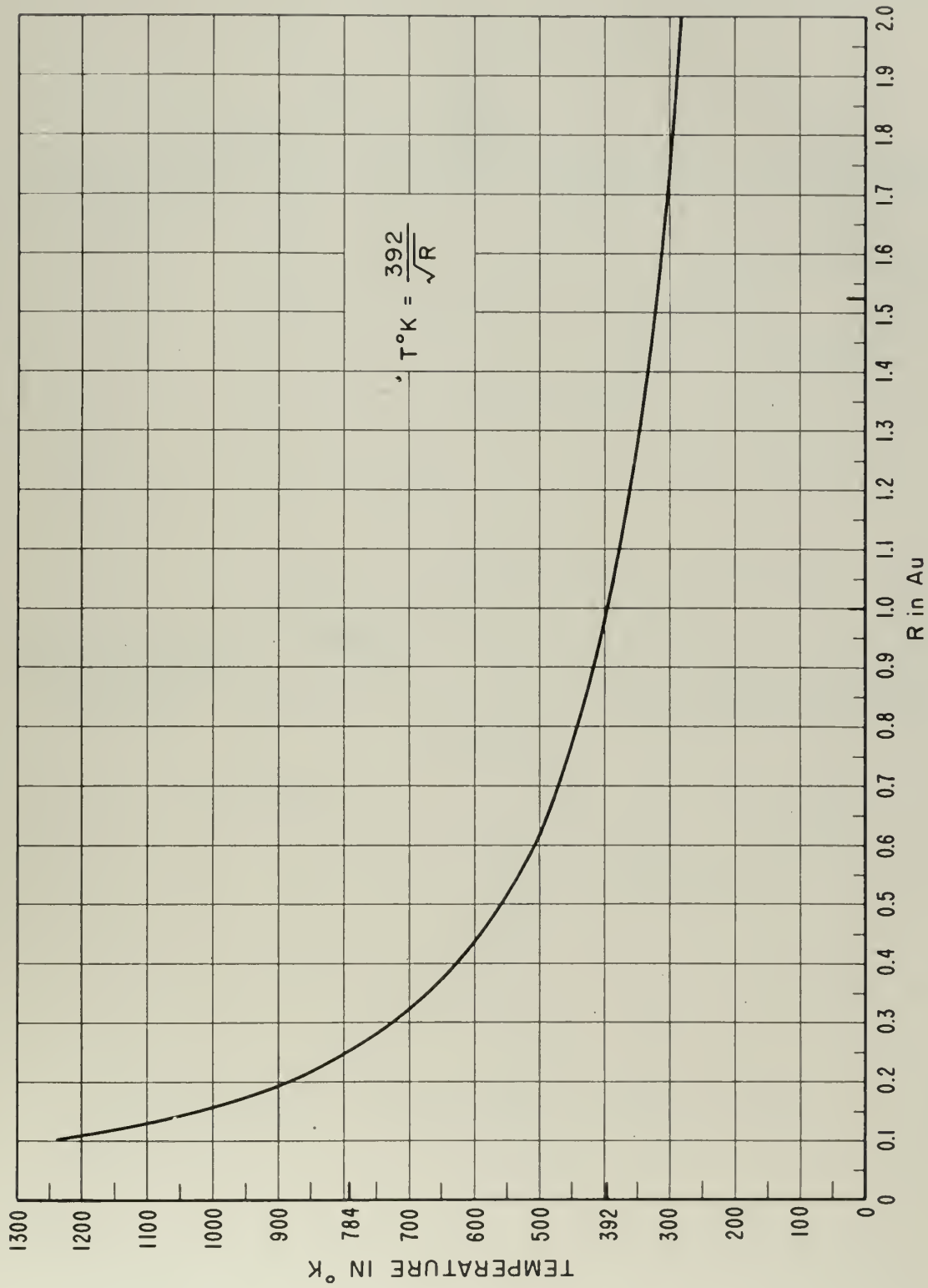


Fig. 2.3 Black body temperature as a function of distance from Sun

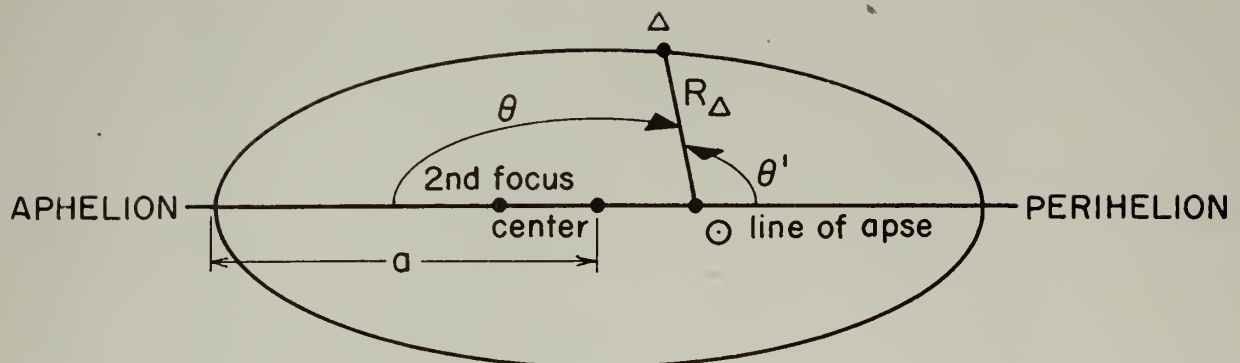


Fig. 2.4 Basic ellipse

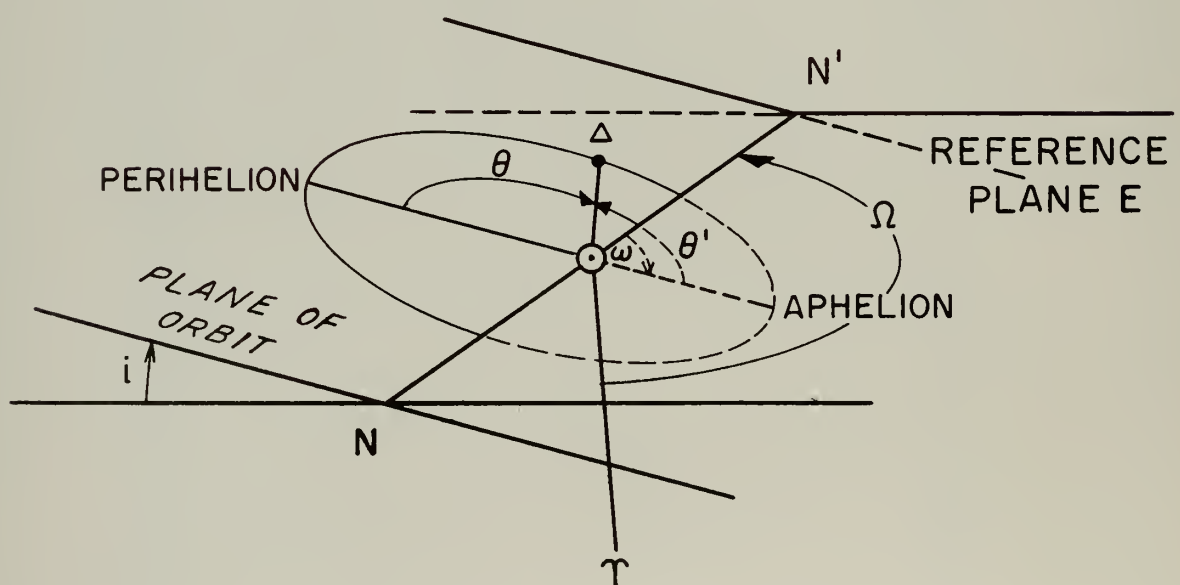


Fig. 2.5 Basic ellipse oriented to reference plane

3. The square of the time of revolution is proportional to the cube of the mean distance.

2.4 Perturbations of Planetary Orbits

The actual motion of the planets may best be described as follows:

1. The orbits of the planets are not fixed but gradually change in eccentricity, inclination, (etc.). These changes are classified as secular perturbations; however, these perturbations are so slow that during any one revolution the orbit is altered very little and during the time of any given single interplanetary flight, can be neglected.
2. A planet in its motion does not exactly follow Kepler's Laws but is seen to vary in three dimensions relative to its ideal Keplerian Ellipse. Such changes are very small and are called periodic perturbation. These values expressed in heliocentric longitude (λ_p) are:

Mercury	15"
Venus	30"
Earth	1'
Mars	2'
Jupiter	30'
Saturn	70'
Uranus	60'
Neptune	35'

In general the larger the terms the longer the period of periodic perturbation. For example Jupiter and Saturn exhibit periods of periodic perturbations of about 913 years.

2.5 The Invariable Plane

The most stable property of the solar system is the so called invariable plane. This is defined by the condition that the total angular momentum of the solar system is zero about any axis in this plane. The invariable plane can be considered as the fundamental reference plane of the solar system and is inclined $1^{\circ} 38' 7''$ to the ecliptic reference plane of 1900 with ascending node in longitude $106^{\circ} 42'$ measured from Υ . This inclination is decreasing at the rate of $.144''$ per year and will reach $47'$ in about 20,000 years at which time it will begin to increase again.

2.6 Cislunar Motion

Cislunar (earth-moon) motion in the plane of the ecliptic is that of two unequal revolving masses in a central force field, whose center of mass follows a slightly distorted Keplerian ellipse of eccentricity (e)= $.01674$. This cislunar center of mass is approximately 2880 miles from the earth center in the direction of the moon. See Fig. 2.6 and 2.7.

The moon's path around the earth has an eccentricity $.055$ and a mean inclination to the ecliptic of $5^{\circ} 9'$. The average distance from earth to moon is 238,857 miles (60.207 earth radii) with maximum distance of 252,710 miles and minimum distance of 221,463 miles.

If we represent the cislunar orbit by a circle of radius 100 feet, the moon will deviate from this circle approximately 3 inches on either side in one transit around the earth. During this time the geocenter will deviate approximately .04 inches either side of the orbit.

2.7 Solar Motion

Campbell and Moore in 1920 found the solar system to be moving at about 12.2 miles per second with respect to the nearer

3. The square of the time of revolution is proportional to the cube of the mean distance.

2.4 Perturbations of Planetary Orbits

The actual motion of the planets may best be described as follows:

1. The orbits of the planets are not fixed but gradually change in eccentricity, inclination, (etc.). These changes are classified as secular perturbations; however, these perturbations are so slow that during any one revolution the orbit is altered very little and during the time of any given single interplanetary flight, can be neglected.
2. A planet in its motion does not exactly follow Kepler's Laws but is seen to vary in three dimensions relative to its ideal Keplerian Ellipse. Such changes are very small and are called periodic perturbation. These values expressed in heliocentric longitude (λ_p) are:

Mercury	15"
Venus	30"
Earth	1'
Mars	2'
Jupiter	30'
Saturn	70'
Uranus	60'
Neptune	35'

In general the larger the terms the longer the period of periodic perturbation. For example Jupiter and Saturn exhibit periods of periodic perturbations of about 913 years.

2.5 The Invariable Plane

The most stable property of the solar system is the so called invariable plane. This is defined by the condition that the total angular momentum of the solar system is zero about any axis in this plane. The invariable plane can be considered as the fundamental reference plane of the solar system and is inclined $1^{\circ} 38' 7''$ to the ecliptic reference plane of 1900 with ascending node in longitude $106^{\circ} 42'$ measured from Υ . This inclination is decreasing at the rate of $.144''$ per year and will reach $47'$ in about 20,000 years at which time it will begin to increase again.

2.6 Cislunar Motion

Cislunar (earth-moon) motion in the plane of the ecliptic is that of two unequal revolving masses in a central force field, whose center of mass follows a slightly distorted Keplerian ellipse of eccentricity (e) = .01674. This cislunar center of mass is approximately 2880 miles from the earth center in the direction of the moon. See Fig. 2.6 and 2.7.

The moon's path around the earth has an eccentricity .055 and a mean inclination to the ecliptic of $5^{\circ} 9'$. The average distance from earth to moon is 238,857 miles (60.207 earth radii) with maximum distance of 252,710 miles and minimum distance of 221,463 miles.

If we represent the cislunar orbit by a circle of radius 100 feet, the moon will deviate from this circle approximately 3 inches on either side in one transit around the earth. During this time the geocenter will deviate approximately .04 inches either side of the orbit.

2.7 Solar Motion

Campbell and Moore in 1920 found the solar system to be moving at about 12.2 miles per second with respect to the nearer

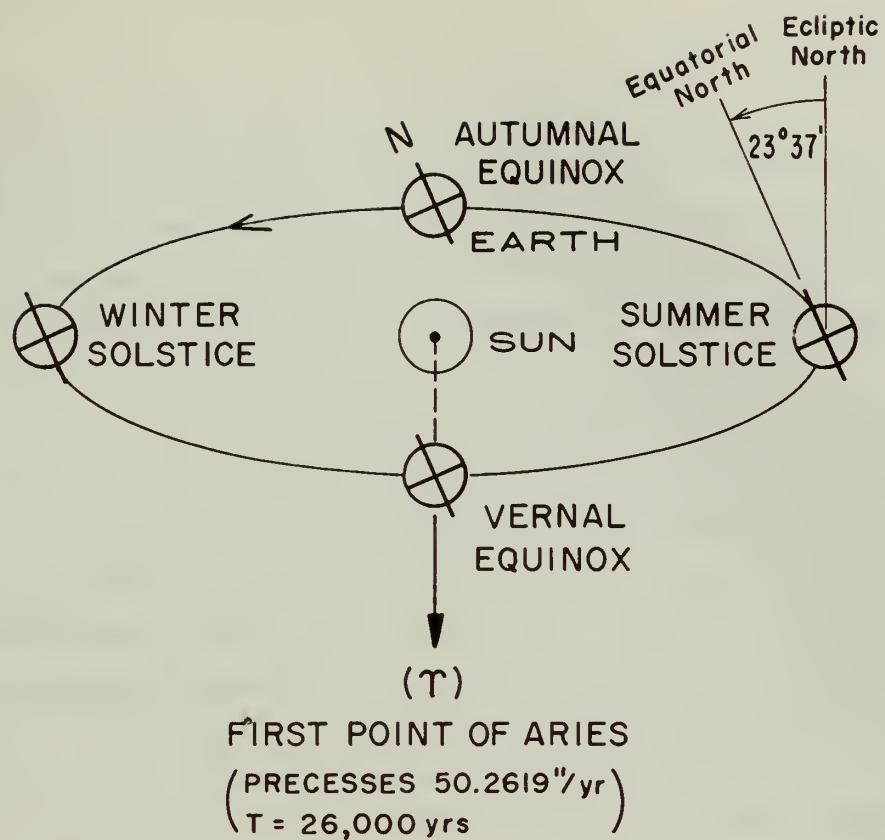


Fig. 2.6 Motion of the Earth in the ecliptic plane

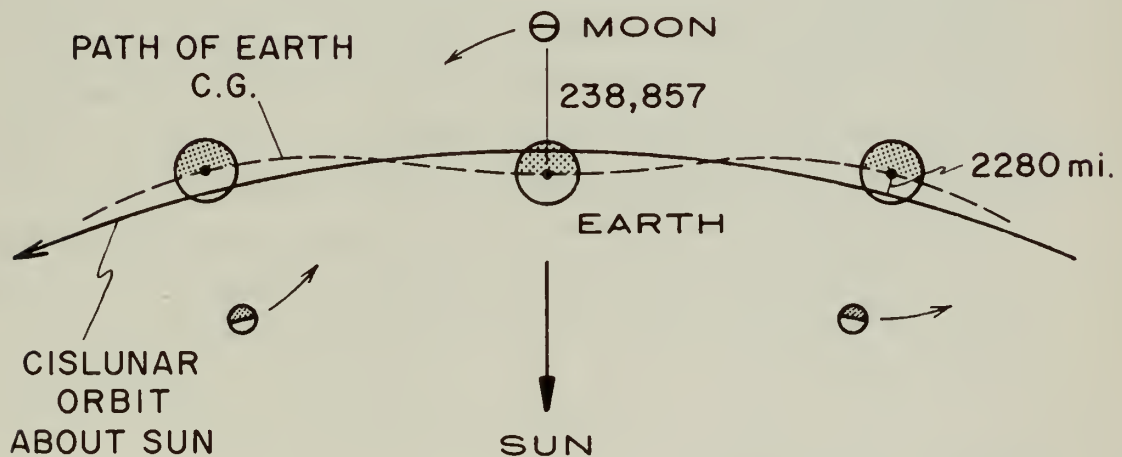


Fig. 2.7 Cislunar Motion

few hundred stars toward the constellation Hercules. Jay, Sanford, Stromberg, and Hubble, among others, estimate that the solar system and the neighboring stars are moving at about 170 miles per second toward the constellation Cygnus.

Conclusions reached by Oort place the solar system about 32,000 light years from the center of the galaxy which is in Sagittarius and that this position is about two thirds of the distance from center to circumference. At 170 miles per second the period of galactic revolution of our sun is approximately 2,200,000 years, indicating that during the time covered by any given flight within the solar system, the sun may be considered as a rather stable reference point.

2.8 Fixed Stars

The nearest star, Alpha Centauri, is at a distance from our sun of 4.3 light years or 2.53×10^{13} miles. It has also been determined that no star exhibits a parallax of more than .76 seconds and only 200 stars have proper motion greater than one tenth of "Barnard's Runaway Star" which traverses 10.25 seconds of arc per year. For the purposes of this paper a "Fixed" star, as the term is used for establishment of celestial inertial reference, will be considered to be a star exhibiting a parallax and a proper motion of less than one quarter second of arc. Of the stars checked to date only about .01% do not fall within this classification of "Fixed" stars.

2.9 Gravitational Effects

Newton's general Law of Gravitation states that, "Any two particles of matter attract each other with a force proportional to the product of their masses and inversely proportional to the square of the distance between them"⁵⁴ or $f = K \frac{mM}{R^2}$, where K is the so called Gaussian gravitational constant equal to

$6.67 \times 10^{-8} \frac{\text{cm}^3}{\text{gM(m) sec}^2}$. From this the acceleration of gravity is then $g = \frac{KM}{R^2}$.

Values of the acceleration of gravity for the various solar bodies are tabulated in Table 2.2 with the mean surface gravity for earth equal to 1. Fig. 2.8 presents "g" versus the radial distance from the earth, moon and Mars and the variation in the effect of the sun's gravitational attraction over the distance between the orbits of Earth and Mars.

Herrick has pointed out¹⁸ that Gauss was able to determine mathematically the value of K^2 , for heliocentric orbits with distance in AU, accurate to nine significant figures but neither the laboratory value of gravitational acceleration nor laboratory units of measurements at present will permit any greater accuracy than 3 or 4 significant figures.

An interesting discussion of Gravitational and tidal effects which has direct bearing on any travel between Earth and Mars has been presented by Schaub⁵⁶. Schaub states that the inner most moon of Mars, Phobos, is within Rocke's limit⁵⁴. This means that since Phobos is assumed to have the same density as Mars and is traveling in an orbit of less than 2.44 times Mars radius (see Table 2.2) its surface is now free of all loose material. Eventually, due to the bombardment by rays from space, more and more of this moon will be torn away forming a ring of dust particles around Mars. This implies that any terminal orbit about Mars should stay well clear of Phobos less it hasten this disintegration possibly destroying the vehicle in the process.

Table 2.1

PRINCIPAL ELEMENTS

Name	Semi-Major Axis of Orbit	Mean Dist. (Millions of Km.)	Sidereal Period (Mean Solar Days)	Period in Sidereal Years	Mean Orbital Velocity (Km./Sec.)	Eccentricity	Inclination to Ecliptic	Longitude of Ascending Node	Longitude of Perihelion	Mean Longitude of Epoch
Mercury	0.387099	57.94	87.9693	0.24085	47.90	0.20562	7°00'14"	47°47'-32.2"	76°-45'-19.0"	305°-50'-55.73"
Venus	0.723331	108.10	224.7008	0.61521	34.99	0.00681	3°23'39.1"	76°-16'-28.8"	130°-56'-16.5"	127°07'-55.46"
Earth	1.000000	149.45	365.2564	1.00004	29.76	0.01674	0°00'00"		102°-09'-59.3"	99°-22'-49.59"
Mars	1.523688	227.72	686.9797	1.88088	24.11	0.09333	1°50'59.9"	49°-12'-37.7"	335°-131-50.2"	21°-17'-21.34"
Jupiter	5.202803	777.6	4332.588	11.86223	13.05	0.04837	1°18'20.3"	99°-59'-37.9"	13°-35'-51.5"	107°-57'-13.18"
Saturn	9.538843	1427.7	10759.201	29.45772	9.65	0.05582	2°29'24.5"	113°-15'-49.7"	92°-09'-59.2"	219°-28'-14.59"
Uranus	19.190978	2872.4	30685.93	84.01323	6.80	0.04710	0°46'22.9"	73°-46'-14.6"	169°-55'-47.4"	119°-48'-02.38"
Nepituna	30.070672	4500.8	60187.64	164.79365	5.43	0.00855	1°46'27.1"	131°-17'-04.7"	44°-13'-49.1"	205°-56'-36.87"
Pluto	39.51774	5914.8	90737.2	248.4302	4.74	0.24684	17°08'38.4"	109°-38'-0.2"	223°-10'-30.2"	137°-38'-08.0"

Table 2.2

SATELLITES OF EARTH AND MARS

PRINCIPAL ELEMENTS

Name	Mean Dist. in Equatorial Radii of Planet	Mean Distance Km.	Sidereal Period	Inc. of Orbit to Planet's Equator or to "Proper Plane"	Eccentricity	Diameter Km.	Name	Mean Diameter $\oplus = 1$	Mass $\oplus = 1$	Inclination of Equator to Orbit	Mean Surface Gravity $\oplus = 1$	Semi-Diam. at Unit Distance ($1 = AU$)
Satellite of Earth Moon \odot	60.2643	384403	$27^{\text{d}}7^{\text{h}}43^{\text{m}}18^{\text{s}}.5$	$28^{\circ}35^{\prime}$ to $18^{\circ}19^{\prime}$	0.05490	3.476	Sun \odot	109.3	333.420	$7^{\circ}10^{\prime}.5$	27.91	$15^{\circ}58.63^{\prime}$ at mean distance $16-32.58$
Satellites of Mars							Mercury \odot	0.273	81.27	$6^{\circ}40^{\prime}.7$	0.165	
Phobos	2.79	9380	$0^{\text{d}}7^{\text{h}}39^{\text{m}}13^{\text{s}}.651$	$0^{\circ}57^{\circ}.5$	0.017	15?	Venus \odot	0.39	0.045	0.29	3.34	
Deimos	6.96	23460	$1^{\text{d}}6^{\text{h}}17^{\text{m}}54^{\text{s}}.9$	$1^{\circ}44^{\circ}.0$	0.003	8?	Earth \oplus	1.000	1.000	$23^{\circ}26^{\prime}59^{\prime}$	1.00	
							Mars \odot	0.532	0.108	$25^{\circ}12^{\prime}$	0.37	4.68
							Jupiter \odot	10.97	318.25	$3^{\circ}6^{\prime}.9$	2.64	$1-38.47$ (equa.)
							Saturn \odot	9.03	95.3	$26^{\circ}44^{\prime}.7$	1.17	$1-31.91$ (polar)
							Uranus \odot	4.00	14.58	$98^{\circ}.0$	0.91	$1-23.33$ (equa.)
							Neptune \odot	3.90	17.26	29°	1.12	$1-14.57$ (polar)
							Pluto \odot	1.0?	0.93	1?	36.56	

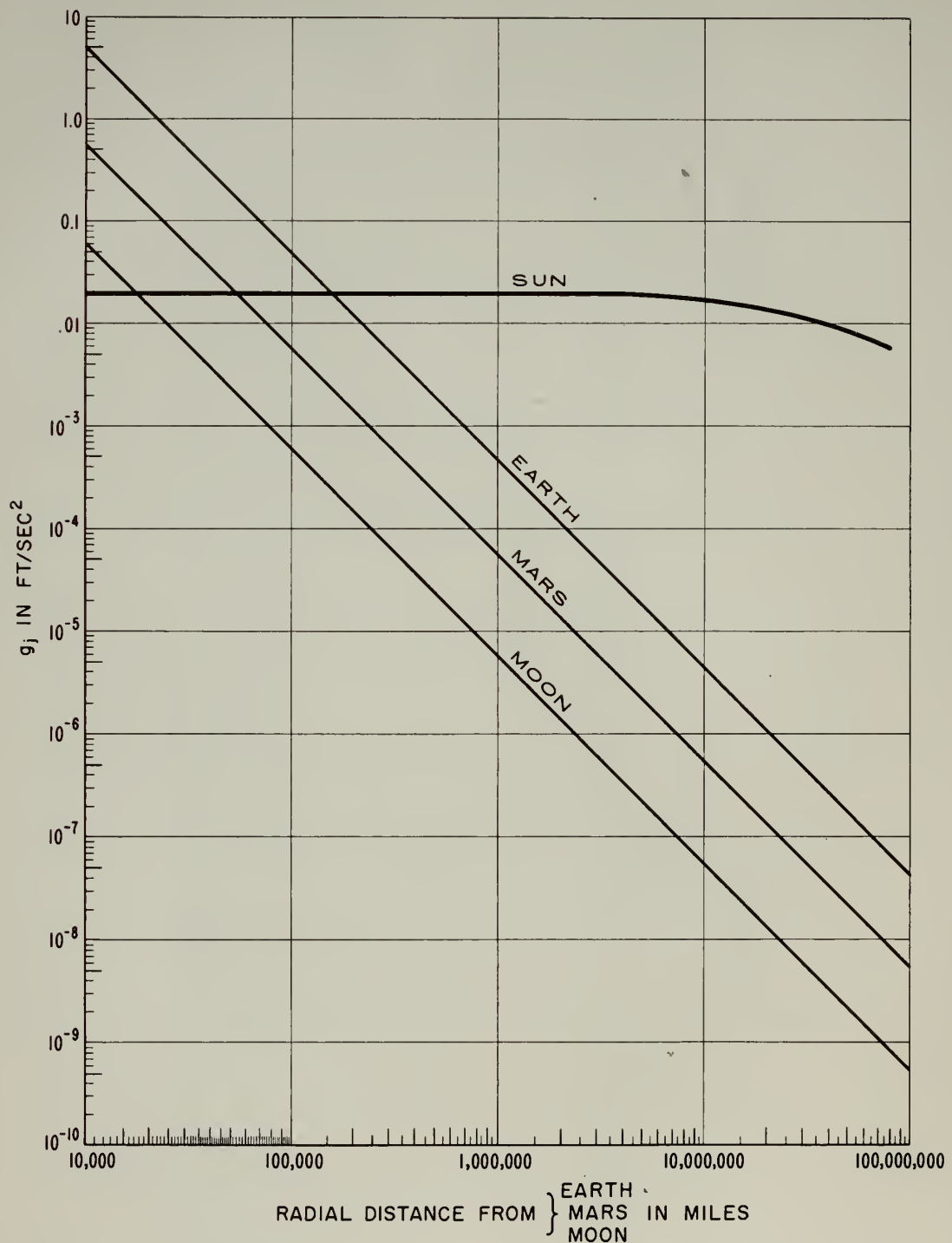


Fig. 2.8 Gravitational field effects

CHAPTER 3

THE PROBLEM SIMPLIFIED

3.1 Introduction

The Law of Universal Gravitation as enunciated by Newton states "Every particle of matter in the universe attracts every other particle with a force which acts in a line joining them, and whose intensity varies as the product of the masses and inversely as the squares of their distances apart."

Moulton⁴⁴ presents an excellent discussion of this law and states, "It will be observed that the law of gravitation involves considerably more than can be derived from Kepler's Laws of Motion; and it was by a master stroke of genius that Newton grasped it in its immense generality and stated it so exactly that it has not been necessary to change a single syllable in over two hundred years. When contemplated in its entirety it is one of the grandest conceptions in the physical sciences."

It is evident that the various bodies comprising the Solar System will exert certain forces upon a rocket in flight among them. Because of the extremely large masses and distances involved we will omit consideration of the minor bodies, such as asteroids and meteor swarms, and show later by inference that this omission is justifiable. Considering then only the Sun, Moon, rocket, and nine planets, we are faced with a twelve-body problem. It would appear expedient to simplify this problem if possible since twelve bodies require thirty-six second order differential equations (thirty-three, if referred to the Sun) to adequately describe their motions.

3.2 Differential Equation of Motion of the Rocket

In order to reduce the complexity of the problem let us first examine the terms of the equation of motion of the rocket and consider their magnitudes. With reference to Fig. 3.1 define I as an inertial reference frame in the convention of Wrigley⁷¹ and 0 as a frame within the Solar System non-rotating with respect to I and with axes parallel to those of I. Note that at this point 0 is restricted only to lie somewhere in the vicinity of the Solar System. Δ represents the position of the rocket, a variable.

We may write Newton's Second Law in vector notation as follows;

$$[\ddot{\bar{R}}_{I\Delta}]_I = \frac{\bar{F}}{m_\Delta} = \bar{f}_f + \bar{f}_{nf} \quad (3-1)$$

where $[\ddot{\bar{R}}_{I\Delta}]_I$ is the second derivative of the vector $\bar{R}_{I\Delta}$ with respect to the frame I and the other terms are previously defined.

Then;

$$\begin{aligned} \bar{f}_f = & \bar{G}_{\odot\Delta} + \bar{G}_{\oplus\Delta} + \bar{G}_{\zeta\Delta} + \bar{G}_{\dot{\zeta}\Delta} + \bar{G}_{\dot{\oplus}\Delta} + \bar{G}_{\dot{\odot}\Delta} \\ & + \bar{G}_{4\Delta} + \bar{G}_{h\Delta} + \bar{G}_{\dot{h}\Delta} + \bar{G}_{\psi\Delta} + \bar{G}_{\dot{\psi}\Delta} \end{aligned} \quad (3-2)$$

where $\bar{G}_{j\Delta}$ is defined in Derivation Summary 1.

If there is a particle at point 0 of mass m_0 then;

$$m_0 [\ddot{\bar{R}}_{I0}]_I = m_0 (\bar{G}_{\odot 0} + \bar{G}_{\oplus 0} + \bar{G}_{\zeta 0} + \bar{G}_{\dot{\zeta} 0} \dots) \quad (3-3)$$

and the masses may be cancelled.

By geometry

$$[\ddot{\bar{R}}_{I\Delta}]_I = [\ddot{\bar{R}}_{0\Delta}]_I + [\ddot{\bar{R}}_{I0}]_I \quad (3-4)$$

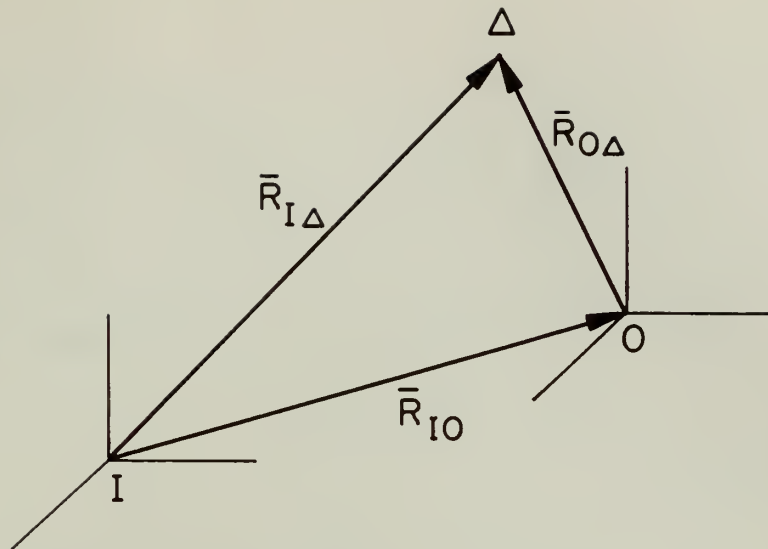


Fig. 3.1 Reference frames

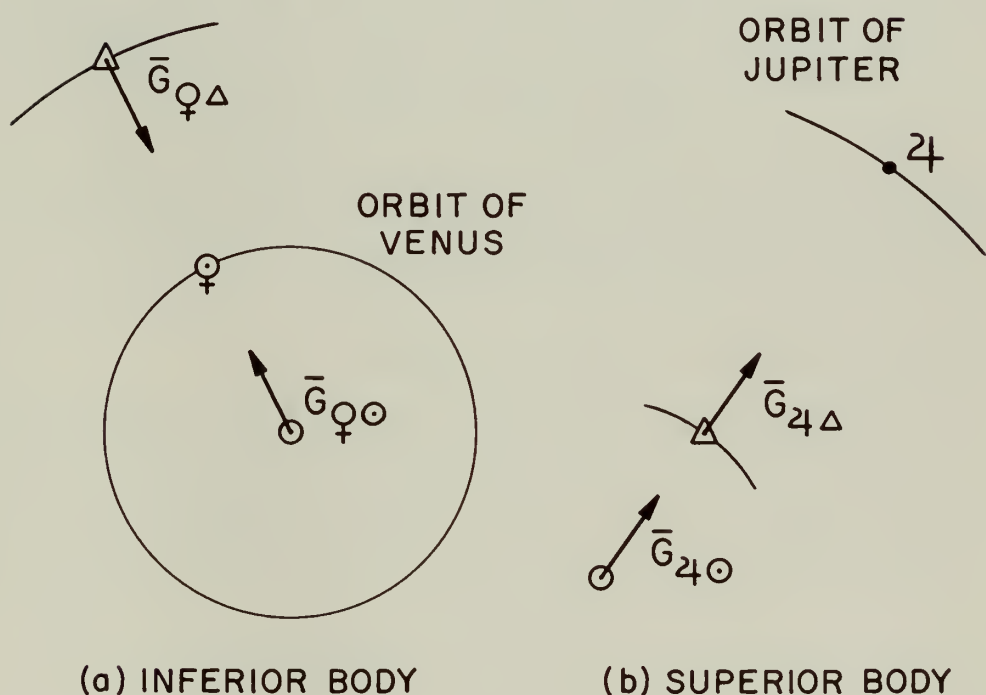


Fig. 3.2 Planetary configurations for Table 3.1

Hence by substitution

$$[\ddot{\overline{R}}_{I_0}]_I + [\ddot{\overline{R}}_{o\Delta}]_I = \overline{f}_f + \overline{f}_{nf} \quad (3-5)$$

or

$$(\overline{G}_{\odot o} + \overline{G}_{\oplus o} + \overline{G}_{\zeta o} + \dots) + [\ddot{\overline{R}}_{o\Delta}]_I = \overline{f}_{nf} \\ + (\overline{G}_{\odot\Delta} + \overline{G}_{\oplus\Delta} + \overline{G}_{\zeta\Delta} + \dots) \quad (3-6)$$

Hence in full

$$[\ddot{\overline{R}}_{o\Delta}]_I = \overline{f}_{nf} + (\overline{G}_{\odot\Delta} - \overline{G}_{\odot o}) + (\overline{G}_{\oplus\Delta} - \overline{G}_{\oplus o}) + (\overline{G}_{\zeta\Delta} - \overline{G}_{\zeta o}) \\ + (\overline{G}_{\dot{\zeta}\Delta} - \overline{G}_{\dot{\zeta} o}) + (\overline{G}_{\dot{\oplus}\Delta} - \overline{G}_{\dot{\oplus} o}) + (\overline{G}_{\dot{\odot}\Delta} - \overline{G}_{\dot{\odot} o}) \\ + (\overline{G}_{\dot{\zeta}\Delta} - \overline{G}_{\dot{\zeta} o}) + (\overline{G}_{\dot{\oplus}\Delta} - \overline{G}_{\dot{\oplus} o}) + (\overline{G}_{\dot{\odot}\Delta} - \overline{G}_{\dot{\odot} o}) \\ + (\overline{G}_{\dot{\psi}\Delta} - \overline{G}_{\dot{\psi} o}) + (\overline{G}_{\dot{\rho}\Delta} - \overline{G}_{\dot{\rho} o}) \quad (3-7)$$

We shall now consider applying this derivation (frame 0) to various members of the Solar System.

3.3 Inertial Points Within the Solar System

Looking first at the motions of the Sun, or the Solar System as a unit, it appears from a statistical analysis of the motions of the "nearer" stars that the Solar System possesses a velocity of approximately 12.2 miles per second relative to these "nearer" stars. The "nearer" stars range from 4 to 300 light-years distant from the Sun. Further, the Sun is thought to occupy a position approximately 20,000 light-years from the center of our Galaxy (The Milky Way) with a period of revolution about the galactic center on the order of 2,200,000 years. (See Section 2.7 for further details on the Solar System). In addition our Galaxy is a member of the so-called Local Group consisting of 17 galaxies, clusters, and clouds including the Andromeda Galaxy, The

Large and Small Magellanic Clouds, and several small clusters. It is thought that these 17 members rotate about a common center of mass located somewhere between our galaxy and the Andromeda Galaxy. Lastly, current theories on the "Red Shift" of the optical spectra of distant galaxies conclude that these galaxies are receding from the Solar System at such tremendous relative velocities that certain effects attributed to the Theory of Relativity must surely be present. It is not the purpose of this paper to argue any of the current theories or to attempt any analysis including Relativity Effects. These motions to which the Solar System is subject are mentioned solely as a basis for the following statements:

The Sun is probably undergoing motions involving intricate and complex accelerations; however, the vast macrocosmic scale of distances involved is such that during the time of flight of our rocket the effect of these ill-defined accelerations is neither appreciable nor measurable. This then permits the statement, "Newtonian space is that unaccelerated with respect to the 'fixed' stars",⁷¹ particularly since it is not known that any stars are fixed, but only that their motions are very small during recorded history.

The foregoing definition of Newtonian space is preferred by the authors since it appears at least semantically more definitive than the statement "Newtonian space is that space wherein Newton's Laws are valid."⁷¹ We say then "The possible motions of the center of the Solar System, however complex, within our detective ability are not known to interfere measurably with the information obtained while ignoring these motions and effects thereof."

3.4 Simplified Differential Equations of Rocket Motion

On the foregoing basis we allow ourselves to define the center of (1) the Sun, (2) the Earth, and (3) Mars each in turn as the lo-

cation of our inertial reference frame 0. Equation (3-7) may then be written successively;

$$[\ddot{\bar{R}}_{\odot\Delta}]_I = \bar{f}_{nf} + \bar{G}_{\odot\Delta} + (\bar{G}_{\oplus\Delta} - \bar{G}_{\oplus\odot}) + (\bar{G}_{\zeta\Delta} - \bar{G}_{\zeta\odot}) \dots \dots \dots \quad (3-8)$$

$$[\ddot{\bar{R}}_{\oplus\Delta}]_I = \bar{f}_{nf} + \bar{G}_{\oplus\Delta} + (\bar{G}_{\odot\Delta} - \bar{G}_{\odot\oplus}) + (\bar{G}_{\zeta\Delta} - \bar{G}_{\zeta\oplus}) \dots \dots \dots \quad (3-9)$$

$$[\ddot{\bar{R}}_{\odot\Delta}]_I = \bar{f}_{nf} + \bar{G}_{\odot\Delta} + (\bar{G}_{\odot\Delta} - \bar{G}_{\odot\odot}) + (\bar{G}_{\zeta\Delta} - \bar{G}_{\zeta\odot}) \dots \dots \dots \quad (3-10)$$

Table 3.1 gives values in ft/sec^2 of the maximum values the above terms in parenthesis will hold, using mean values for the orbital radii of the bodies. Use of these mean radii is considered justifiable since only rarely will the bodies be aligned such that these maximum values actually occur. Figure 3.2 clarifies the manner in which these values do occur.

By inspection of Table 3.1; if we establish that all accelerations less than 10^{-6} ft/sec^2 are to be ignored, we may eliminate from future consideration most of the parenthetical terms in the foregoing equations. We then have;

$$[\ddot{\bar{R}}_{\odot\Delta}]_I = \bar{f}_{nf} + \bar{G}_{\odot\Delta} + (\bar{G}_{\oplus\Delta} - \bar{G}_{\oplus\odot}) + (\bar{G}_{\zeta\Delta} - \bar{G}_{\zeta\odot}) + (\bar{G}_{\odot\Delta} - \bar{G}_{\odot\odot}) \quad (3-11)$$

$$[\ddot{\bar{R}}_{\oplus\Delta}]_I = \bar{f}_{nf} + \bar{G}_{\oplus\Delta} + (\bar{G}_{\odot\Delta} - \bar{G}_{\odot\oplus}) + (\bar{G}_{\zeta\Delta} - \bar{G}_{\zeta\oplus}) + (\bar{G}_{\odot\Delta} - \bar{G}_{\odot\oplus}) \quad (3-12)$$

$$[\ddot{\bar{R}}_{\odot\Delta}]_I = \bar{f}_{nf} + \bar{G}_{\odot\Delta} + (\bar{G}_{\odot\Delta} - \bar{G}_{\odot\odot}) + (\bar{G}_{\zeta\Delta} - \bar{G}_{\zeta\odot}) + (\bar{G}_{\oplus\Delta} - \bar{G}_{\oplus\odot}) \quad (3-13)$$

We have now reduced the problem to one of five bodies rather than twelve. We will investigate the possibility of reducing it even further.

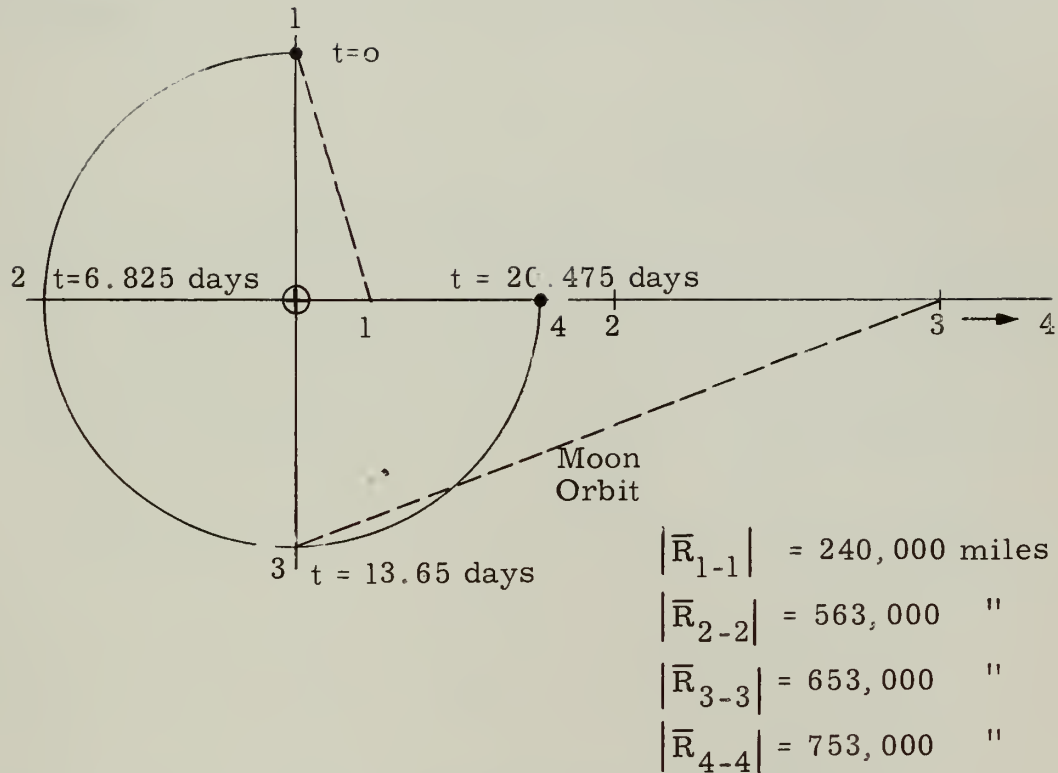


Fig. 3.3 Illustration of Rocket-Moon Separation

3.5 The Lunar Gravity Field Effect

Referring to the Hohmann Ellipse²² it may be shown that in the first 15.2 days of rocket flight along this trajectory the radius vector of the rocket measured from the center of the Earth increases by approximately 600,000 miles. During this period the rocket is in almost linear flight, hence the magnitude of the Lunar gravity field is easily estimated and is shown in Fig. 3.3. At the end of the 15.2 days the value of the gravity field has decreased to less than $1 \times 10^{-5} \text{ ft/sec}^2$ and is continually decreasing.

As a result of these rudimentary estimations it is evident that the effect of the lunar gravity field need be considered only during the initial portion of the trajectory. The example selected

above is unique in that it has been shown to require the least possible rocket velocity hence the rocket would be subjected to Lunar influence for a longer time than in any other trajectory. The foregoing estimates then are an upper bound to the values which actually may occur.

3. 6 The Flight-Phase Concept

Similar arguments to those of the preceding section may be employed to justify ignoring the effect of the Earth and Mars gravity fields over certain portions of the flight. Certainly if a computer is designed to employ the values of these fields there will be a certain sensitivity level below which no cognizance of these values will be taken.

Thus we may write with some degree of justification the following equations;

$$[\ddot{\overline{R}}_{\odot\Delta}]_I = \overline{f}_{nf} + \overline{G}_{\odot\Delta} \quad \text{Phase II} \quad (3-14)$$

$$[\ddot{\overline{R}}_{\oplus\Delta}]_I = \overline{f}_{nf} + \overline{G}_{\oplus\Delta} \quad \text{Phase I} \quad (3-15)$$

$$[\ddot{\overline{R}}_{\odot\Delta}]_I = \overline{f}_{nf} + \overline{G}_{\odot\Delta} \quad \text{Phase III} \quad (3-16)$$

where the limits of the Phases are to be identified.

Thus by consideration of the trajectory and the magnitudes of the forces involved we reduce our problem from one of 12 bodies to three separate two-body problems.

TABLE 3.1

This table displays values for the parenthetical terms of equation 3-7. In the general form we have;

$$|(\bar{G}_{j\Delta} - \bar{G}_{jo})| = k_j R_{oj}^2 \left(\frac{1}{R_{j\Delta}^2} - \frac{1}{R_{jo}^2} \right)$$

where k_j is the surface gravity of the indicated body

R_{oj} is the radius of the body in AU

$R_{j\Delta}$ is the distance separating the body and the rocket in AU

R_{jo} is the distance separating the body and point 0 in AU

# Term	0 = \odot	0 = \oplus	0 = \ominus
$ G_{\odot\Delta} - G_{\odot} $	—	2.78×10^2	2.78×10^{-2}
$ G_{\oplus\Delta} - G_{\oplus} $	~ 32.2	—	~ 32.2
$ G_{\ominus\Delta} - G_{\ominus} $	1×10^{-4}	$* 1 \times 10^{-4}$	$* 1 \times 10^{-4}$
$ G_{\varphi\Delta} - G_{\varphi} $	2.025×10^{-8}	8.03×10^{-9}	8.03×10^{-9}
$ G_{\varphi\Delta} - G_{\varphi} $	1.635×10^{-7}	6.21×10^{-7}	6.21×10^{-7}
$ G_{\odot\Delta} - G_{\odot} $	~ 12.25	~ 12.25	—
$ G_{4\Delta} - G_{4} $	7.1×10^{-7}	9.21×10^{-7}	9.21×10^{-7}
$ G_{h\Delta} - G_{h} $	1.732×10^{-8}	4.025×10^{-8}	4.025×10^{-8}
$ G_{\odot\Delta} - G_{\odot} $	4.65×10^{-10}	7.17×10^{-10}	7.17×10^{-10}
$ G_{\psi\Delta} - G_{\psi} $	1.585×10^{-10}	2.01×10^{-10}	2.01×10^{-10}
$ G_{\rho\Delta} - G_{\rho} $	$\dagger 6.62 \times 10^{-13}$	$\dagger 1.01 \times 10^{-12}$	$\dagger 1.01 \times 10^{-12}$

* by judicious choice of firing time

† Assuming that Pluto and Earth have the same value for surface gravity.

‡ Sample calculations are given in Table 3.2.

TABLE 3.2

Sample Calculation for the Values Listed in Table 3.1.

 $\odot = \odot$

j	K_j	$(R_{oj})^2$	$(R_{j\Delta})^{-2}$	$(R_{jo})^{-2}$	$ \bar{G}_{j\Delta} - \bar{G}_{jo} $
♀	10.45	$\times 10^{10}$	(-)0.780	6.66	2.025×10^{-8}
☿	85.27	2250	0.074	0.034	7.1×10^{-7}

 $\odot = \oplus$

j	K_j	$(R_{oj})^2$	$(R_{j\Delta})^{-2}$	$(R_{jo})^{-2}$	$ \bar{G}_{j\Delta} - \bar{G}_{jo} $
♀	10.45	$\times 10^{10}$	(-)0.274	2.67	8.03×10^{-9}
☿	85.27	2250	0.074	0.026	9.21×10^{-7}

 $\odot = \oplus$

j	K_j	$(R_{oj})^2$	$(R_{j\Delta})^{-2}$	$(R_{jo})^{-2}$	$ \bar{G}_{j\Delta} - \bar{G}_{jo} $
♀	10.45	$\times 10^{10}$	(-)2.67	0.274	8.03×10^{-9}
☿	85.27	2250	0.026	0.074	9.21×10^{-7}

CHAPTER 4

THE TRAJECTORY

A. SOME POSSIBLE TRAJECTORIES

4.1 Basic Criterion for Selection

Selection of the type of trajectory to be followed during the mid-course phase of an interplanetary exploratory trip of any type is dependent upon the basic criterion of when, in the future we contemplate attempting the flight. If we desire to make the attempt within less than ten years it is reasonable to postulate that presently developed power plants and guidance systems must be used with considerable refinement a necessity. If the attempt will not be made until some time after 1970, more exotic power plants and guidance can probably be postulated. However, the basic trajectories can be summarized and a selection made for further study in this paper.

4.2 Classifications of Trajectories

All trajectories, based on thrust available, can be divided into three classifications: (1) Powered, (2) Unpowered and (3) Combination of Powered and Unpowered. Although this statement is simple, the actual engineering and instrumentation requirements are exceedingly complex and somewhat dissimilar.

4.3 Powered Trajectories

The term "Powered Trajectory" implies continuous thrust with either acceleration or deceleration used during the entire flight. Also implied is the ability to apply this thrust in any direction by multiple thrust units or vehicle reorientation with respect to the trajectory.

The upper limit of this type trajectory can be considered to be strictly interceptor, while the lower limit is that of a distorted Keplerian Ellipse. Interceptor trajectories, using proportional navigation, collision course, line of sight, or constant lead⁴³ similar to present day antiaircraft and air-to-air guided missiles, require nearly unlimited thrust. However, many simplifications in guidance methods can be realized due to reduced time of flight and reduction in accuracy requirements if high speed interceptor methods are used.

With small thrust power units such as the ion gun, solar furnace, or Nuclear-chemical, etc.^{47, 62} the trajectory can be a logarithmic spiral such as developed by Forbes¹⁴ or a series of constantly changing ellipses with the actual trajectory being the envelope of the series. In addition the vehicle could be forced to traverse a predetermined elliptical path. This latter method would be extremely wasteful of both fuel and time.

Powered trajectories are difficult to compute and almost infinite in number. The practicality of detailed powered trajectory study with any more than a general overall look at the field appears to be limited at present until the perfection of suitable thrust devices warrant the effort.

4.4 Unpowered Trajectories

Basically the unpowered trajectory is a ballistic flight - incorporating the Fire Control Problem^{22, 43, 72} with that of determining the path of a comet in space.^{21, 44, 60} This implies the application of a large impulsive thrust applied over a very short interval of time with respect to total time of flight. This would result in a hyperbolic path with respect to a planet during application of thrust.^{47, 68} At the end of this time the hyperbolic trajectory would merge with an elliptical path with respect to the sun, and the vehicle would be in free flight, acted upon basically by gravitational attraction of the sun with slight perturbations

caused by the planets, (see Section 3.6).

A trajectory of this sort leads to simplification or elimination of a guidance system for mid-course. However, extreme accuracy in the orientation of the velocity vector at termination of impulse is mandatory. Very small errors in magnitude or direction, or unforeseen gravitational gradients during transit can cause large errors at the trajectory terminus as shown in Section 8.6.

4.5 Combination Trajectories

Trajectories containing thrust periods and ballistic no-thrust periods are complicated by virtue of attempting to combine two separately difficult problems into one. This method does permit slightly lower accuracies of the initial velocity vector but requires accurate mid-course position determination to be of any use.

The basic advantage of this method is that presently developed thrust units can be used for correcting or changing the trajectory during mid-course, thereby increasing the probability that the mission will be completed. Using contemplated low thrust corrective units^{47, 62} powered phases could be of long duration and be equally as effective as high thrust, short burning time chemical units.

4.6 Trajectory Selected for Further Study

The basic mid-course trajectory chosen for further study in this paper is that of a combination of unpowered and powered. The ideal or hoped for situation is one in which no corrective thrust is needed during the time of transit. This would mean that a relatively unperturbed ellipse could be flown within the limits of terminal accuracy requirements. However, if it becomes apparent during transit that corrective action is needed, a new ellipse is computed and proper thrust applied to get on the new

trajectory. The position determination accuracy requirements for such a system are rather high as are the thrust control requirements. However, it is felt that these requirements are not entirely beyond present day engineering capabilities.

B. THE UNPOWERED TRAJECTORY

4.7 Introduction

To intelligently decide upon a trajectory to be traveled to Mars one must weigh many aspects of the problem. In previous portions of this paper we have investigated some properties which influence a vehicle in flight in the Solar System; and, in addition, investigated some vehicular behaviors and parameters which could be selected or adjusted to our benefit.

As previously described, the "unpowered" trajectory is a trajectory provided with an initial impulsive velocity, which, when perfectly instituted, needs no corrective action. This type trajectory lends itself well to analysis since the vehicle is essentially a body acting in a central force field (subject to perturbations). Primarily due to considerations of available fuel and performance characteristics it was decided early in this work to proceed with an analysis of this type trajectory. It is emphasized here that this type trajectory may by no means be considered more attractive than any other because of any inherent property associated with it. It simply appears more feasible due to the current state of the art in the development of rocket vehicles.

Hohmann²² appears to be the first author (circa 1925) to seriously consider the solution of space flight problems. One of the most important results of his excellent study is the description of the minimum energy ellipse, which as the name implies requires the least rocket velocity of any configuration of two planets. This trajectory has become known as the "Hohmann" ellipse and has the characteristic that the arrival of the rocket at Mars occurs when Mars is diametrically opposite Earth position at

time of firing in their respective orbits about the Sun. Note Fig. 4.1 .

Preston-Thomas^{51, 52} agrees with Hohmann and shows some simple relations of the Hohmann ellipse with other ellipses. Other than this the literature shows a decided lack of information on other trajectories of the "unpowered" type.

It is the purpose of this chapter to show some relations existing among the "unpowered" trajectories. These are the trajectories which when corrected for errors are described as the "combination" trajectories of Section 4.5 .

4.8 Basic Relations

The basic relations of a vehicle in motion under the influence of a central force field are set forth by Moulton⁴⁴, Smart⁶⁰, Kooy and Uyttenbogaart²⁶, and others. Those general equations selected by the authors which appear to best fit the problem are:

$$r = \frac{a(1-e^2)}{1-e \cos \theta} \quad (4-1)$$

$$v = \sqrt{GM} \left(\frac{1}{2r} - \frac{1}{a} \right)^{\frac{1}{2}} \quad (4-2)$$

$$\tan \phi = \frac{e \sin \theta}{1 - e \cos \theta} \quad (4-3)$$

A fourth equation⁴⁷ which will be of interest is

$$\frac{e \sqrt{1-e^2} \sin \theta}{1 - e \cos \theta} + \sin^{-1} \left[\frac{e - \cos \theta}{1 - e \cos \theta} \right] + \frac{\pi}{2} = \frac{2\pi t}{T} \quad (4-4)$$

A general trajectory situation is shown in plan view in Fig. 4.2
 Figs. 4.2 and 4.3 illustrate the quantities appearing in the
 foregoing equations.

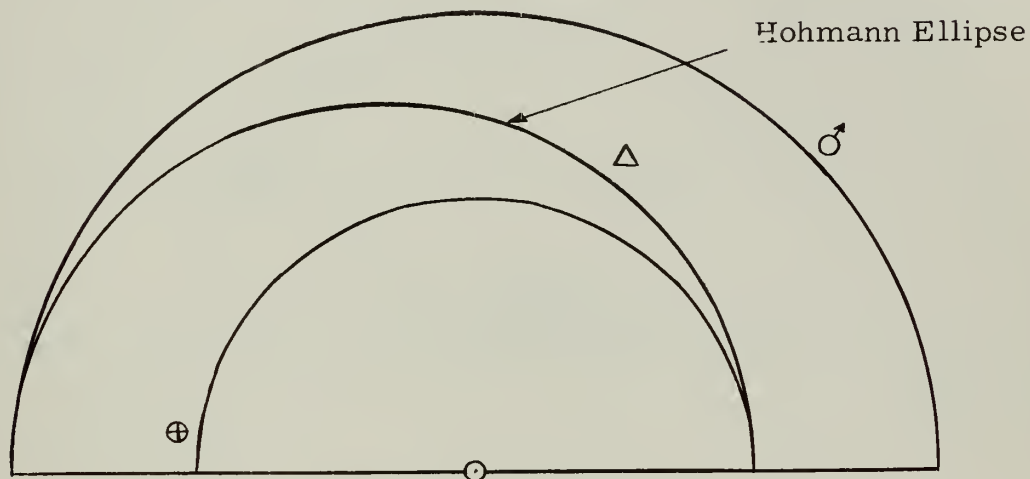


Fig. 4.1 The Hohmann Ellipse

4.9 Some Simplified Trajectory Parameters

We logically begin our analysis by considering the effect of the most massive member of the Solar System, the Sun. Referring to Fig. 4.2; for a given trajectory we may establish initial and final positional conditions (i.e. - we know we are on the Earth and hopefully we will arrive at Mars). Hence we write (4-1) as

$$r_o = \frac{a(1 - e^2)}{1 - e \cos \theta_o} \quad (4-5)$$

and

$$r_A = \frac{a(1 - e^2)}{1 - e \cos \theta_A} \quad (4-6)$$

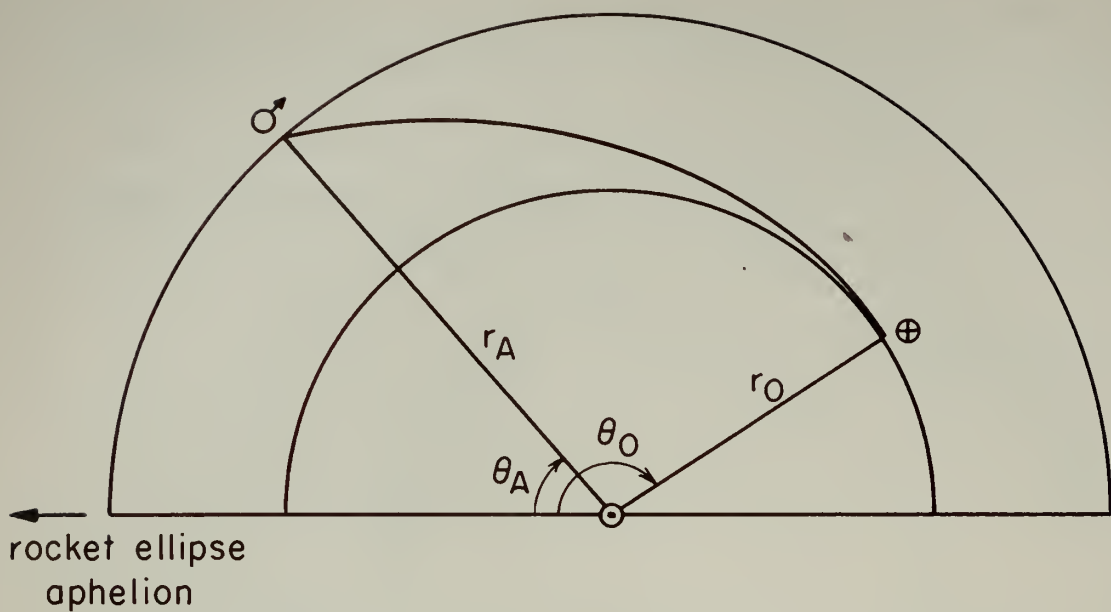


Fig. 4.2 General trajectory configuration

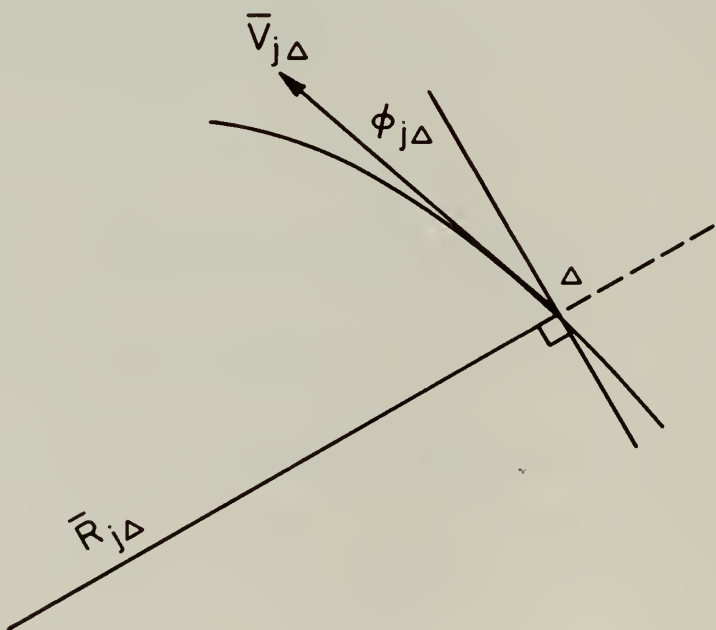


Fig. 4.3 Some vector-angle relations for the general trajectory

where $r_o = |\bar{R}_{\odot o}|$ at $t = t_o$, and $r_A = |\bar{R}_{\odot A}|$ at $t = t_o + t_f$.
 Similar definitions apply to the angles θ_o and θ_A .

Let $r_o = 1$ AU

Let $r_A = 1.5237$ AU

Dividing (4-5) by (4-6) and rearranging, we have

$$e = \frac{0.5237}{1.5237 \cos \theta_A - \cos \theta_o} \quad (4-7)$$

Then from (4-1)

$$a = \frac{(1 - e \cos \theta_o) r_o}{1 - e^2} \quad (4-8)$$

which may be expressed more conveniently

$$\frac{1}{a} = \frac{1 - e^2}{1 - e \cos \theta_o} \quad (4-9)$$

where a is in AU.

This defines two of the parameters (a and e) of any ellipse.

We may now establish the vector velocity of the rocket with respect to the Sun in terms of the trajectory parameters.

Let $V_o \equiv \bar{V}_{\oplus \Delta}$ at $t = t_o$. Then (4-2) may be written

$$V_o = 97,500 \sqrt{2 - 1/a} \quad \text{ft/sec} \quad (4-10)$$

where a is in AU.

Let ϕ_o be the angle shown in Fig. 4.4 at $t = t_o$. Then

$$\phi_o = \tan^{-1} \left[\frac{e \sin \theta_o}{1 - e \cos \theta_o} \right] \quad (4-11)$$

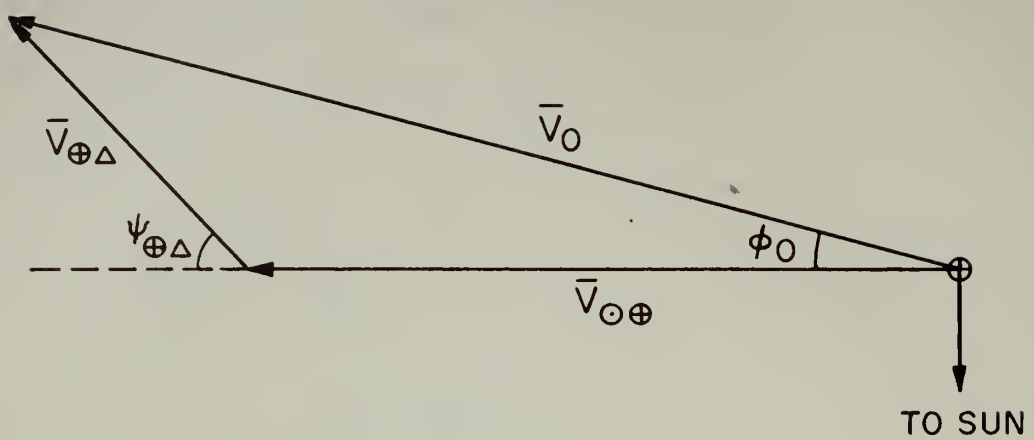


Fig. 4.4 Velocities relative to Earth

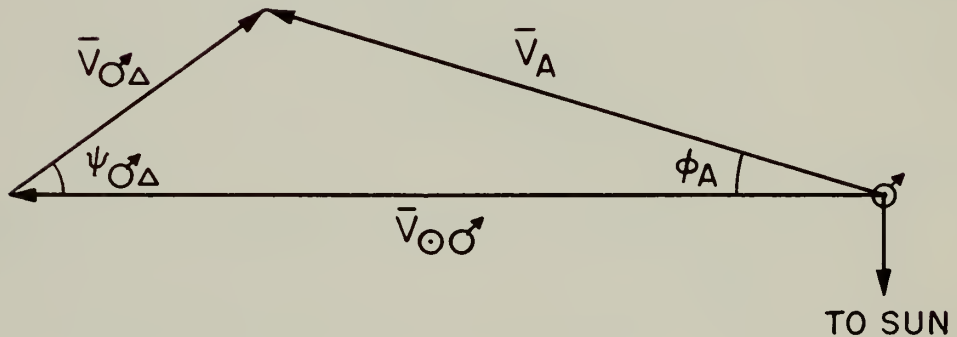


Fig. 4.5 Velocities relative to Mars

Additionally, from Kepler's Laws

$$T = \frac{2\pi}{\sqrt{GM_{\odot}}} \cdot a^{3/2} \quad (4-12)$$

and the period of the ellipse is known.

The boxed equations summarize pertinent parameters in the study of rocket motion with respect to the Sun, and form a basis for the calculations of velocity vector requirements with respect to Earth and Mars.

It might be argued here that greater accuracy should have been demanded of these basic equations (i.e. - Use 1.523688 AU for $|\bar{R}_{\odot\odot}|$ instead of 1.5237 AU). The astronomical unit is known accurately⁵⁴ only to about one part in 10^4 hence no good purpose could be served by extending the required accuracy of these equations beyond the fourth decimal, at least for a preliminary analysis.

Calculations were carried out for about 50 elliptical trajectories and the values for e and $|\bar{V}_{\odot\Delta}|$ are plotted in Fig. 4.6 and 4.7 as aids in future studies. These plots presuppose that θ_o and θ_A are given, known, or selected. A logical basis for the selection of θ_o and θ_A is the subject of another section. Ellipticity < 1 was arbitrarily chosen since excessively high rocket velocities are required for parabolic or hyperbolic trajectories.

4 10 Rocket Velocity Vectors with respect to Earth and Mars

In the preceding section equations were developed to express parameters of the elliptical trajectory and initial velocity of the rocket with respect to the Sun. Obviously, since Earth and Mars are also bodies in motion with respect to the Sun we want the velocity of the rocket with respect to these bodies. The relations are simple, geometric in nature, and are developed herewith.

At $t = t_o$

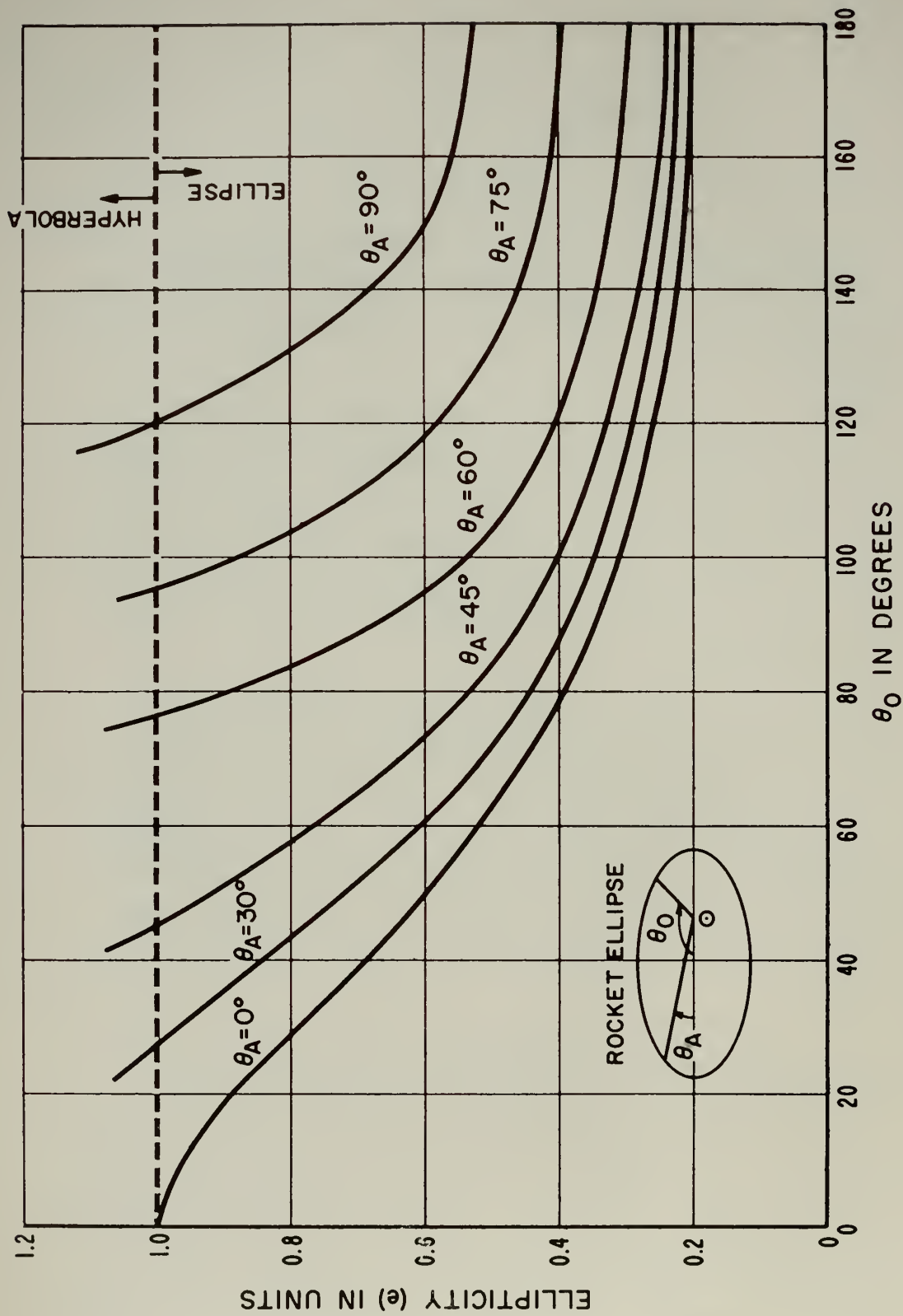


Fig. 4.6 Ellipticity as a function of θ_0 and θ_A

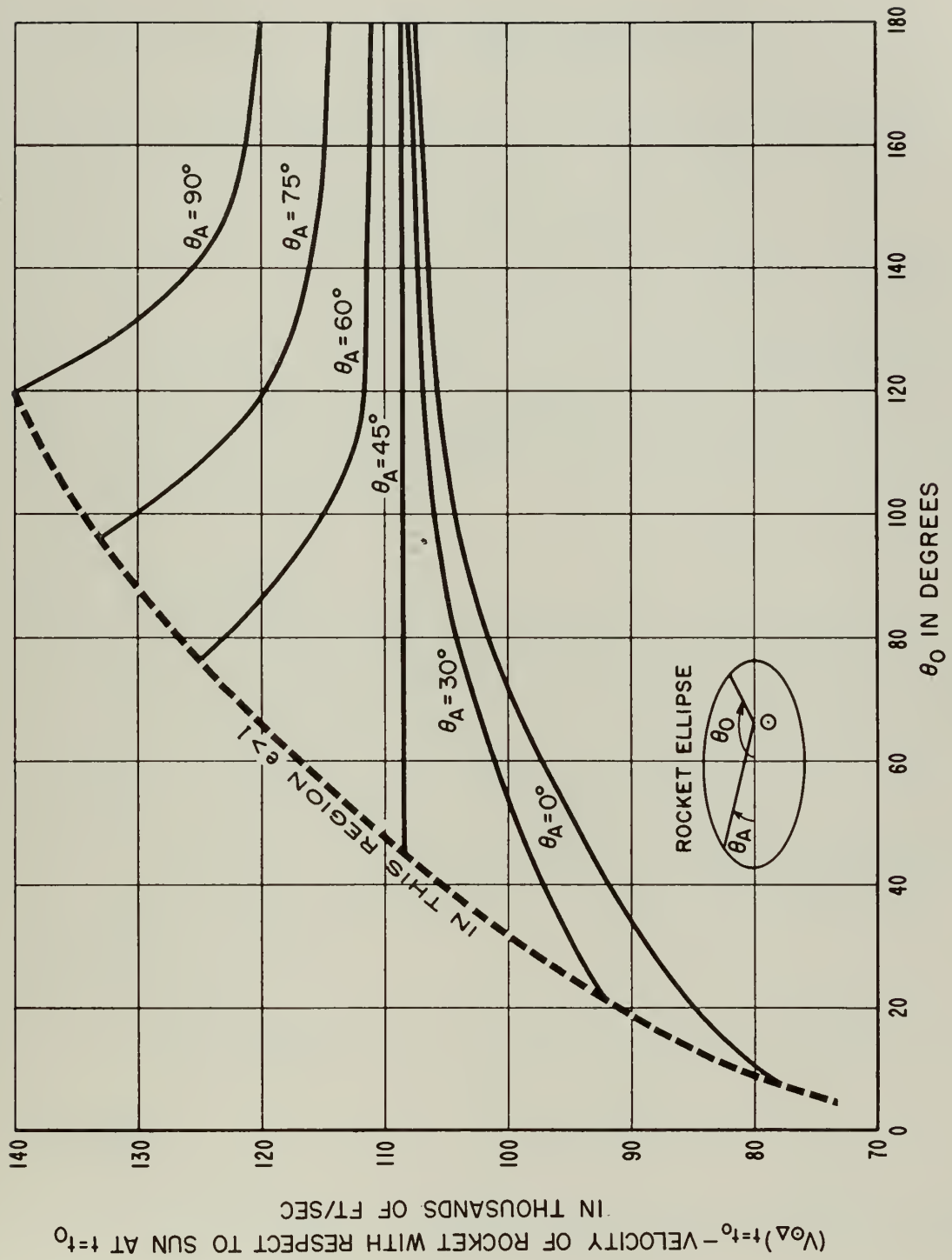


Fig. 4.7 Rocket velocity magnitude with respect to the Sun as a function of θ_O and θ_A

$$\bar{V}_{\odot\Delta} = \bar{V}_{\oplus\Delta} + \bar{V}_{\odot\oplus} \quad (4-13)$$

At $t = t_o + t_f$

$$\bar{V}_{\odot\Delta} = \bar{V}_{\oplus\Delta} + \bar{V}_{\odot\oplus} \quad (4-14)$$

as defined in Definition Summary 1

From equation (4-3)

$$\phi_o = \tan^{-1} \left[\frac{e \sin \theta_o}{1 - e \cos \theta_o} \right] \quad (4-15)$$

And from Fig. 4.4

$$\psi_{\oplus\Delta} = \tan^{-1} \left[\frac{V_o \sin \phi_o}{V_o \cos \phi_o - V_{\oplus}} \right] \quad (4-16)$$

$$V_{\oplus\Delta} = \frac{V_o \cos \phi_o - V_{\oplus}}{\cos \psi_{\oplus\Delta}} \quad (4-17)$$

The properties of an ellipse identify

$$V_A = \frac{r_o}{r_A} V_o \quad (4-18)$$

if $V_A = \bar{V}_{\odot\Delta}$ at $t = t_o + t_f$

$$\phi_A = \tan^{-1} \left[\frac{e \sin \theta_A}{1 - e \cos \theta_A} \right] \quad (4-19)$$

and from Fig. 4.5 and equation (4-14).

$$\psi_{\oplus\Delta} = \tan^{-1} \left[\frac{V_A \sin \phi_A}{V_A \cos \phi_A - V_{\oplus}} \right] \quad (4-20)$$

$$V_{\odot\Delta} = \frac{V_{\odot\oplus} - V_A \cos \phi_A}{\cos \psi_{\odot\Delta}} \quad (4-21)$$

If $r_o = 1.0000$ AU and $r_A = 1.5237$ AU then

$$V_{\odot\oplus} = 97,500 \text{ ft/sec}$$

and

$$V_{\odot\Delta} = 78,990 \text{ ft/sec}$$

Figures 4.8 and 4.9 show $V_{\oplus\Delta}$ and $V_{\odot\Delta}$ as functions of θ_o and θ_A . These values are important primarily as a step in solving the trajectory problem and are given here for possible future use by the reader.

4.11 Time of Flight

The calculation of time of flight is necessary at this point in order to determine the angular separation of Earth and Mars at the instant of rocket firing. Furthermore, it is necessary to know t_f in sidereal or calendar time since the inclination of Mars' orbit with the ecliptic is a function of real time.

If we substitute t_c and t_d as defined in Definition Summary 1 each in turn in Equation (4-4) and recognize $\theta_A \equiv \theta_c$ and $\theta_o \equiv \theta_d$ we have

$$\frac{e\sqrt{1-e^2} \sin \theta_o}{1 - e \cos \theta_o} + \sin^{-1} \left[\frac{e - \cos \theta_o}{1 - e \cos \theta_o} \right] + \frac{\pi}{2} = t_d \sqrt{\frac{GM}{a^3}} \odot \quad (4-22)$$

and

$$\frac{e\sqrt{1-e^2} \sin \theta_A}{1 - e \cos \theta_A} + \sin^{-1} \left[\frac{e - \cos \theta_A}{1 - e \cos \theta_A} \right] + \frac{\pi}{2} = t_c \sqrt{\frac{GM}{a^3}} \odot \quad (4-23)$$

Substituting $t_f = t_d - t_c$ after subtracting (4-23) from (4-22) we have

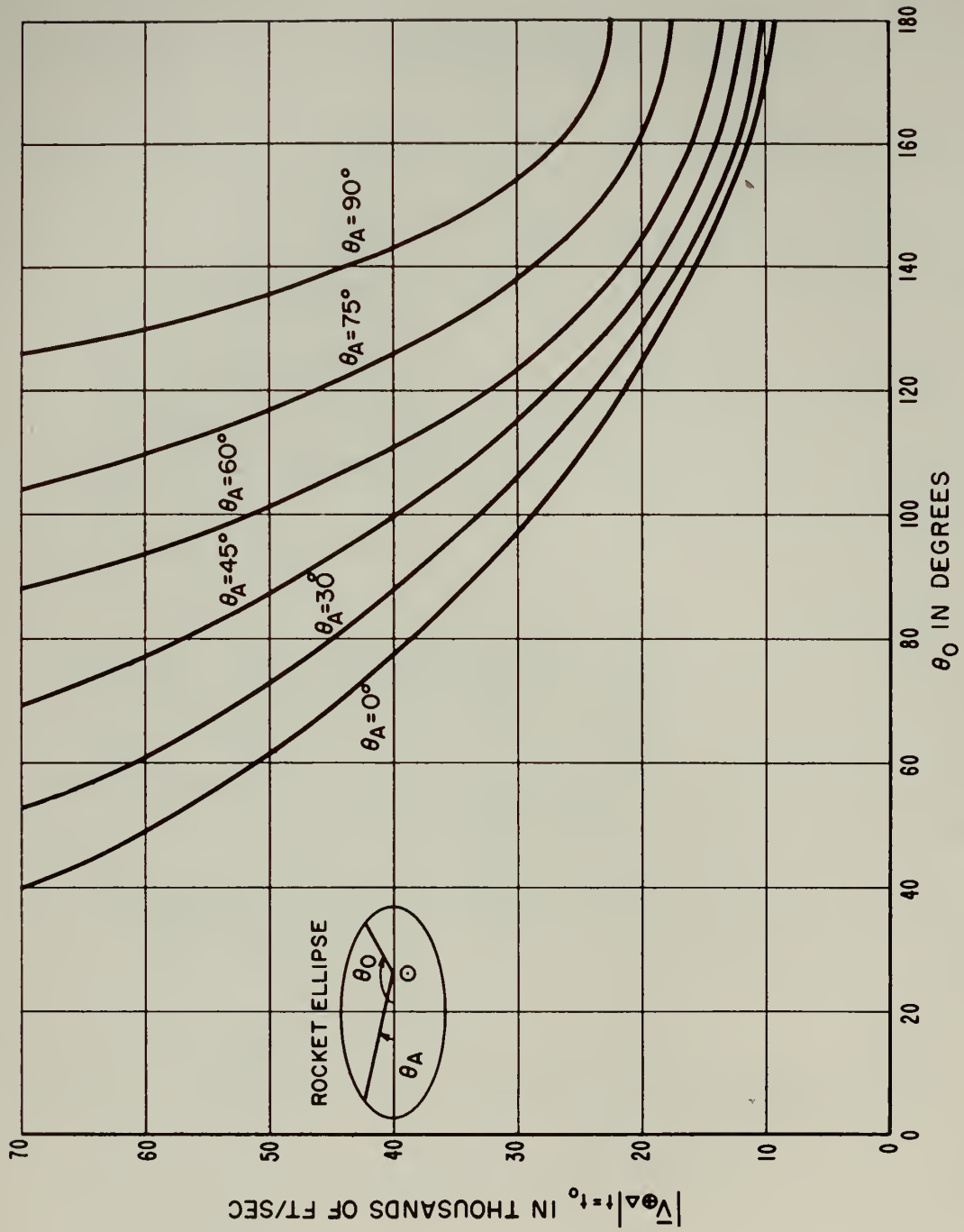


Fig. 4.8 Rocket velocity magnitude with respect to Earth as a function of θ_O and θ_A

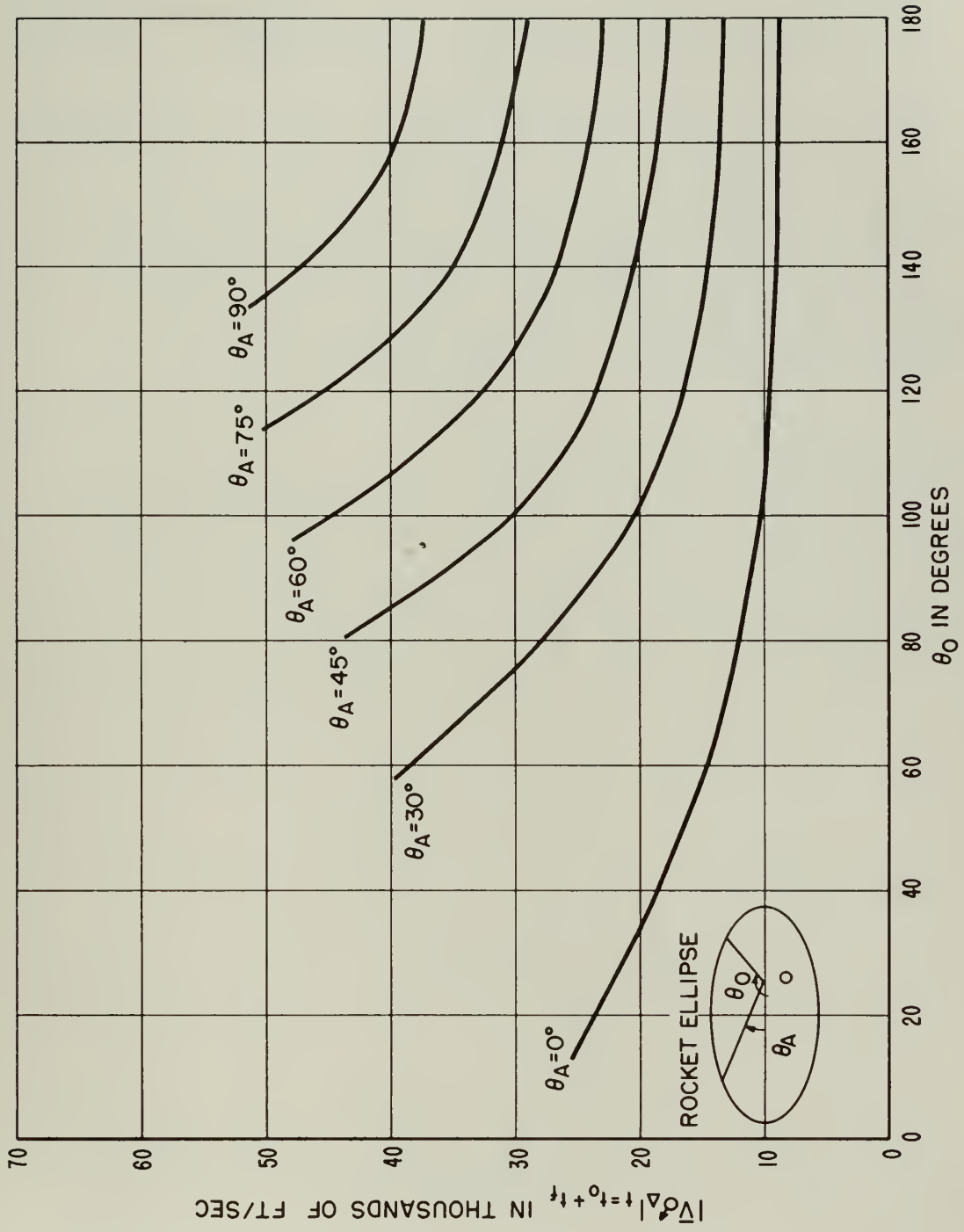


Fig. 4.9 Rocket velocity magnitude with respect to Mars as a function of θ_O and θ_A

$$e\sqrt{1-e^2} \left[\frac{\sin \theta_o}{1-e \cos \theta_o} - \frac{\sin \theta_A}{1-e \cos \theta_A} \right] + \left[\sin^{-1} \left(\frac{e - \cos \theta_o}{1-e \cos \theta_o} \right) - \sin^{-1} \left(\frac{e - \cos \theta_A}{1-e \cos \theta_A} \right) \right] \\ = t_f \sqrt{\frac{1}{a^3}} \sqrt{GM} \quad (4-24)$$

where $GM = 0.01716$ if a is given in AU. t_f is in days (sidereal).

Values for a large number of trajectory time of flights were calculated and the results plotted in Fig. 4.10. Fig. 4.2 illustrates pertinent factors in the foregoing equations.

4.12 Angular Separation of Earth and Mars

Having found the time of flight for a given trajectory we may compute the angular separation of Earth and Mars at the instant of firing ($\theta_o - \theta_s$). Since Mars is in motion about the Sun ($\theta_o - \theta_s$) is a quantity which must be known in order to fire at the correct time to produce an intercept. It is evident from Definition Summary 1 that

$$\theta_s = \theta_A + \dot{\theta}_{\odot} t_f \quad (4-25)$$

It may be shown²⁷ that

$$\dot{\theta}_{\odot} = \frac{2\pi}{T} \frac{(1-e \cos \theta_s)^2}{(1-e^2)^{5/2}} \quad (4-26)$$

$$= \text{constant} (1 - e \cos \theta_s)^2 \quad (4-27)$$

Since $\dot{\theta}_{\odot}$ is a function of θ_{\odot} we are inexorably engaged with a quantity which varies not only with real time but also with angular position. A convenient method of expressing $\dot{\theta}_{\odot} t_f$ is to plot θ_{\odot} as a function of time; then, knowing t_f and choosing t_o we can obtain the angle

$$\dot{\theta}_{\odot} t_f \equiv \theta_s - \theta_A \quad (4-28)$$

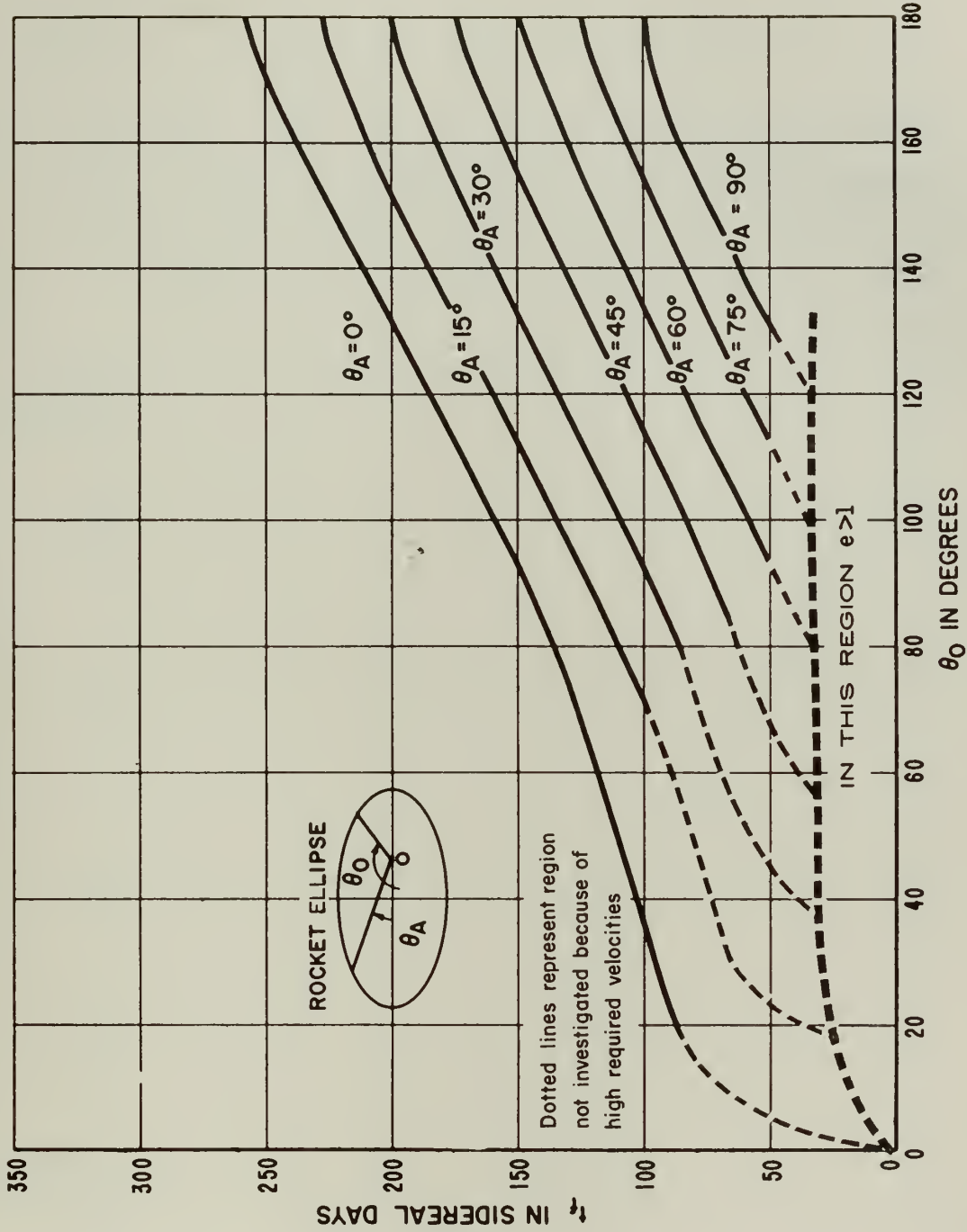


Fig. 4.10 Time of flight as a function of θ_O and θ_A

and

$$(\theta_o - \theta_s) = (\theta_o - \theta_A) - (\theta_s - \theta_A) \quad (4-29)$$

The aforementioned plot appears as Fig. 4.11. To assist in the logical selection of t_o an overlay (Fig. 4.12; in envelope attached to back cover) has been constructed. The basis of construction and description of use is given in Information Summary 4.1.

MARS ANGLE IN DEGREES FROM EARTH APHELION

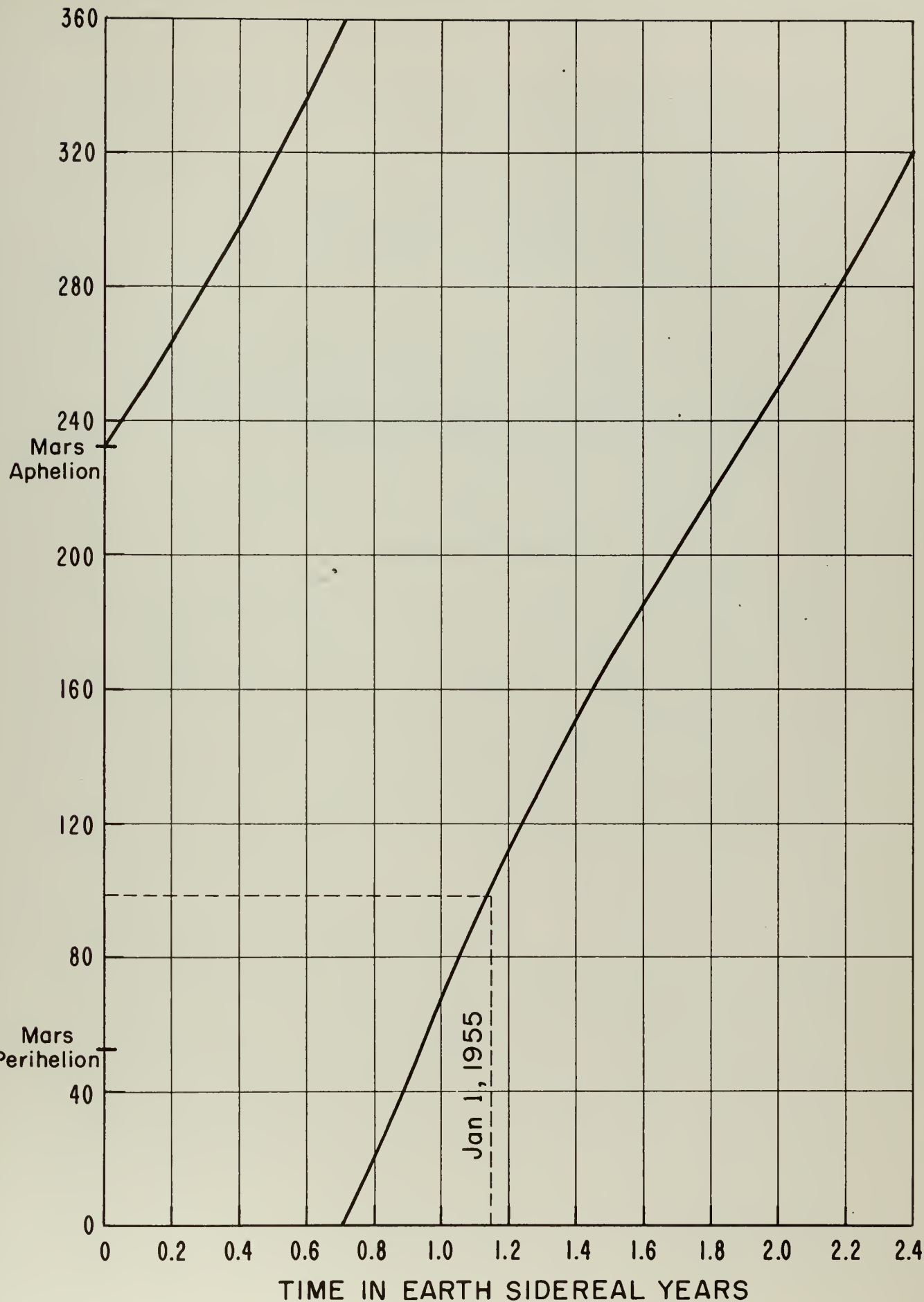


Fig. 4.11 Mars angular position measured from Earth aphelion as a function of time

Fig. 4.12 (Overlay #1)

Earth angular position measured from earth
aphelion as a function of time

(In pocket on back cover)

INFORMATION SUMMARY 4.1

Construction and Use of Overlay #1.

Assuming the "state of the art" of interplanetary travel is such that an Earth-Mars trip is planned to occur about 1980, we note^{2, 54} that on January 1, 1979 Earth is 177° ahead of her aphelion (see insert on Fig. 4.12). Mars is 2° behind Earth's aphelion. In other words Mars is 181° ahead of the Earth. During the succeeding 1.135 sidereal years Earth overtakes Mars, and they are in conjunction 227° past Earth aphelion (about February 17, 1980). Hence from January 1, 1979 to February 17, 1980 ($\theta_o - \theta_s$) takes on all values from 0 to π . With all pertinent parameters of both Earth and Mars orbits known,⁵⁴ Fig. 4.11 and 4.12 were drawn so that information for the period in question would be easily accessible. The assumption has been implicitly made herein that Mars aphelion precesses only slightly about the Sun (a few seconds of arc in about 10,000 years).⁵⁴

(a) Basis for Construction of Overlay

The angular position of Earth is indicated for January 1, 1955 and will repeat every sidereal year. Mars angular position is marked on graph 4.11 for January 1, 1955, but its period is not an even multiple of years, hence its angular position for any given time must be found either from an Ephemeris or by the following method:

Divide the difference in time between January 1, 1955 and the time for which Mars angular position is desired by the number 1.88 (Mars period in sidereal years). Slide the mark for January 1, 1955 on the overlay to the right of the mark for January 1, 1955 on the underlying graph an amount equal in sidereal years to the remainder in the foregoing division. The real time scales have now been superimposed so that the angular positions of Earth and Mars are coincident on the time scale. The values of θ_o and θ_s may be picked off the curves and ordinate scale. If a time other than January 1, for a given year is desired, make auxilliary pencil marks for Earth position and use that rather than January 1, as a reference.

(b) To find $(\theta_o - \theta_s)$ for a given t_o

During the period of interest all values of $(\theta_o - \theta_s)$ from 0 to π occur, hence set the overlay as before and read t_o corresponding to the given θ_o and θ_s as a decimal fraction of a year after the chosen reference time.

(c) To find t_o for a given θ_o and θ_s

This problem is somewhat more complex. We are primarily concerned with a real time firing time in late 1979. This is true because it is about this time that $(\theta_o - \theta_s)$ takes on values in which we are interested (note Section 4.12 and Fig. 4.11 and 4.12). Fortunately; Mars' angular rate in late 1979 is approximately constant at 0.47 degrees per sidereal day. If we multiply 0.47 times the t_f this determines a rough value of $(\theta_s - \theta_A)$. Subtracting $(\theta_s - \theta_A)$ from $(\theta_o - \theta_A)$ provides $(\theta_o - \theta_s)$ for which a t_o can be found as explained in part (c). By noting the angular positions of Earth and Mars and by moving a straight-edge up or down the superimposed curves one may obtain a more accurate value of $(\theta_o - \theta_s)$ for the given data.

(Page 2 of 3)

(d) To find t_o for a given t_f , θ_o and θ_A

January 1, 1955 was chosen as reference time because accurate values were available to the authors.

The method described herein is a rough graphical method of finding required quantities for preliminary work. Actual calculation would of necessity be made by computer.

(e) Notes

(Page 3 of 3)

4.13 $V_{\oplus\Delta}$ and $V_{\ominus\Delta}$ as functions of $(\theta_o - \theta_s)$

Since we now may find $(\theta_o - \theta_s)$ for any given trajectory, it appears pertinent to note any relations which may exist between this angle and the velocity required to fly the trajectory. From an inspection of the basic equations in Section 4.8 it is obvious that the relationship is quite complex. For this reason $V_{\oplus\Delta}$ and $V_{\ominus\Delta}$ were plotted graphically for a large number of trajectories in a manner analogous to that of Preston-Thomas⁵¹. The minimum $V_{\oplus\Delta}$ was found to be the envelope of the curves as θ_o took on various values. (See Fig. 4.13) The minimum $V_{\ominus\Delta}$ was found to be identically the curve for $\theta_A = 0^\circ$. (See Fig. 4.14) This is not inconsistent since the first case represented minimum velocities for a non-maximum radius vector of an ellipse; whereas the second case represented the minimum velocities that exist at aphelion (maximum radius) of an ellipse. In both cases the Hohmann Ellipse ($\theta_o = 180^\circ$; $\theta_A = 0^\circ$) provided the absolute minimum velocities.

4.14 The Rocket Plane (Δ plane) Concept

Let us define the plane containing $\bar{R}_{\odot\oplus}$ and $\bar{V}_{\odot\Delta}$ at $t = t_o$ as the rocket plane (Δ plane). If the rocket were not perturbed during its flight it could remain in this Δ plane (this being a

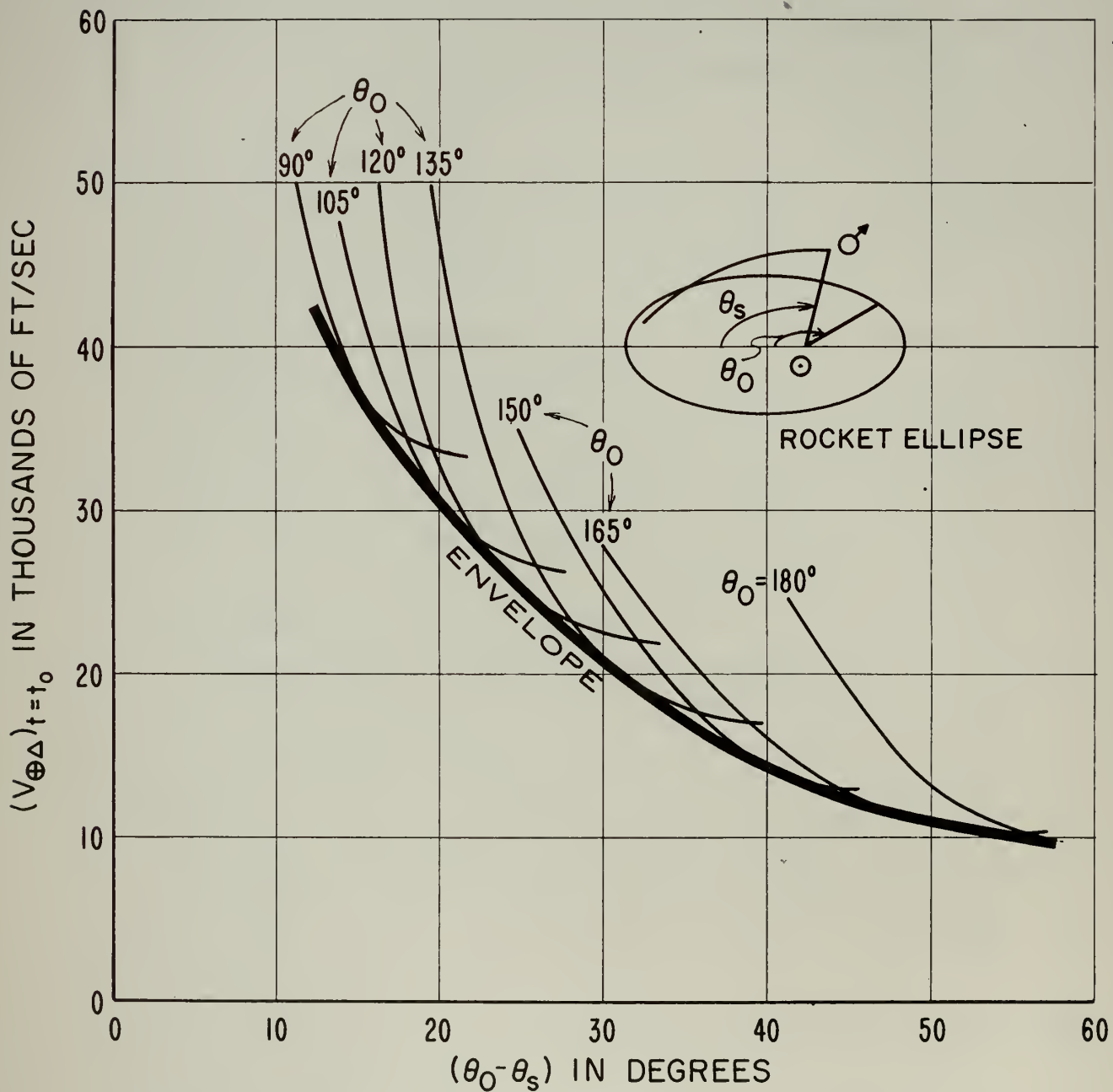


Fig. 4.13 Rocket velocity magnitude with respect to Earth as a function of θ_0 and $\theta_0 - \theta_s$

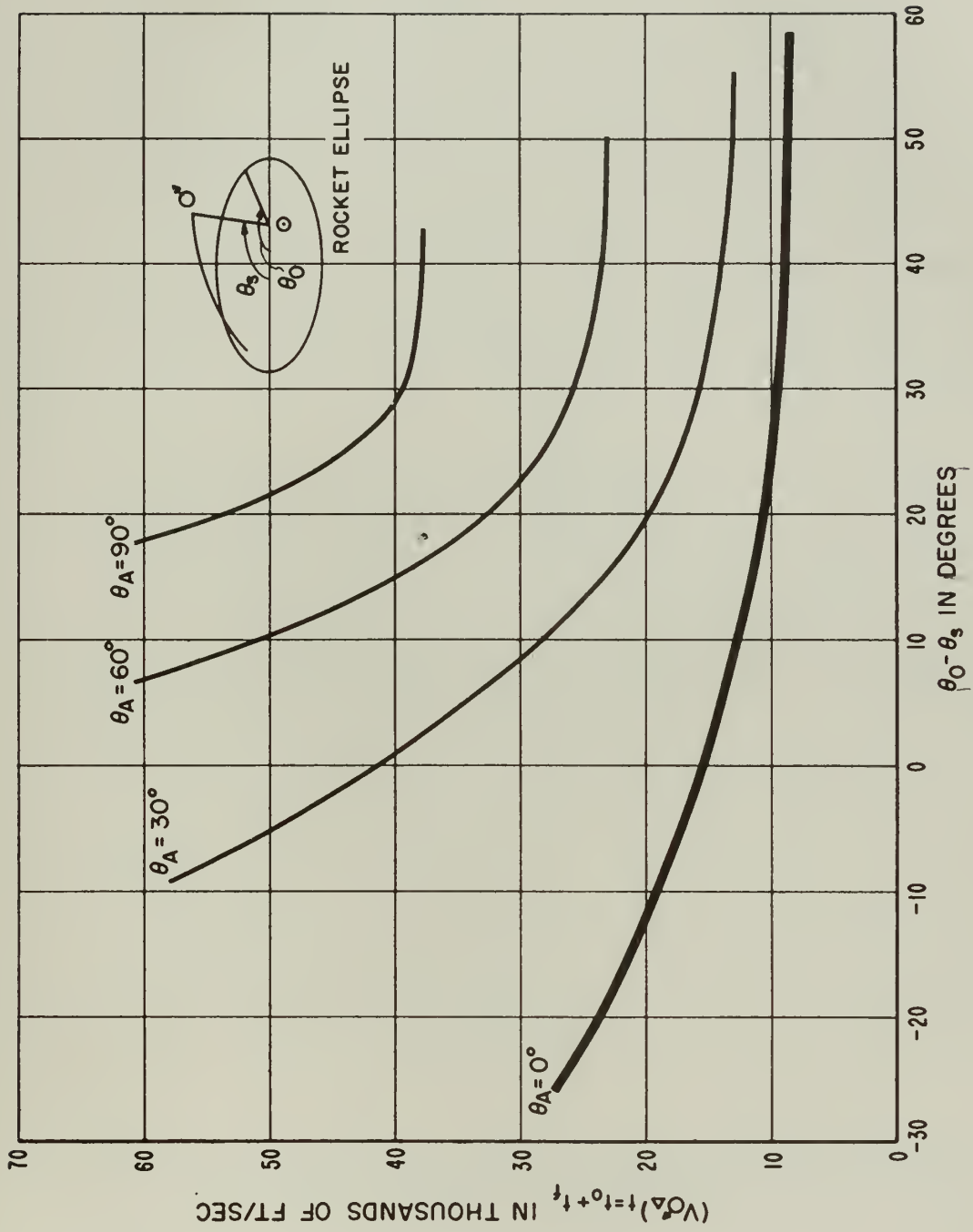


Fig. 4.14 Rocket velocity magnitude with respect to Mars as a function of $\theta_O - \theta_s$ in degrees

property of the motion of a body in a central force field⁴⁴). The Δ plane need not necessarily, and generally will not, lie in the Earth ecliptic plane since Mars passes through the Earth ecliptic plane only twice every 1.88 sidereal years. Unfortunately, for calculation purposes, the orientation of $\bar{V}_{O\Delta}$ in Solar System space depends on the real time firing time and time of flight. Hence every possible trajectory requires a complete individual solution. The labor involved is so mountainous that solution by high-speed digital computer is mandatory; and even these solutions must be based on a selected future firing time.

If we can show that the displacement of the rocket normal to the Δ plane is negligibly small we may be justified in saying that for practical purposes the rocket remains essentially in the rocket plane and our problem reduces to two dimensions. Neglecting the possible perturbations of bodies such as meteors, distant planets, asteroids, etc., the bodies causing displacement of the rocket from the Δ plane are Earth, Moon, and Mars. In an effort to show the minor nature of the aforementioned displacements calculations were made on a single "typical" trajectory. This trajectory was chosen because $V_{inc} = 10,000$ ft/sec, which is a velocity probably within the capabilities achievable in the near future. Since we are concerned with the period from late 1979 to early 1980 the firing time is established by $(\theta_o - \theta_s)$ to be about December 6, 1979. Note Figs. 4.15 and 4.18.

Referring to Derivation Summary 4.1 the cumulative displacement of the rocket from the Δ plane was found by accumulating the values determined from Equation 11 over the trajectory traveled by an unperturbed rocket (see Fig. 4.19). Certain errors are inherent in the calculations but will be seen to be negligibly small. The arc length of the trajectory

ROCKET ELLIPSE
APHELION

DATE OF FIRING
APPROX. DEC. 6, 1979

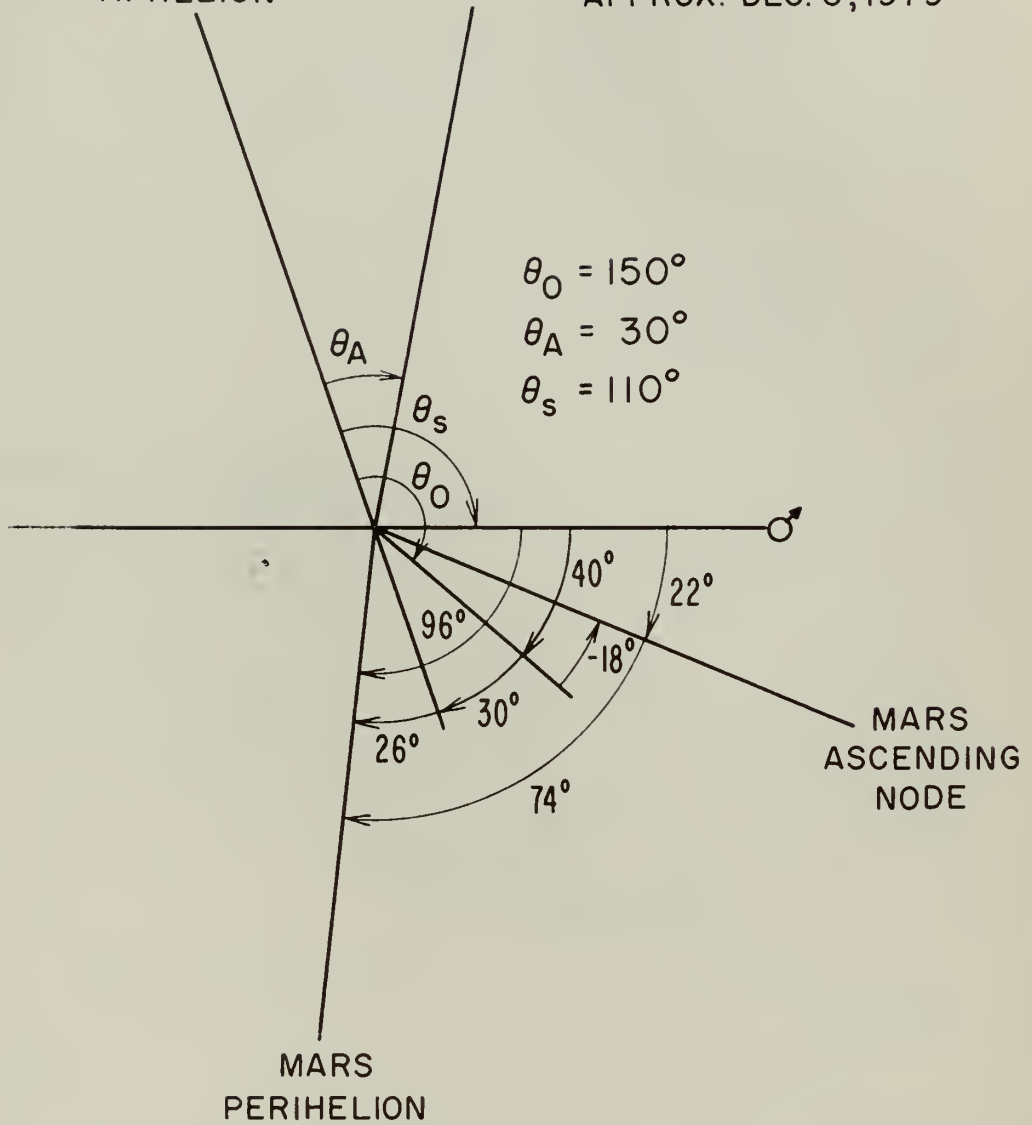


Fig. 4.15 Angular quantities of a representative trajectory discussed in section 4.14

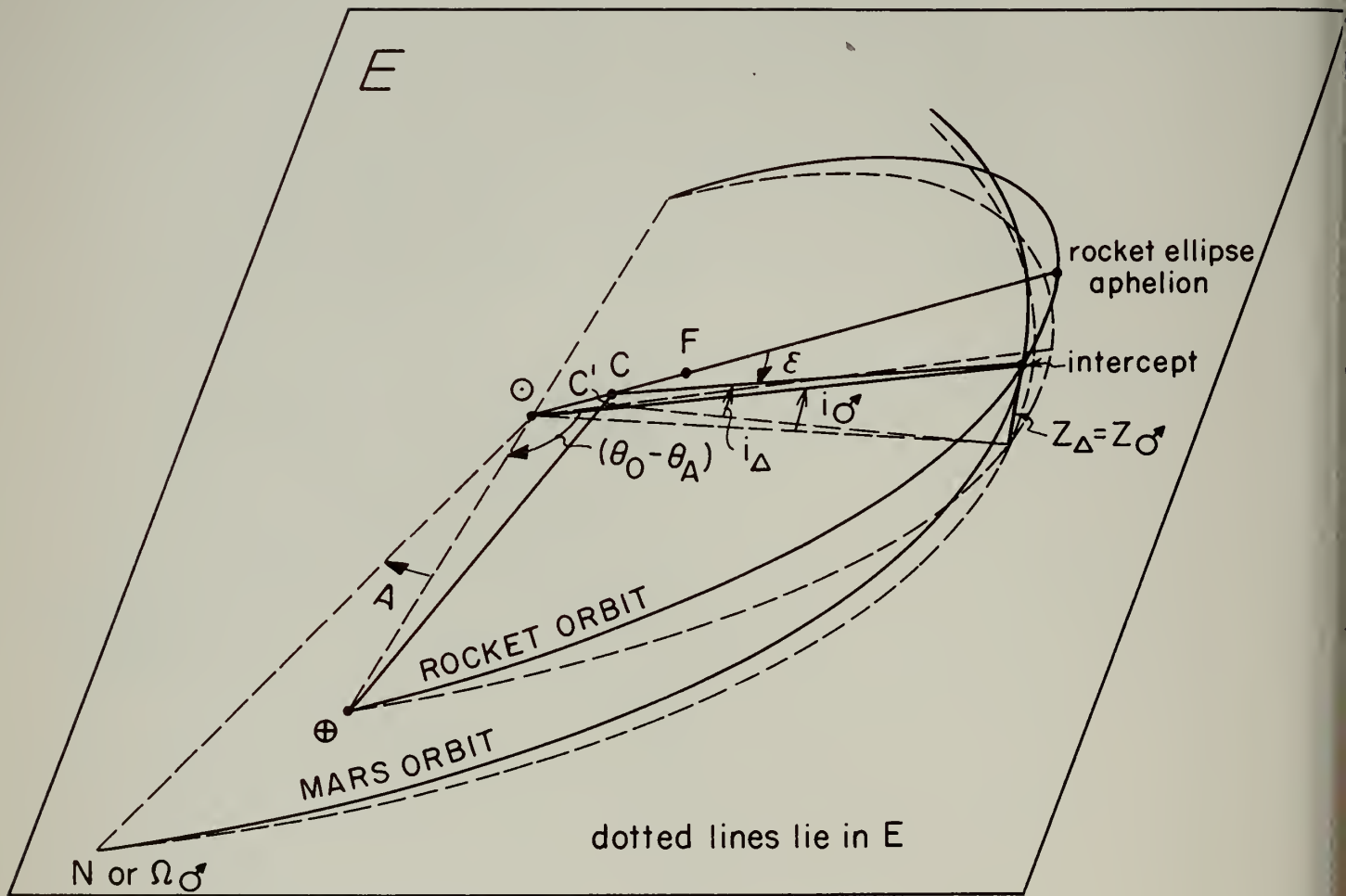


Fig. 4.16 A typical trajectory showing the effect of tilt to account for non-co-planarity of Earth and Mars motion

AN IMAGINARY CYLINDER
RADIUS EQUAL TO r_{σ^*} , Z
PERPENDICULAR TO E

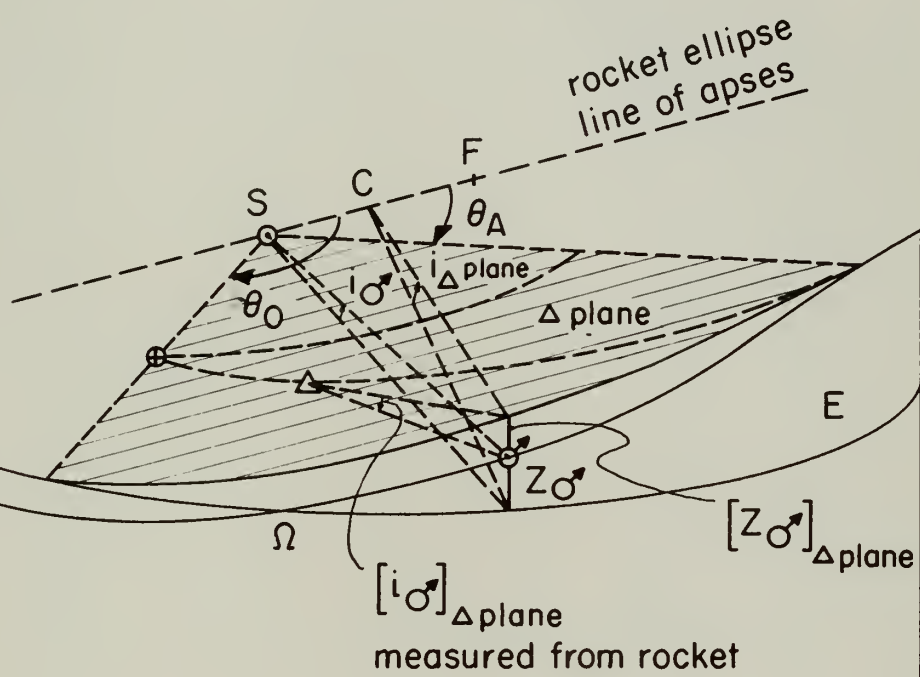


Fig. 4.17 Assisting supplementary view to figure 4.16

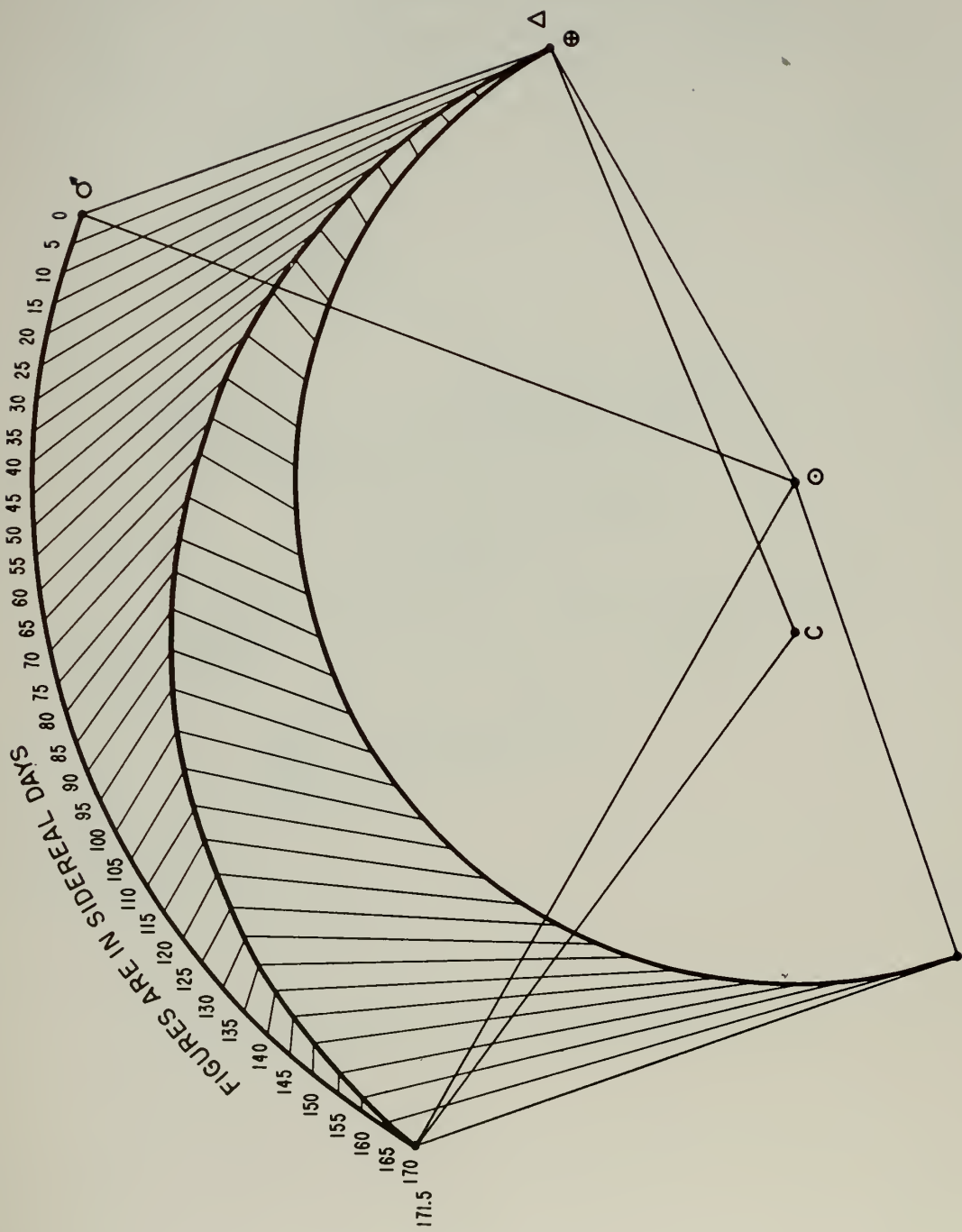
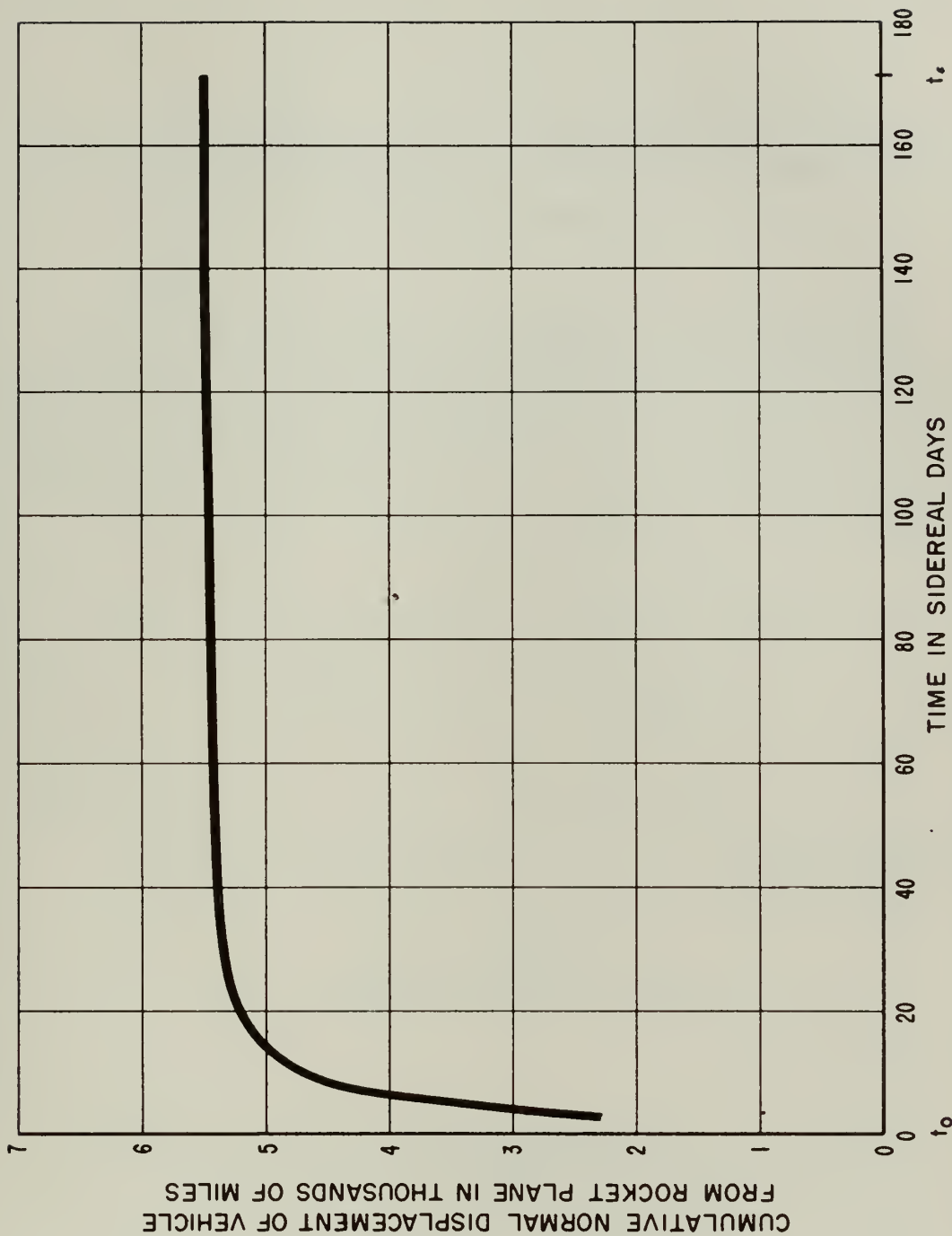


Fig. 4.18 Plan view of body motions for trajectory discussed in section 4.14



DERIVATION OF THE EQUATION FOR THE DETERMINATION
OF THE DISPLACEMENT OF THE ROCKET NORMAL TO THE
"ROCKET PLANE"

Four relations are available from consideration of the geometrical properties of the trajectories or orbits. Two assumptions are made which greatly simplify the solution. The error introduced by these assumptions is on the "high" side and will be shown to be negligible (Fig. 4.16 refers).

$$i_{\Delta} = (i_{\max})_{\Delta} \sin \epsilon \quad (1)$$

$$i_{\circlearrowleft} = (i_{\max})_{\circlearrowleft} \sin (A + \theta_o - \theta_{\circlearrowleft}) \quad (2)$$

$$z_{\Delta} = R_{C\Delta} \sin i_{\Delta} \quad (3)$$

$$z_{\circlearrowleft} = r_{\circlearrowleft} \sin i_{\circlearrowleft} \quad (4)$$

From (3) and (4)

$$i_{\Delta} = \sin^{-1} \left[\frac{r_{\circlearrowleft}}{R_{C\Delta}} \sin i_{\circlearrowleft} \right] \quad (5)$$

(a) Basic Equations

To aid in clarification of the development that follows and the assumptions made, the following list of symbols is presented:

$(g_{\text{orth}})_j$ Magnitude of that component of \bar{G}_j normal to the "rocket plane".

DERIVATION SUMMARY 4.1
(Page 1 of 4)

i_j Inclination of indicated quantity with reference plane, or with ecliptic plane if no reference is given - positive direction in the conventional sense.

$(i_{\max})_j$ Maximum inclination as defined above.

z_j Displacement of indicated quantity normal to indicated reference or to ecliptic plane if no reference is given.

A Angle as shown in Fig. 4.16

ξ Eccentric anomaly as shown in Fig. 4.16

δ Increment (Magnitude as defined).

(b) Definitions

Referring to Fig. 4.16 and 4.17 the two assumptions made are

(1) that the "rocket ellipse" is almost circular about its center (C).

(2) that the line CC' in Fig. 4.16 is negligibly small.

(c) Assumptions

To derive the required equation we solve (3), then (4) for the final condition $\theta_{\odot} = \theta_A$. We then find i_{Δ} from (5) and $(i_{\max})_{\Delta}$ from (1). Having discovered $(i_{\max})_{\Delta}$ for a given trajectory we are now able to write i_{Δ} as a function of θ_{\odot} (Equation 1).

Any [z] $_{\Delta\text{plane}}$ may be found thusly:

DERIVATION SUMMARY 4.1

(Page 2 of 4)

From Fig. 4.17 ;

$$[Z_{\Delta\text{plane}}]_{\text{at } \odot} = [R_{C\Delta} \sin i_{\Delta}]_{\text{at } \odot} \quad (6)$$

and

$$Z_{\odot} = [r_{\odot} \sin i_{\odot}]_{\text{at } \odot} \quad (7)$$

obviously

$$[Z_{\odot}]_{\Delta\text{plane}} = [Z_{\Delta\text{plane}}]_{\text{at } \odot} - Z_{\odot} \quad (8)$$

now

$$[i_{\odot}]_{\Delta\text{plane}} = \sin^{-1} \frac{[Z_{\odot}]_{\Delta\text{plane}}}{|\bar{r}_{\odot} - \bar{r}_{\Delta}|} \quad (9)$$

measured from
rocket

then

$$[g_{\text{orth}}]_{\odot} = |\bar{G}_{\odot} \text{at } (\bar{r}_{\odot} - \bar{r}_{\Delta})| \frac{[Z_{\odot}]_{\Delta\text{plane}}}{|\bar{r}_{\odot} - \bar{r}_{\Delta}|} \quad (10)$$

and

$$[\delta Z_{\Delta}]_{\Delta\text{plane}} \text{ (due to Mars)}$$

$$= \frac{[g_{\text{orth}}]_{\odot}}{2} (\delta t)^2$$

$$= [g_{\text{orth}}]_{\odot} (\delta t)^2 \times 7.15 \times 10^5 \quad (11)$$

if δt is in sidereal days

g_{orth} is in ft/sec^2

δZ_{Δ} is in miles

DERIVATION SUMMARY 4.1

(Page 3 of 4)

A similar derivation may be made for the cis-lunar Barycenter.

(d) Derivation

DERIVATION SUMMARY 4.1
(Page 4 of 4)

traveled by the rocket is approximately 354,000,000 miles; the cumulative displacement from the Δ plane is approximately 5,500 miles: a ratio of about 1.55 to 100,000, certainly negligible. Further, the calculations show that the displacement due to the mass attraction of Mars is only 33 miles, the remainder being the effect of the Earth-Moon mass attraction. About 3,250 miles displacement occurs in the first five days of travel; hence, if a computer program were established to counteract this, the displacement could be reduced even further.

The obvious advantages of reducing the problem to two dimensions are many-fold. These include (a) reduction in weight and complexity of the guidance mechanism; (b) simplification of component construction; (c) savings in fuel; (d) improvement of payload ratio; (e) saving in material, labor, and cost; (f) contraction of production time-tables; and many others.

CHAPTER 5

DEPARTURE AND ARRIVAL ORBITS

5.1 Introduction

The capability of a rocket to achieve required velocities depends so critically upon the energy carried within itself that every effort must be made to minimize these energy requirements. This section investigates one aspect of this minimization -- the selection of departure and arrival orbits about the respective planets to minimize kinetic energy, hence velocity, that the rocket must provide itself in order to fly a given trajectory.

Fig. 5.1 illustrates the relationships of pertinent velocities. For complete definitions see Definition Summary 1 .

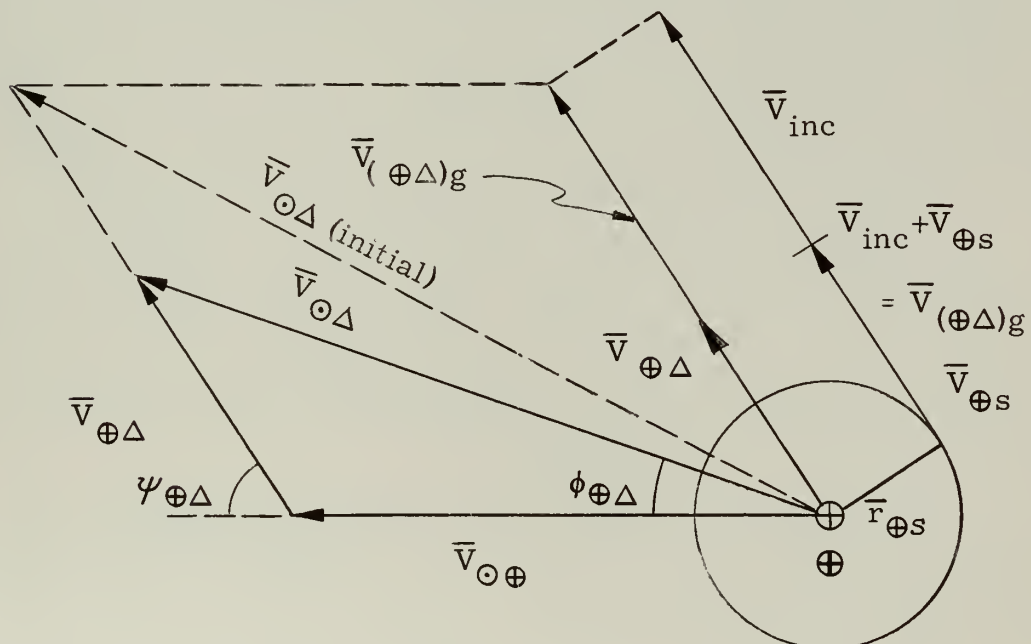


Fig. 5.1 Pertinent Velocity Relations

5.2 Optimum Orbit Radii

In order to fly any given trajectory, or ellipse, a velocity of the rocket with respect to the Sun ($\bar{V}_{\odot\Delta}$) must somehow be attained. Referring to Section 4.9, we note that this is the velocity vector required for an intercept of the orbit of Mars, treating both Earth and Mars initially as massless points. However, this is obviously not the case. Referring to Fig. 5.2 we can say, figuratively, that we must climb up the side of the Earth potential "well", over the intervening "hump", then down into Mars potential "well". Jupiter's potential "well" is shown for comparison. From Fig. 5.1 we note that the rocket already possesses a certain velocity with respect to the Sun by virtue of the Earth's orbital motion, thus the rocket must be provided the velocity, $\bar{V}_{\oplus\Delta}$. In order to "overcome" the effect of the earth gravity field, the rocket must be provided a greater velocity, $\bar{V}_{(\oplus\Delta)g}$. The rocket also possesses a velocity, $\bar{V}_{\oplus s}$, by virtue of being in orbit about the earth, therefore it remains for the rocket to provide by its own efforts an increment of velocity V_{inc} . Initially $\bar{V}_{\odot\Delta}$ will be along the dotted line labeled in Fig. 5.1, however, the earth gravity effect decreases rapidly so that $\bar{V}_{\odot\Delta}$ lies almost identically on the solid line. In addition the ratio $|\bar{r}_{\oplus s}/\bar{R}_{\odot\oplus}|$ is of the order 10^{-4} , hence the displacement of the rocket from the earth $\bar{r}_{\oplus s}$ is negligible for purposes of calculating initial velocity requirements.

Regardless of validity, if $\bar{V}_{\odot\Delta}$ is known we may obtain relations between \bar{V}_{inc} and $\bar{r}_{\oplus s}$. This has been done in Derivation Summary 5.1. Although the relations have been developed for the planet Earth the derivation is perfectly general and applies to any body; with different constants.

Parts (b) and (c) of Derivation Summary 5.1 develop and prove the optimal relationship of V_{inc} and $\bar{r}_{\oplus s}$. Part (d) expresses the relation non-dimensionally.

Pertinent ranges of \bar{V}_{inc} vs $\bar{r}_{\oplus s}$ have been plotted in Fig. 5.3 and the non-dimensional function is shown over an applicable range in Fig. 5.4.

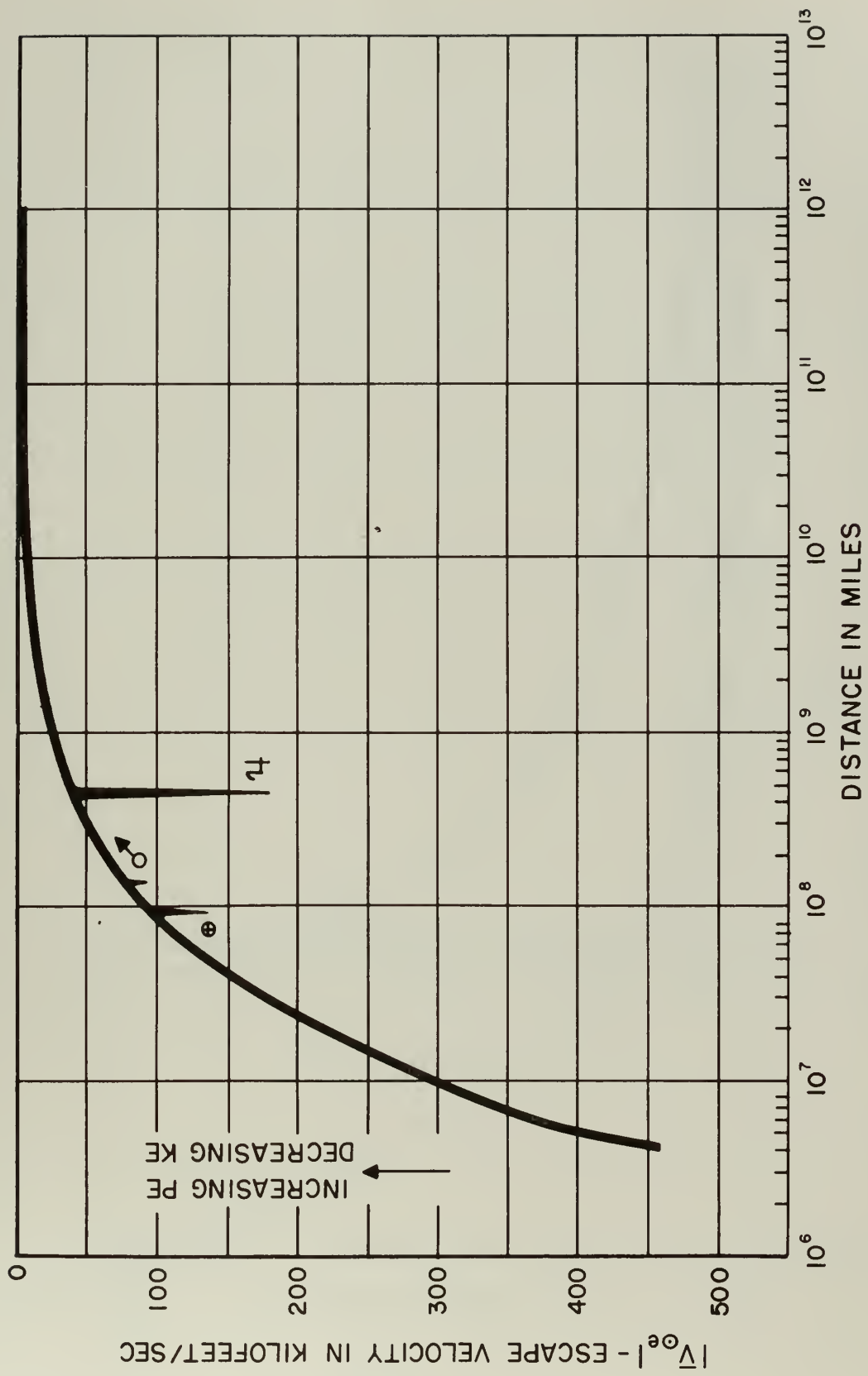


Fig. 5.2 Velocity of "escape" from the Sun and some planets as a function of distance

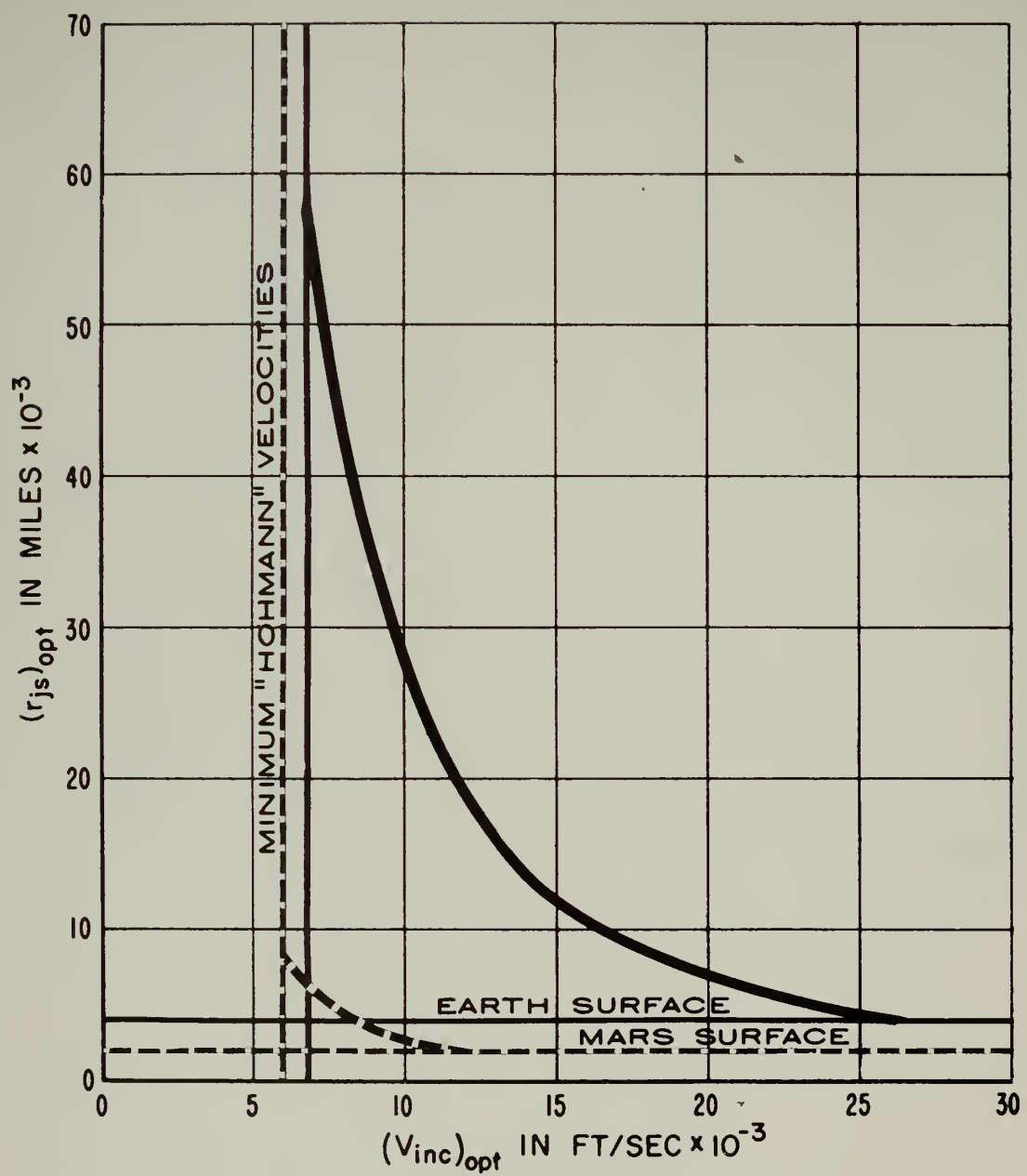


Fig. 5.3 Optimal relationships between V_{inc} and r_{js} for Earth and Mars

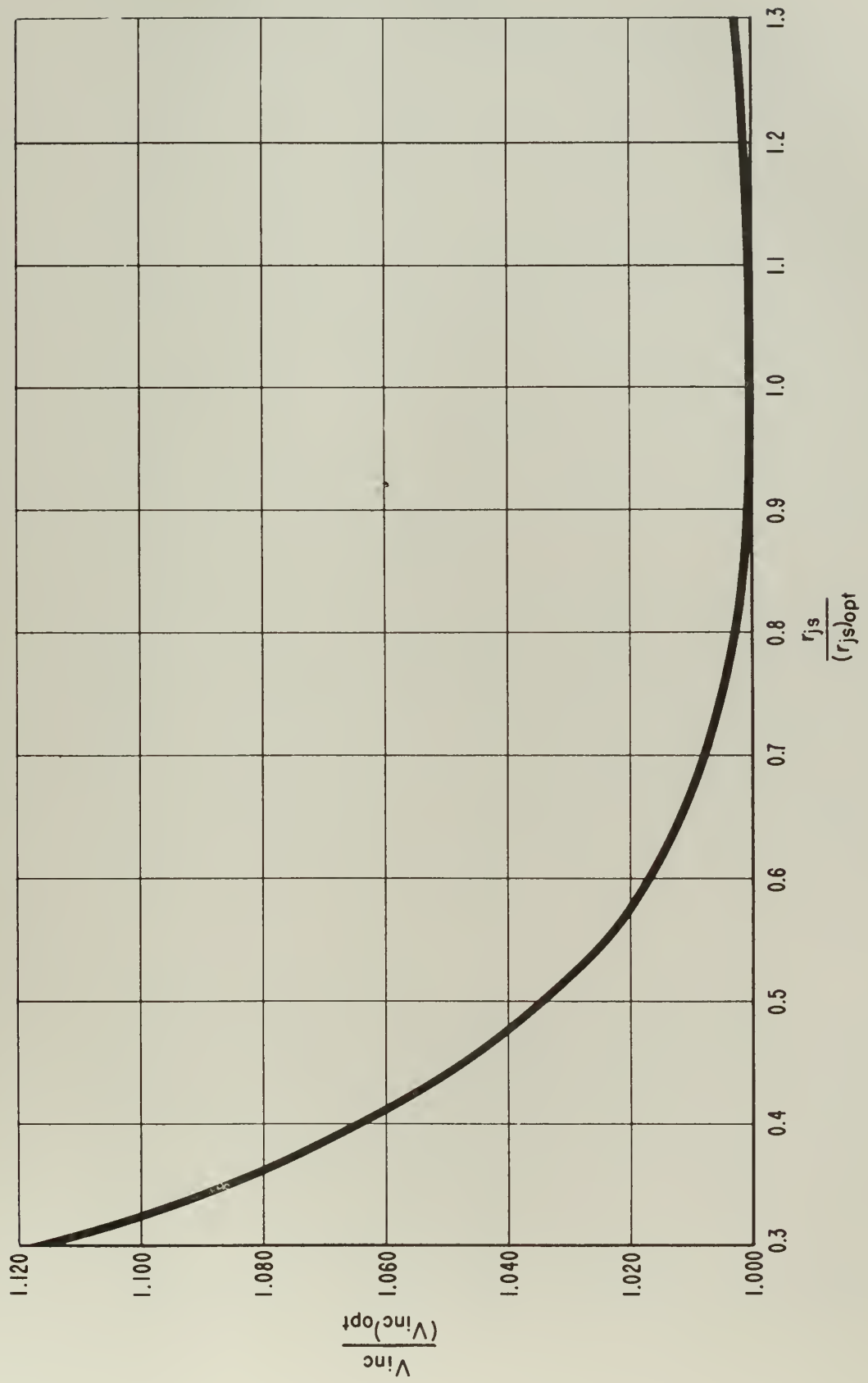


Fig. 5.4 Non-dimensional relationships for $\frac{V_{inc}}{V_{inc\,opt}}$ and $\frac{r_{js}}{(r_{js})_{opt}}$

is the frequency of occurrence of the rather special Earth-Mars configurations required by the Hohmann ellipse. This, among other considerations has been taken up in preceding sections.

5.3 Use of Optimum Orbit Concept

Almost paradoxically, the optimum orbit concept is of particular use in the selection of non-optimum orbits or trajectories. As an example, assume that a rocket has been developed with a capacity to provide itself with a V_{inc} of approximately 10,000 ft/sec. The optimal orbit radius corresponding to 10,000 ft/sec, as an optimal velocity, from graph 5.3 is approximately 27,500 miles above Earth center. If 27,500 miles is unacceptable due to other considerations we can reduce (from graph 5.4) this radius by 42.5% simply by allowing a 2% increase in the required velocity. In other words, for $V_{inc} = 10,200$ ft/sec $r_{\oplus s} = 15,800$ miles, or approximately 12,000 miles above the Earth's surface. It must be borne in mind, however, that these relations exist only for that trajectory for which $(V_{inc})_{opt} = 10,000$ ft/sec.

Applying the foregoing reasoning to the "Hohmann" type ellipse $-(V_{inc})_{opt} = 6,818$ ft/sec; $(r_{\oplus s})_{opt} = 57,300$ miles - we may reduce $r_{\oplus s}$ to 33,000 miles by increasing V_{inc} to 6,936 ft/sec. Hence, if we can provide the energy to increase $(V_{inc})_{opt}$ by 118 ft/sec we not only gain the obvious advantages of a lesser $r_{\oplus s}$ but also the flexibility inherent in a greater freedom of choice in the angular positions of Earth and Mars. This has been discussed more fully in Chapter 4.

5.4 The Least Orbit Concept

If the problem is posed that $V_{inc} = 7,500$ ft/sec., what is the least orbit the rocket may depart from and still travel a trajectory to arrive at Mars? This obviously is not an optimum orbit problem as previously posed. For $(V_{inc})_{opt} = 7,500$ ft/sec $(r_{\oplus s})_{opt} = 47,000$ miles (graph 5.3). For $(V_{inc})_{opt} = 6,818$ ft/sec (the minimum "Hohmann" ellipse velocity) the ratio $V_{inc}/(V_{inc})_{opt} = 1.1$ and from graph 5.4 the ratio $r_{\oplus s}/(r_{\oplus s})_{opt} = 0.327$ and $r_{\oplus s} = 18,750$ miles. The limiting restriction herein

DEPARTURE AND ARRIVAL ORBITS

Optimum Planetary Orbits

In order to "escape" any bodies mass attraction a vehicle must attain kenetic energy at least equal to the potential energy inherent in the field or fields to be "overcome"; hence

$$KE = m_{\Delta} \int \left| \bar{G}_{j\Delta} \right| dR \quad (1A)$$

or

$$\frac{KE}{m_{\Delta}} = \int_R^{\infty} \frac{GM_j}{R^2} dR \quad (1B)$$

Following the convention $Q = \left| \bar{Q} \right|$ we integrate

and
$$\frac{KE}{m_{\Delta}} = \frac{GM_j}{R_{j\Delta}} \quad (2)$$

but
$$\frac{KE}{m_{\Delta}} = 1/2 V_{je}^2 \quad (3)$$

hence
$$V_{je} = \sqrt{\frac{2GM_j}{R_{j\Delta}}} \quad (4)$$

It has been shown⁶³ that a rocket in circular orbit about a body possesses a so-called circular velocity.

$$V_{js} = \sqrt{\frac{GM_j}{R_j \Delta}} \quad (5)$$

hence

$$V_{je} = \sqrt{2} V_{js} \quad (6)$$

From Fig. in the case of the earth and a rocket

$$V_{(\oplus\Delta)g} = V_{inc} + V_{\oplus s} \quad (7)$$

Further, by equating the kinetic energy requirements for the rocket we have,

$$\frac{1}{2} m_{\Delta} \frac{V_{\Delta}}{\Delta}^2 + \frac{1}{2} m_{\Delta} \frac{V_e}{\Delta}^2 = \frac{1}{2} m_{\Delta} \frac{V_{(\oplus\Delta)g}}{\Delta}^2 \quad (8)$$

where the first term represents the kinetic energy requirement to achieve the velocity $V_{\oplus\Delta}$; the second term represents the kinetic energy requirement to "escape" the earth gravity field; and the third term describes the sum of the first and second.

From (8) we have

$$V_{(\oplus\Delta)g} = \sqrt{V_{\oplus\Delta}^2 + V_{\oplus s}^2} \quad (9)$$

Hence, substituting in (7) and rearranging

$$V_{inc} = \sqrt{V_{\oplus\Delta}^2 + 2V_{\oplus s}^2} - V_{\oplus s} \quad (10)$$

and if initially $R_{\Delta} = r_s$ then

$$V_{inc} = \sqrt{V_{\oplus\Delta}^2 + \frac{2GM_{\oplus}}{r_{\oplus s}}} - \sqrt{\frac{GM_{\oplus}}{r_{\oplus s}}} \quad (11)$$

(a) Development of V_{inc} in terms of rocket orbital radius

DERIVATION SUMMARY 5.1

(Page 2 of 5)

In order that $r_{\oplus s}$ be the optimum radius on a kinetic energy basis V_{inc} must be a minimum for $r_{\oplus s} = (r_{\oplus s})_{opt}$ which is the equivalent of the conditions

$$(1) \frac{\delta V_{inc}}{\delta r_{\oplus s}} = 0 \quad (12)$$

$$(2) \frac{\delta^2 V_{inc}}{\delta r_{\oplus s}^2} > 0 \quad (13)$$

To satisfy (1) we take the first partial derivative of (11) and equate to zero.

$$\frac{\delta V_{inc}}{\delta r_{\oplus s}} = \frac{\frac{GM_{\oplus}}{r_{\oplus s}^2}}{\sqrt{V_{\oplus \Delta}^2 + \frac{2GM_{\oplus}}{r_{\oplus s}}}} + 1/2 \quad \frac{\frac{GM_{\oplus}}{r_{\oplus s}^2}}{\sqrt{\frac{GM_{\oplus}}{r_{\oplus s}}}} = 0 \quad (14)$$

Solving for $r_{\oplus s} = (r_{\oplus s})_{opt}$

$$\sqrt{\frac{2GM}{(r_{\oplus s})_{opt}} + V_{\oplus \Delta}^2} - \sqrt{\frac{GM_{\oplus}}{(r_{\oplus s})_{opt}}} = 0 \quad (15)$$

$$(r_{\oplus s})_{opt} = \frac{2GM_{\oplus}}{V_{\oplus \Delta}^2} \quad (16)$$

and as corollaries

$$V_{\oplus \Delta} = \sqrt{2} (V_{\oplus s})_{opt} \quad (17A) \quad (V_{inc})_{opt} = \sqrt{\frac{GM_{\oplus}}{r_{\oplus s}}} \quad (17B)$$

(b) Derivation of $(r_{\oplus s})_{opt}$

DERIVATION SUMMARY 5.1

(Page 3 of 5)

To satisfy condition (2) above we take the second partial derivative of V_{inc} with respect to $r_{\oplus s}$ and evaluate at $r_{\oplus s} = (r_{\oplus s})_{\text{opt}}$ to show it is indeed positive.

$$\frac{\delta^2 V_{\text{inc}}}{\delta r_{\oplus s}^2} = -\frac{1}{2} \frac{GM_{\oplus}}{r_{\oplus s}^2} \left[\frac{-\left(-2 \frac{GM_{\oplus}}{r_{\oplus s}^2}\right)}{\left(\frac{2GM_{\oplus}}{r_{\oplus s}} + V_{\oplus}^2 \Delta\right)^{3/2}} - \frac{\left(-\frac{GM_{\oplus}}{r_{\oplus s}^2}\right)}{\left(\frac{GM_{\oplus}}{r_{\oplus s}}\right)^{3/2}} \right]$$

(18)

$$+ \left[-\frac{1}{2} \left(-\frac{2GM_{\oplus}}{r_{\oplus s}^3} \right) \left[\frac{2}{\sqrt{\frac{2GM_{\oplus}}{r_{\oplus s}} + V_{\oplus}^2 \Delta}} - \frac{1}{\sqrt{\frac{GM_{\oplus}}{r_{\oplus s}}}} \right] \right]$$

Combining

$$\frac{\delta^2 V_{\text{inc}}}{\delta r_{\oplus s}^2} = -\frac{\left(\frac{GM_{\oplus}}{r_{\oplus s}^2}\right)^2}{\left(\frac{2GM_{\oplus}}{r_{\oplus s}} + V_{\oplus}^2 \Delta\right)^{3/2}} + \frac{\frac{1}{2} \left(\frac{GM_{\oplus}}{r_{\oplus s}^2}\right)^2}{\left(\frac{GM_{\oplus}}{r_{\oplus s}}\right)^{3/2}}$$

(19)

$$+ \frac{\frac{2GM_{\oplus}}{r_{\oplus s}^3}}{\sqrt{\frac{2GM_{\oplus}}{r_{\oplus s}} + V_{\oplus}^2 \Delta}} - \frac{\frac{GM_{\oplus}}{r_{\oplus s}^3}}{\sqrt{\frac{GM_{\oplus}}{r_{\oplus s}}}}$$

Evaluating (19) for $r_{\oplus s} = \frac{2GM_{\oplus}}{V_{\oplus}^2 \Delta}$ or $V_{\oplus}^2 \Delta = \frac{2GM_{\oplus}}{r_{\oplus s}}$

DERIVATION SUMMARY 5.1

(Page 4 of 5)

$$\frac{\delta^2 V_{\text{inc}}}{\delta r_{\oplus s}^2} = -\frac{\frac{1}{4} V_{\oplus \Delta}^4}{2\sqrt{2} r_{\oplus s}^2 V_{\oplus \Delta}^3} + \frac{\frac{1}{8} V_{\oplus \Delta}^4}{\frac{1}{2\sqrt{2}} r_{\oplus s}^2 V_{\oplus \Delta}^3} \quad (20)$$

$$+ \frac{V_{\oplus \Delta}^2}{\sqrt{2} r_{\oplus s}^2 V_{\oplus \Delta}} - \frac{\frac{1}{2} V_{\oplus \Delta}^2}{\frac{1}{\sqrt{2}} r_{\oplus s}^2 V_{\oplus \Delta}}$$

$$= \frac{V_{\oplus \Delta}}{r_{\oplus s}^2} \left(\frac{1}{2\sqrt{2}} - \frac{1}{8\sqrt{2}} \right) \quad (21)$$

$$= \frac{3 V_{\oplus \Delta}}{8\sqrt{2} r_{\oplus s}^2} \quad (22)$$

which is positive for positive values of the radical

(c) Proof of Minimality of $(r_{\oplus s})_{\text{opt}}$

Dividing (11) by (17B) and noting (17A) we have

$$\frac{V_{\text{inc}}}{(V_{\text{inc}})_{\text{opt}}} = \sqrt{\frac{2}{\frac{r_{\oplus s}}{(r_{\oplus s})_{\text{opt}}}} + 2} - \sqrt{\frac{1}{\frac{r_{\oplus s}}{(r_{\oplus s})_{\text{opt}}}}} \quad (23)$$

(d) Non-dimensional Relations

DERIVATION SUMMARY 5.1

(Page 5 of 5)

CHAPTER 6

THRUST AND ENERGY CONSIDERATIONS

A. THRUST REQUIREMENTS

6.1 Introduction

It is of interest to examine the thrust requirements and payload ratios for a rocket departing circular orbit about earth. Such figures appear to be more or less well known for the journey from earth's surface into orbit (as for earth satellites). However, the orbit-to-orbit requirements are not commonly available, although easily calculable. This information is consistent with the optimal orbit concept developed previously and verifies the validity of such an approach for the conditions assumed.

Although the data have been based upon the departure and arrival orbit concept, an extension to surface departure can easily be made by extrapolation to lower altitudes. The penalty of departing a lower altitude will be evident after an investigation of this section

6.2 The Optimal Payload Ratio

The change in velocity necessary to affect transfer from orbital motion about earth to departure path has been designated, V_{inc} . This change in velocity is accomplished by applying thrust for a controlled period of time. If the power-on period is sufficiently brief, the maneuver trajectory can be neglected and the transition from circular orbit to departure path thought to occur instantaneously at tangency. The justification of this assumption will be discussed shortly after the development of the equations.

The commonly used expressions for an idealized single

step thrust study of this nature are derived from the equations of motion written along the orbit flight path.⁶³

$$m \frac{dv}{dt} = \bar{T} - \bar{D} - Mg \sin \theta$$

In circular orbit, however, for the above assumptions, \bar{D} is presumed negligible and $\theta = 0$.

$$m \frac{dv}{dt} = \bar{T} = M_o - \frac{M_p t}{t_b} \frac{dv}{dt} \text{ for } 0 \leq t \leq t_b$$

where M_o = initial gross mass

M_p = mass of propellant

t_b = time of burning

A constant thrust device is assumed of specific impulse, I.

$$T = \frac{M_p}{t_b} Ig$$

$$\frac{dv}{dt} = \frac{\frac{M_p}{t_b} Ig}{\frac{M_o - M_p}{t_b} t} = \frac{\delta \frac{Ig}{t_b}}{1 - \delta t} \text{ where } \delta = \frac{M_p}{M_o}$$

Integrating between $t = 0$ and $t = t_b$

$$V_{t_b} - V_o = V_{inc} = - Ig \ln (1 - \delta) = - Ig \ln (PR)$$

$$PR = \text{Payload Ratio} = \frac{M_o - M_p}{M_o}$$

It is to be remembered that this, V_{inc} , applies only to the departure maneuver, as does PR . For entry into circular orbit about Mars, a similar expression is obtained. The total payload ratio(PR_t) for an orbit-to-orbit maneuver, ignoring corrective thrust requirements, is

$$PR_t = PR_{\oplus} PR_{\sigma}$$

These equations have been expressed in tabular and graphical form for various values of specific impulse, which has been chosen as the propellant parameter. The subscripts in the headings of Table 6.1 refer to the three assumed values of specific impulse. Table 6.1 for example, lists Payload ratios for various sample trajectories developed by the methods of chapter 4. The importance of improved propellant performance is noted. Although the corrective thrust requirements have not been included, reference 47

$\theta_o - \theta_s$	t_f	$V_{inc\oplus}$	$PR_{\oplus 250}$	$PR_{\oplus 300}$	$PR_{\oplus 350}$
55.8°	201	7391	.022	.042	.063
58.2°*	259.6	6818	.065	.101	.139
21.7°	145.8	23,696	.004	.011	.021
16.2	125.5	24,529	.002	.005	.011
20.1	181.0	19,045	.009	.021	.037
27.0	134.5	16,763	.003	.008	.017
7.0	241.5	15,181	.018	.036	.057
33.2	153.1	13,055	.008	.017	.030
39.3	204.1	11,932	.031	.054	.082
43.0	228.2	9358	.045	.075	.108
48.1	185.4	8151	.019	.037	.060
45.3	255.4	7290	.060	.095	.134
38.7*	171.5	10,146	.005	.011	.021

TABLE 6.1
SOME REPRESENTATIVE TRAJECTORIES WITH CORRESPONDING
PAYLOAD REQUIREMENTS

has indicated that a suitable payload ratio for corrective thrust requirements is .79. If the above figures are altered by this multiplier, it is seen that the most optimistic Payload Ratio to be hoped for is .11. The calculations of Table 6.1 presume departure and arrival orbits at "optimal" altitude as defined earlier. Since these altitudes inevitably vary for various trajectories, little correlation is to be expected between Payload Ratio (PR_T) and angular separation at instant of fire ($\theta_o - \theta_s$) other than to indicate a lower bound for certain specified parameters.

6.3 An Interpretation of "Optimum" Altitude

At first glance, it appears that the higher the optimal departure and arrival orbit altitudes, the more favorable the total Payload Ratio. To invalidate this idea as well as to demonstrate the advisability of employing optimal altitude two trajectories have been selected for study: one is the familiar Hohmann semi-ellipse trajectory: the other merely a representative one selected for contrast. Both are defined by the * in Table I.

If the PR_{\oplus} and PR_{\ominus} for these two trajectories are calculated as functions of altitude (including optimal altitude) on a non-dimensional basis, as in Fig.6.1 and 6.2 it can be seen that a peak payload ratio is achieved at precisely $(r_s)_{OPT}$. A slight fall-off occurs at values of $(r_s) > 1$. Thus, the choice of optimum altitudes, in the sense defined, insures a maximum total payload ratio for any given specification of $V_{inc\oplus}$ and $V_{inc\ominus}$. The great saving in Payload Ratio is noted when one departs from circular orbit altitude for $\frac{r_s}{(r_s)_{OPT}} \geq .5$.

6.4 The Assumption of Impulsive Thrust

A justification of the assumption of impulsive thrust is dependent upon a comparison of burning time and period of orbit. Obviously, for a low thrust device of considerable duration, the

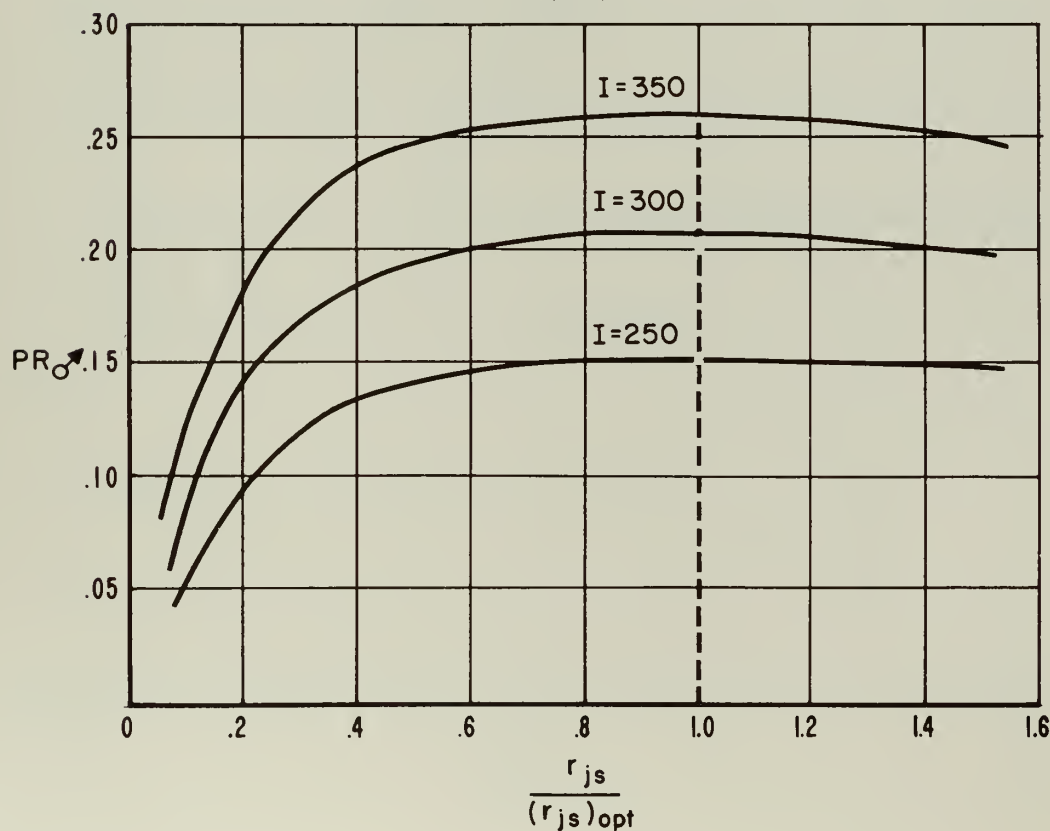
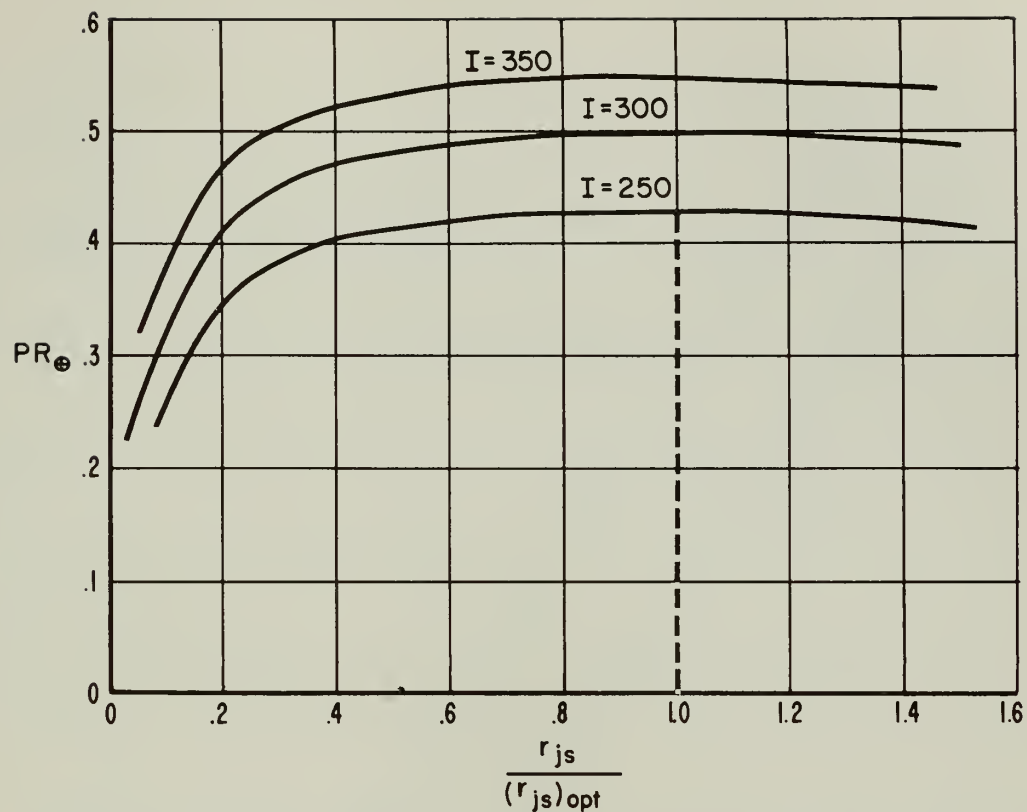


Fig. 6.1 Payload ratios VS. orbit altitude for the Hohmann ellipse

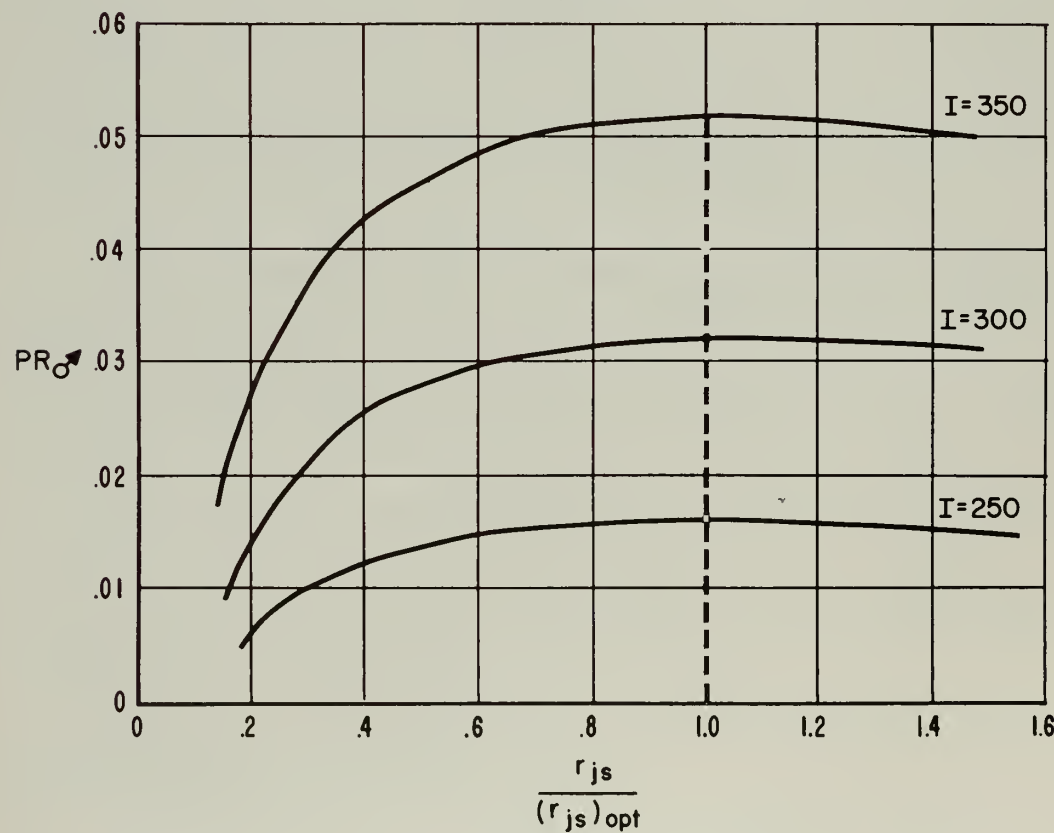
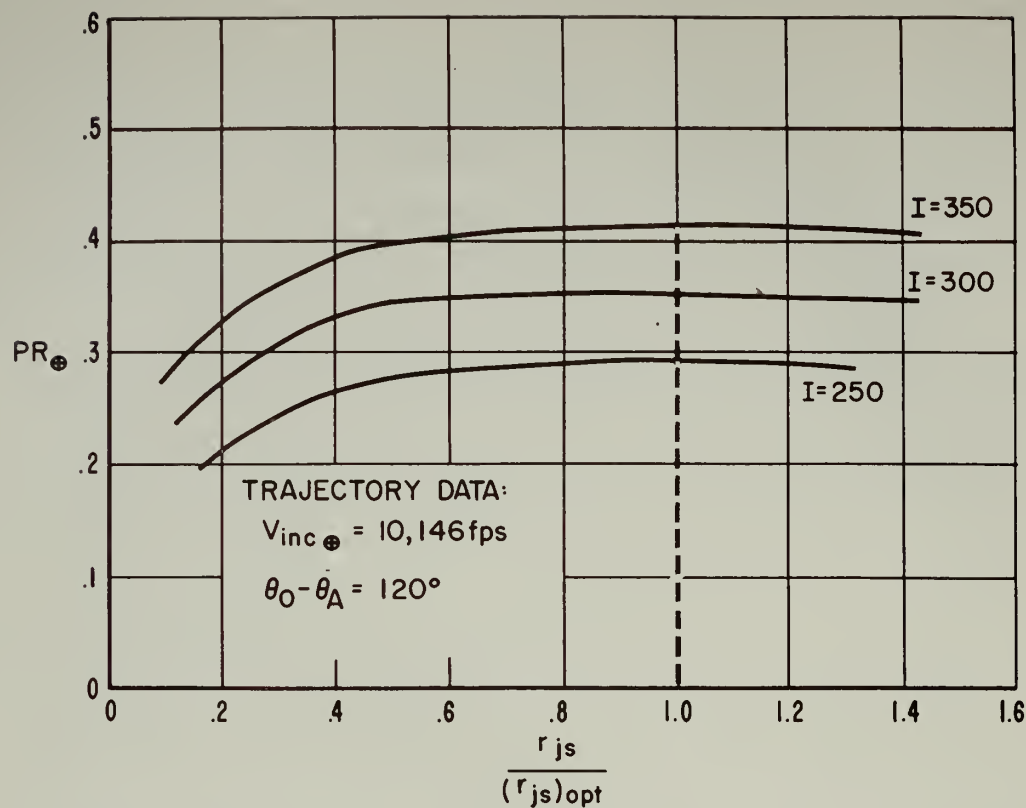


Fig. 6.2 Payload ratios vs. orbit altitude for a representative trajectory

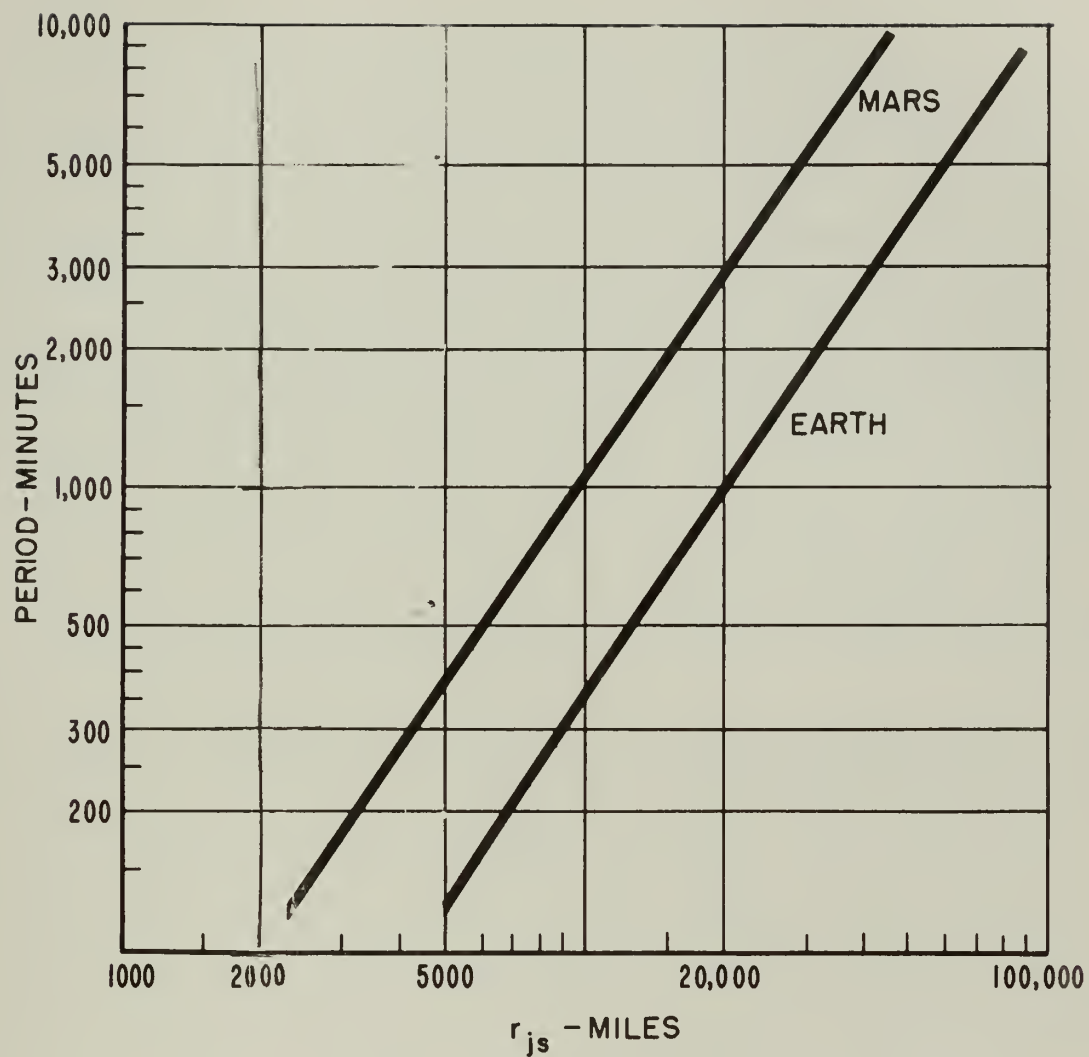


Fig. 6.3 Orbit period as a function of altitude above planet center

assumption is not valid.

The period of orbit for both Mars and Earth is plotted in Fig. 6.3 as a function of distance from Earth and Mars center. If we assume that instrumentation is capable of withstanding an axial load of 10g upon departure from Earth orbit the minimum acceptable burning time can be determined.⁶³ Careful design can then be employed to produce a favorable burning time. The minimum burning times as functions of orbital period for optimum Earth and Mars orbit are listed in Table 6.2 for the trajectories previously considered: A specific impulse of 350 seconds is assumed.

$r_{s\oplus}$	T_{\oplus} (min)	t_b sec.	$r_{s\odot}$	T_{\odot}	t_b
48,772	3550	33	3353	210	254
57,295*	4650	29	7792	735	102
4,744	115	252	4571	330	171
4,424		275	2585	142	334
7,344	220	154	5471	430	142
9,481	320	120	2127	108	438
11,558	400	100	6315	530	123
15,630	680	76	2607	145	334
18,709	880	66	6918	620	113
30,416	1900	45	7404	680	108
40,099	2750	37	7689	700	247
51,782	4000	32	3261	200	102
25,277*	1420	51	1631	71	640

TABLE 6.2

A COMPARISON OF ORBITAL PERIOD AND BURNING TIME

B. ENERGY CONSIDERATIONS

6.5 Introduction

It would seem appropriate at this stage to mention optimization of the trajectory. The term, optimization, however, invariably leads to ambiguity and requires explanation. Do we desire optimization with regard to time, fuel expenditure, or initial velocity? -- or possibly cost? Previously, an attempt was made to minimize the initial velocity requirements, but it is clear that this does not necessarily represent the optimum as far as other variables are concerned.

An overriding consideration during early interplanetary flights will undoubtedly be minimization of fuel expenditure. By minimization of fuel expenditure, we imply a determination of not only the minimum duration of powered flight but also the direction in which this power or thrust is applied. Accordingly, these are all considerations in the minimization problem. It is the intent of this section to describe the problem in general terms and summarize, without proof, the findings of other authors who have written at length on this particular subject. ^{34, 35, 36, 37}

6.6 General Theory

Let us first consider the problem of optimum transfer (with respect to fuel expenditure) between two terminals lying in a plane. If we consider an inertial orthogonal coordinate system, the equations of motion for the rocket are

$$\ddot{X} + G_x = -\cos \alpha \frac{c}{M} \frac{dM}{dt} \quad (6-1)$$

$$\ddot{Y} + G_y = -\cos \beta \frac{c}{M} \frac{dM}{dt} \quad (6-2)$$

$$\ddot{Z} + G_z = -\cos \gamma \frac{c}{M} \frac{dM}{dt} \quad (6-3)$$

where G_x , G_y , and G_z are the components of the resultant attractive force per unit mass and α , β and γ are the angles between rocket thrust direction and coordinate axes. The expression $\frac{c}{M} \frac{dM}{dt}$ is the well known simplified term for rocket thrust and is defined in the section describing thrust considerations. c is the effective exhaust velocity and M is the mass of the rocket at any time t .

G_x , G_y , G_z depend explicitly on x , y , z , and t only.
Squaring and adding 6-1, 6-2, and 6-3.

$$[\ddot{X} + G_x]^2 + [\ddot{Y} + G_y]^2 + [\ddot{Z} + G_z]^2 = \left[\frac{c}{M} \frac{dM}{dt} \right]^2 [\cos^2 \alpha + \cos^2 \beta + \cos^2 \gamma] \quad (6-4)$$

Integrating,

$$c \log_e \frac{M_0}{M_1} = \int_{t_0}^{t_1} \left[[\ddot{X} + G_x]^2 + [\ddot{Y} + G_y]^2 + [\ddot{Z} + G_z]^2 \right]^{1/2} dt$$

It is assumed that the boundary or terminal conditions are specified

$$\begin{array}{llll} X_0(t_0) = X_0 & \dot{X}(t_0) = \dot{X}_0 & X_1(t_1) = X_1 & \dot{X}_1(t_1) = \dot{X}_1 \\ Y_0(t_0) = Y_0 & \dot{Y}(t_0) = \dot{Y}_0 & Y_1(t_1) = Y_1 & \dot{Y}_1(t_1) = \dot{Y}_1 \\ Z_0(t_0) = Z_0 & \dot{Z}(t_0) = \dot{Z}_0 & Z_1(t_1) = Z_1 & \dot{Z}_1(t_1) = \dot{Z}_1 \end{array}$$

The objective is to select the functions $x(t)$, $y(t)$, and $z(t)$ so that the fuel ratio $\frac{M_0}{M_1}$ is a minimum (i.e., we desire initial fuel mass, M_0 as small as possible and still attain our objective subject to the boundary conditions).

The minimization of the above integral is a problem in the calculus of variations. Its solution is highly detailed and is not presented here. The conclusions and interpretations of existing

solutions are helpful and interesting, however, and are stated here without proof.³⁷

These conclusions are due to D. F. Lawden, one of the more active writers in the field.

Let us consider a rocket orbiting the earth circularly. The optimal path is desired for travel from this orbit to entry into circular orbit about another planet. The conclusions of Lawden indicate that an optimal path can only be followed in a vacuum by the application of certain impulsive thrusts from the rocket motor, the rocket coasting freely under gravity during the intervals between such thrusts. These coast periods are essentially null-thrust arcs and are minimal in the sense that neighboring arcs can be followed only by an actual expenditure of fuel. To establish an absolute minimal mode of transfer for a definite planet configuration, cases for various numbers of impulses must be computed³⁵ and the minimum selected. Lawden suggests that two impulses usually lead to the optimal solution. It should be remembered, however, that there will be a large number of optimal solutions corresponding to different planet positions. Only one of these will be an absolute optimal solution for all planet configurations. The absolute optimal solution for an Earth-Mars flight has been known theoretically for some time if certain fundamental assumptions are made. The analysis²² is that of Hohmann, who concluded in 1925 that the problem of transferring a rocket from one circular orbit into another coplanar with the first and about the same attracting body would be most economical if effected along an elliptical trajectory tangential at its apses to both circular orbits. Fuel would be expended rapidly at each apse to carry the rocket into and out of the transfer ellipse. A state of free flight would exist between the two impulse trajectory. This classic development, the so-called Hohmann ellipse, has been verified by Lawden and is consistent with the remarks above. Note that the optimum path as developed and computed in this paper on

the basis of a minimum initial velocity is in fact the Hohmann ellipse. The importance, however, of knowing the optimum for other positions of Mars and Earth so that flight can be initiated often, is not to be underestimated.

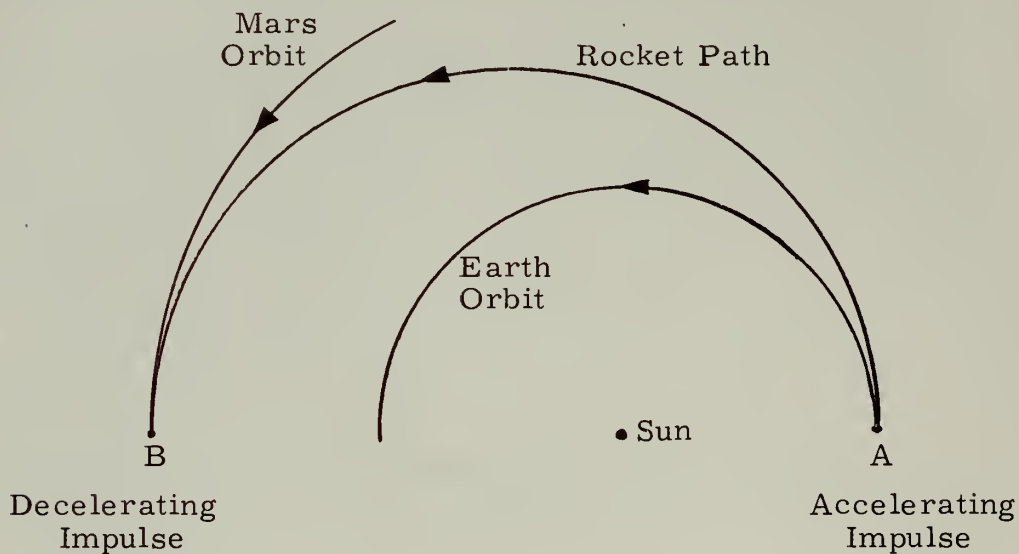


Fig. 6.4 The Theoretical Mode of Transfer

6.7 Rocket Thrust Direction

Ordinarily, the mode of directing the thrust which results in maximum total energy is found to be alignment of the effective exhaust velocity with the velocity vector of the rocket (i.e. align the direction of thrust with the tangent to the trajectory. This will ensure that the rate of increase of total energy is maintained at its maximum value at every instant. This program will be an economical one since the object of the maneuver is to raise the total energy as rapidly as possible in order to achieve escape and sufficient velocity. However, it has been proved³⁴ that this program may not be an absolute optimal method, although close to it. Under some circumstances, when departing a circular orbit, it is not economical to maintain the rate of increase of energy as

its highest value over the entire trajectory of escape. The author claims that after having escaped, it is advantageous first to direct the thrust so as to oppose the motion. The rocket then drifts toward the center of attraction along an elliptical arc. At its closest point of approach, an impulsive thrust is generated in the direction of motion. The velocity is now large, and the total energy increases at a rapid rate. The rocket is transferred into a hyperbolic orbit along which it coasts to its destination and the overall fuel consumption is found to be less than if escape had been achieved by application of a single tangential thrust. The reader is referred to reference³⁸ for information as to how advantage can be taken of such maneuvers for general conservation of energy. A good approximation to the optimal programming of thrust direction under departure from circular orbit may be achieved by maintaining alignment between directions of thrust and motion.

Other writers⁵¹ consider it an empirical rule that a journey from one to another stable orbit round a central body will be completed in the shortest time only if power is applied in two impulses, one at beginning and one at end of journey.

CHAPTER 7

NAVIGATION IN SPACE

A. POSITION IN SPACE

7.1 General Discussion of Problem

Mid-course interplanetary navigation differs quite markedly from terrestrial position determination due primarily to the need to obtain a fix within a volume instead of upon the surface of a sphere (Earth) of known radius. Terrestrial positions can be obtained by simple spherical trigonometric relations and can be further simplified to a problem in plane geometry and time.⁹

Although it is obvious that the problem of Position in Space is three dimensional, several writers have postulated that a sufficiently accurate solution can be obtained by considering the planets to be coplanar and working with only two dimensions in the plane of the ecliptic.^{3, 68} Part of the argument for this approach is found in star tracker limitations, errors in astronomical measurements, the assumption that terminal guidance will correct for errors incurred during mid-course transit, and the relatively small angles of inclinations of the planet orbits from the ecliptic plane.

7.2 Factors Indicating Necessity for "On Board" Automatic Solution

If we postulate that accurate positional data is needed during mid-course transit, several factors indicated that the problem must be solved on board the vehicle and by automatic computers of some sort.

1. Due to high vehicle velocities (in the neighborhood of 1,200 miles per min) time delays of any sort should be avoided wherever possible. This eliminates manual computation and sight taking in the vehicle itself or on the earth.

2. Radio frequency transmission in space has a rather sizeable time delay. (A 10^8 mile round trip signal requires approximately 18 minutes)
3. Radio frequency signal interference in space is uncertain and apparently unpredictable when sent to or from Earth due to the Earth's atmosphere and extraneous radio frequency waves in space itself.¹
4. Power requirements for dependable radio transmissions during mid-course appear to be far too great for installation on any vehicle within the near future.
5. Optical tracking of the vehicle from earth is not possible with any foreseeable astro telescopic equipment.⁶⁹
6. Radar tracking of the vehicle from earth is ruled out by 2 and 3.

7.3 Selection of a Reference Coordinate System

Celestial bodies may be located with respect to several different reference systems which are shown in Fig. 7.1 and Table 7.1 . For mid-course interplanetary position determination two of these systems can be discarded immediately. These are the Geocentric Horizon and Equatorial. Coordinate systems using Galactic quantities are not particularly convenient for travel limited to our solar system. Of the remaining only the heliocentric ecliptic system will be considered for use in this paper. This system has the following features which lead to this choice.

1. The reference zero latitude plane includes the Earth and Sun at all times.
2. All other planet's orbits lie close to this plane.
3. Numerous Ephemerides are available based in this system simplifying programming of any memory drum for a computer

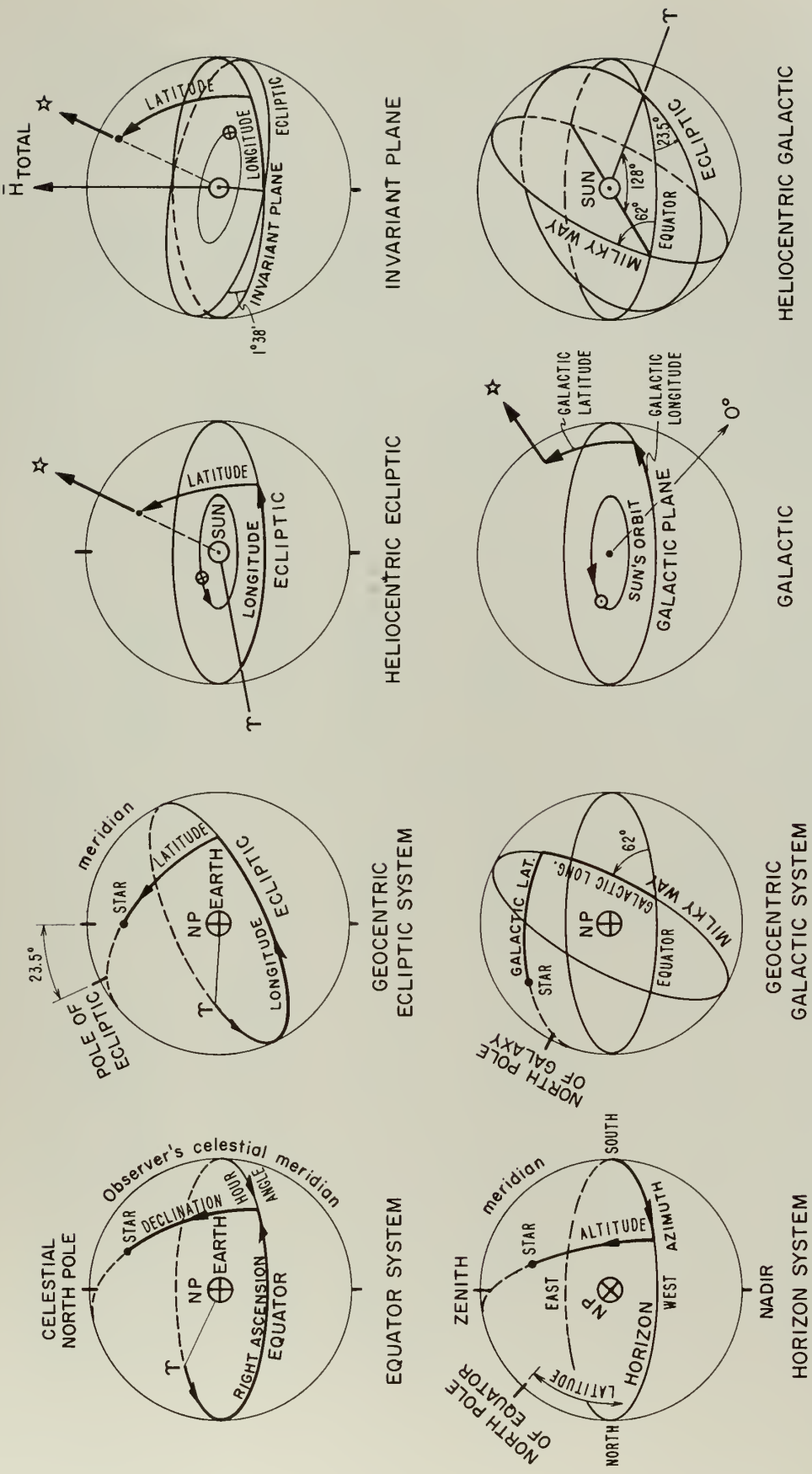


Fig. 7.1 Reference coordinate systems

TABLE 7.1 COORDINATE SYSTEMS

System	Primary Circle Determined by	Primary Circle	Origin of Zero Latitude and Longitude	Secondary Circle (to Primary)	Coordinator	Usual Astronomical Symbol
Horizon	Direction of Gravity	Horizon	South point on Horizon	Vertical Circle through Star	Azimuth Altitude	(A) (h)
Equatorial	Rotation of Earth	Celestial Equator	Intersection of meridian and Equator	Hour circle of Star	Hour Angle Declination	(t) (δ)
			Vernal Equinox (T)		Right Ascension Declination	(α) (δ)
Heliocentric and Geocentric Ecliptic	Plane of Earth's orbit	Ecliptic		Vernal Equinox (T)	Longitude Latitude	(α) (β)
Heliocentric and Geocentric Galactic	Plane of Milky Way	Galactic Equator	Intersection of Galactic and Celestial Equator	Vertical circle (Secondary to Ecliptic) through Star	Galactic Longitude Galactic Latitude	(G) (g)
Galactocentric	Plane perpendicular to total angular momentum of solar system	Galactic Equator	Line from center of galaxy to Sun	Vertical circle or secondary to Galaxy through Star	Galactocentric Longitude Galactic Latitude	(G) (g)
Invariant	Plane perpendicular to total angular momentum of solar system	Invariant plane	Intersection of Ecliptic and Invariant plane	Invariant Longitude Invariant Latitude	Invariant (α) _{inv} (β) _{inv}	

7.4 Establishing the Reference Coordinate System

It appears that the reference system orientation will have to be obtained by use of the fixed stars, an extremely sensitive gyro inertial platform,⁷¹ or a combination of the two. The use of gyroscopic elements by themselves for establishing and maintaining a chosen reference coordinate system to a sufficient degree of accuracy to determine accurate angular measurements and rates in space appears to be beyond engineering capabilities at present. All instrument gyros have drift uncertainties to some extent and very definite lower limits of sensitivities. To be useful for accurate interplanetary guidance the threshold of sensitivity would have to be in the order of 10^{-8} g. Since it is necessary to contemplate transit times of over 100 days, it appears that star trackers locked on the fixed stars will have to be used to a certain degree in either assisting a gyro system or replacing it entirely. At certain periods of the transit it may be advantageous to use gyroscopic elements as a memory circuit or coast device while a star is temporarily obscured or its line of sight becomes nearly coincident to that of a stronger source of light such as a planet or the sun. It also appears that during periods of radical maneuvering or high thrust a gyroscopic device may be needed to insure holding track on a desired star.

If we postulate the use of photoelectric star trackers, establishing the desired reference coordinate system can be accomplished by using only two fixed stars approximately 90° apart in the same meridian. However, three stars near quadrature to each other, or three stars near the chosen zero latitude spaced approximately 120° apart, will establish a more stable and secure reference. Monitoring three fixed stars would allow for the possibility of one of them becoming momentarily obscured or temporarily loosing tracking signal. Section 8.64 discusses the accuracy requirements for such systems.

7.5 Determining Celestial Latitude and Longitude of the Vehicle

After establishing the reference coordinate plane and meridian, the celestial latitude and longitude of the vehicle can be determined from the line of sight to the sun as seen from the vehicle. This is illustrated in Fig. 7.2 and as shown, the vehicle heliocentric latitude is equal to the negative of the angle between the reference zero latitude plane and the vehicle sun line measured in a meridian of the reference coordinate system. The heliocentric longitude of the vehicle is equal to the angle between the reference zero longitude and the meridian containing the vehicle sun line measured in the direction of rotation of the planets, plus 180° .

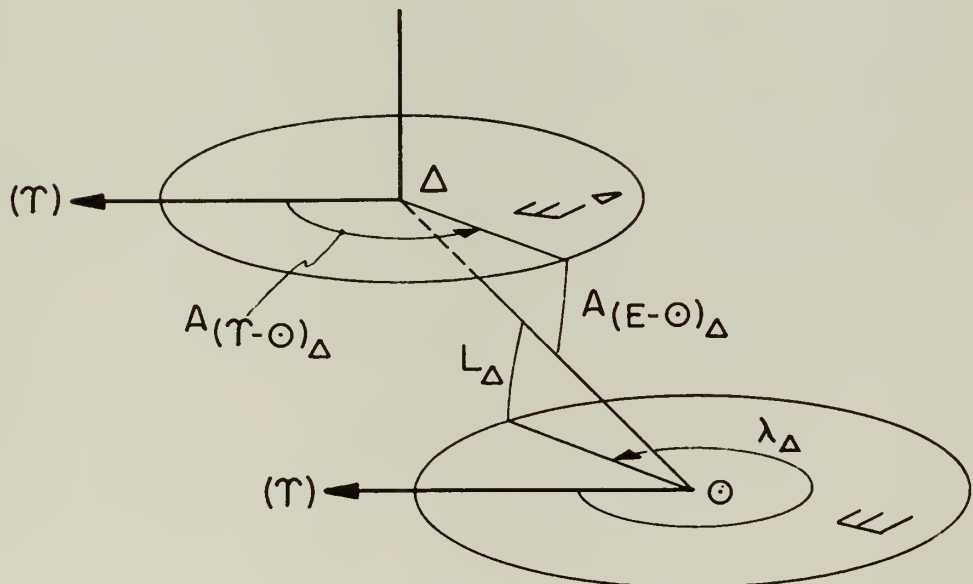
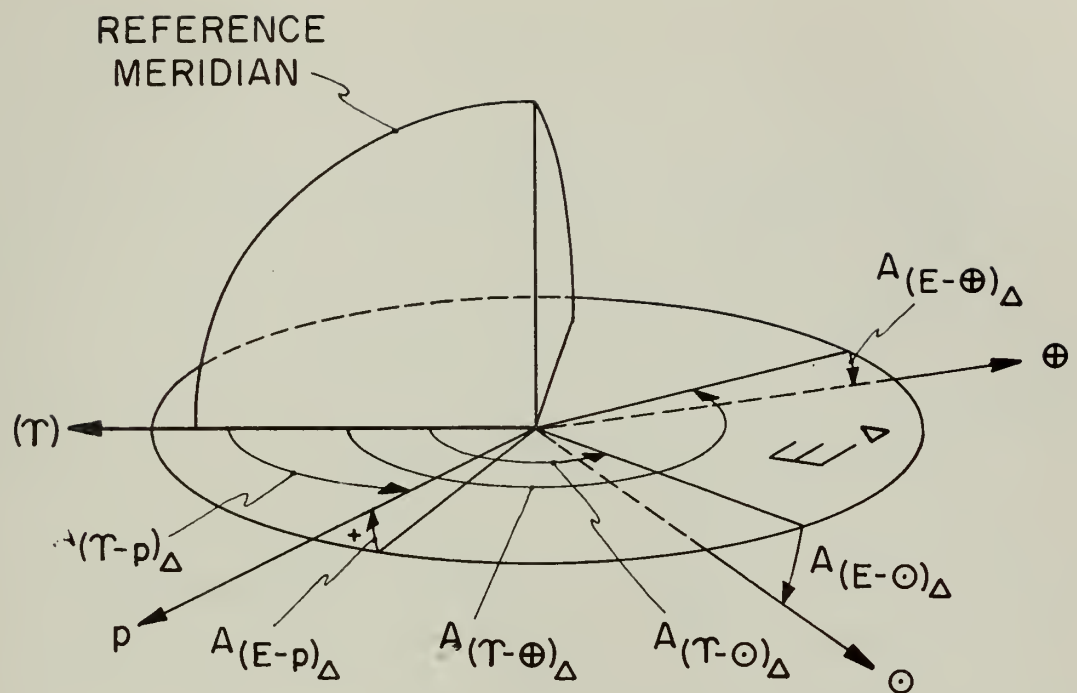
7.6 Determining the Radius Vector to the Sun

After establishing the basic reference, and determining the vehicle latitude and longitude with respect to the sun, it is then necessary to obtain the distance of the vehicle from the sun. This can be accomplished using only one planet tracked with respect to the established reference system by a simple method proposed by Vertregt.⁶⁷

We can obtain from a memory drum or an ephemeris of heliocentric ecliptic positions of the selected planet as a function of time;

1. Longitude of the planet (λ_p)
2. Latitude of the planet (L_p)
3. Distance of planet from sun (R_p)

To obtain the radial distance of the vehicle from the sun referring to Fig. 7.3, we can proceed as follows:



$$L_\Delta = -A_{(E-\ominus)_\Delta} \quad (7-1)$$

$$\lambda_\Delta = 180 + A_{(T-\ominus)_\Delta} \quad (7-2)$$

Fig. 7.2 Determination of heliocentric latitude and longitude

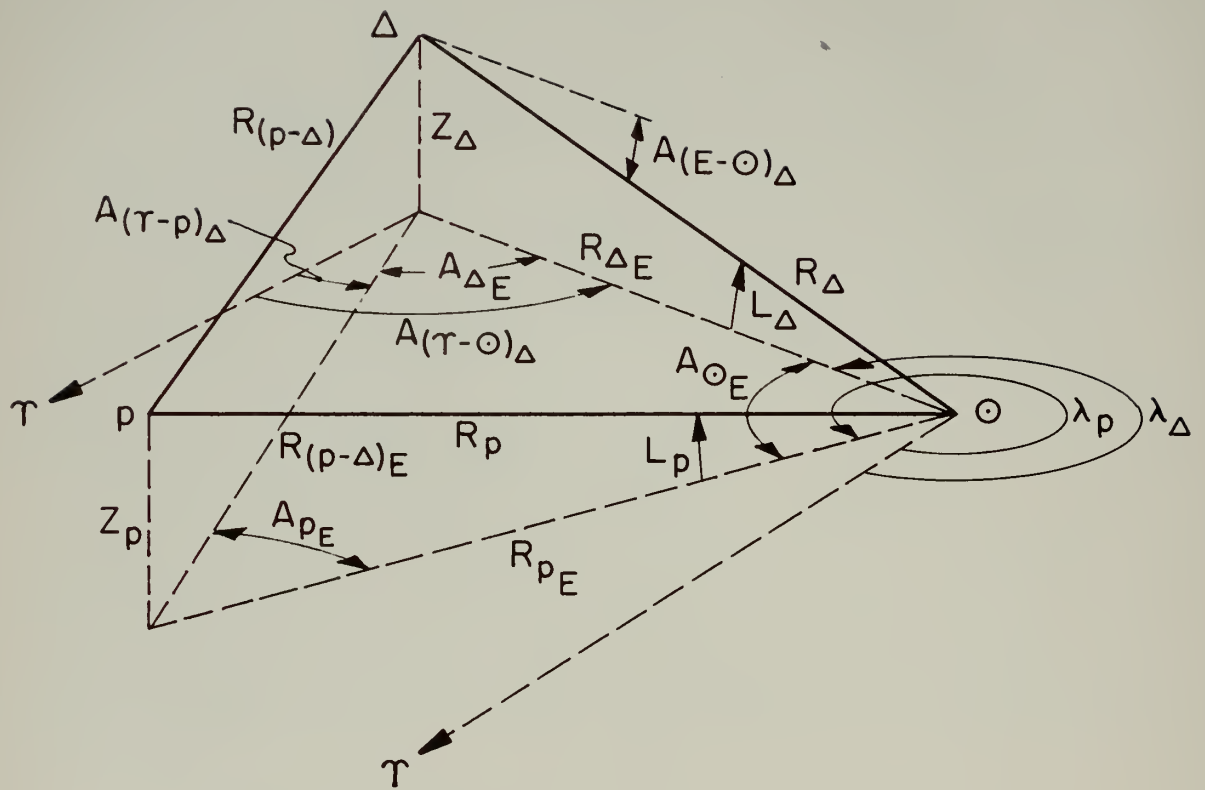


Fig. 7.3 Geometrical relationships determining radial distance from the sun

$$R_{pE} = R_p \cos L_p$$

$$R_{\Delta E} = R_p \frac{\sin A_{pE}}{\sin A_{\Delta E}} = R_p \cos L_p \frac{\sin A_{pE}}{\sin A_{\Delta E}}$$

$$A_{pE} = 360^\circ + \lambda_p - A_{(\tau-p)_\Delta}$$

$$A_{\Delta E} = A_{(\tau-\odot)_\Delta} - A_{(\tau-p)_\Delta}$$

$$R_\Delta = \frac{R_{\Delta E}}{\cos A_{(E-\odot)_\Delta}} = \frac{R_{\Delta E}}{L_\Delta}$$

therefore

$$R_\Delta = \frac{R_p \cos L_p \sin [\lambda_p - A_{(\tau-p)_\Delta}]}{\cos A_{(E-\odot)_\Delta} [\sin(A_{(\tau-\odot)_\Delta} - A_{(\tau-p)_\Delta})]} \quad (7-3)$$

If the earth is one of the planets used for determining position, and we use the plane of the ecliptic as the zero latitude reference plane, the solution is somewhat simplified due to the fact that earth heliocentric ecliptic latitude is at all times zero. (Fig. 7.4)

$$R_{\Delta E} = \frac{R_\oplus \sin A_{\oplus E}}{\sin A_{\Delta E}}$$

$$A_{\Delta E} = A_{(\tau-\oplus)_\Delta} - A_{(\tau-\odot)_\Delta}$$

$$A_{\oplus E} = 360^\circ + \lambda_\oplus - A_{(\tau-\oplus)_\Delta}$$

$$R_\Delta = \frac{R_{\Delta E}}{\cos A_{(E-\odot)_\Delta}} = \frac{R_\oplus \sin [\lambda_\oplus - A_{(\tau-\oplus)_\Delta}]}{\sin [A_{(\tau-\oplus)_\Delta} - A_{(\tau-\odot)_\Delta}] \cos A_{(E-\odot)_\Delta}} \quad (7-4)$$

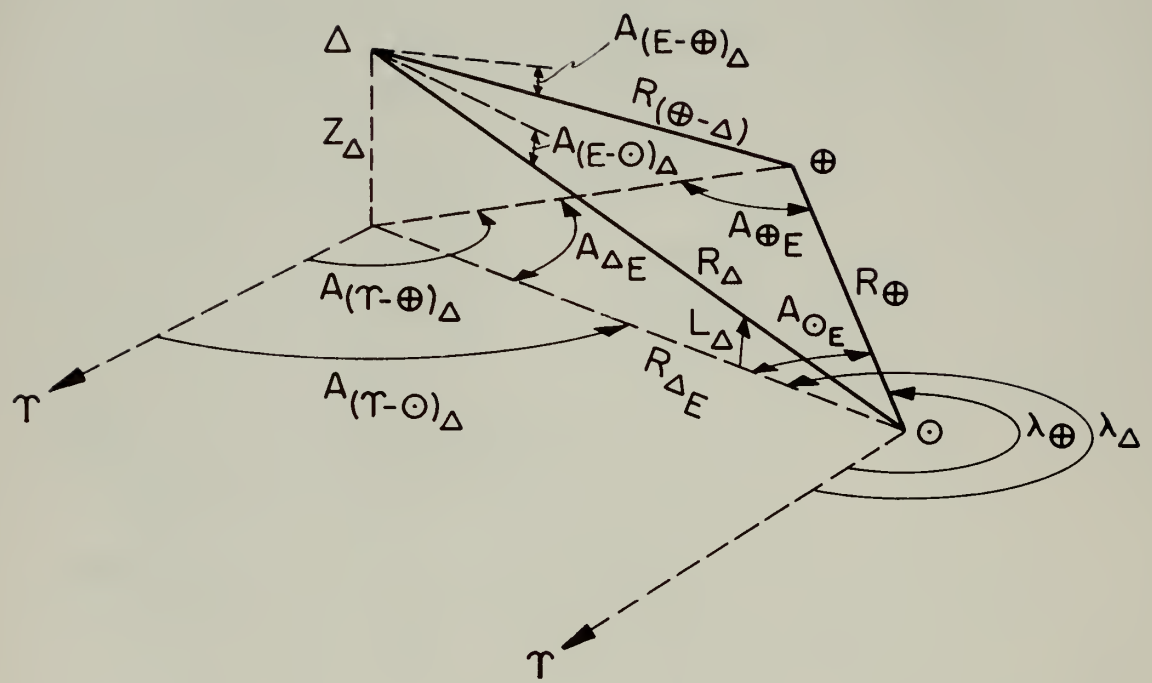


Fig. 7.4 Geometrical relationships determining radial distance from the sun with earth as the reference planet

The determination of range of the vehicle from the sun can be made using only one planet after L_{Δ} and λ_{Δ} are known. However, since we know appreciable errors exist in the values given for planetary positions as shown in Section 8.62, the use of two or more planets should tend to narrow the error down.

7.7 Some Additional Methods for Position Determination

A second method for angular determination of the sun and planets is photographic⁶⁷. By the taking of simultaneous pictures of a given small area (such as 5°) centered about the selected body, the position of the body with respect to the background of recognizable fixed stars can be obtained by taking measurements from the developed plate. This does not appear practical even for a manned vehicle, due to time lag, the need for continuous or very frequent data to effect smooth system performance and, in the case of a manned vehicle, an extra burden upon the crew.

Similarly it has been suggested that the angular measurement of the diameter of solar bodies might be used for range determination. This could be photoelectric or photographic in nature. Both these systems do not appear practical except possibly for terminal guidance where the diameter of the body being approached becomes appreciable.

Further postulated ranging methods are (1) measurement of incident solar radiation intensity,⁴⁹ (2) measurement of reflected solar radiation from planets, and (3) radar ranging.

Some basic arguments against use of the above methods for mid-course ranging are as follows:

1. The variation in intensity of solar radiation does not seem to be great enough for any but the most coarse range determination. Using Fig. 2.2 we see that for a trip between Earth and Mars this variation in radiation is approximately 1 erg per square inch per second for a change in range of one mile.

2. Reflected solar radiation also has the same general gradient as above in (1) plus the uncertain and possible widely varying amounts that might be reflected from a body due to changes in planetary atmospheric condition and orientation of lighted surface relative to the vehicle.
3. Radar ranging has the same disadvantage as listed in Section 7.2

7.8 Determination of the Shape of Actual Transfer Ellipse

If we assume that after obtaining a series of acceptable vehicle positions we want to know the elements and orientation of the ellipse being traversed, we can proceed after first converting the differences in latitude and longitude of three selected positions into angular displacements along their great circle locus ($\theta_2 - \theta_1$). This can be accomplished by standard coordinate transformation.

Determination of three of the basic elements of the unpowered orbit, θ , e , and a , can be accomplished by the use of three selected positions of the vehicle with respect to the sun. For any reasonable degree of accuracy the time interval between selected positions may have to be several days. A method of mathematical reduction which can be easily programmed for a computer has been suggested by Vertregt⁶⁷ and is adapted herein to the nomenclature of this paper in Derivation Summary 7.1.

Two assumptions are made in this method which are common to many proposed non-powered interplanetary mid-course trajectories. These are:

1. Vehicle is following an unperturbed Keplerian ellipse,
2. Sun is only gravitational force considered, and is one of the foci of this ellipse.

From Derivation Summary 7.1 we obtain

DETERMINATION OF THREE BASIC ELEMENTS OF ACTUAL ELLIPTICAL TRAJECTORY FROM OBSERVED DATA

The following method of determining θ , e , and a is adapted from reference 67 to the nomenclature of this paper.

Using a basic equation of any ellipse and referring to Fig. 7.5 we obtain the following:

$$R_{\Delta_1} = \frac{a(1 - e^2)}{1 + e \cos \theta_1} \quad (5)$$

$$R_{\Delta_2} = \frac{a(1 - e^2)}{1 + e \cos \theta_2} \quad (6)$$

$$R_{\Delta_3} = \frac{a(1 - e^2)}{1 + e \cos \theta_3} \quad (7)$$

Combining (5) and (6) and (5) and (7) we get

$$R_{\Delta_1} + R_{\Delta_1} e \cos \theta_1 = R_{\Delta_2} + R_{\Delta_2} e \cos \theta_2 \quad (8)$$

$$R_{\Delta_1} + R_{\Delta_1} e \cos \theta_1 = R_{\Delta_3} + R_{\Delta_3} e \cos \theta_3 \quad (9)$$

Rearranging (8) and (9)

$$R_{\Delta_2} - R_{\Delta_1} = e(R_{\Delta_1} \cos \theta_1 - R_{\Delta_2} \cos \theta_2)$$

$$e = \frac{R_{\Delta_2} - R_{\Delta_1}}{R_{\Delta_1} \cos \theta_1 - R_{\Delta_2} \cos \theta_2} \quad (10)$$

DERIVATION SUMMARY 7.1

(Page 1 of 3)

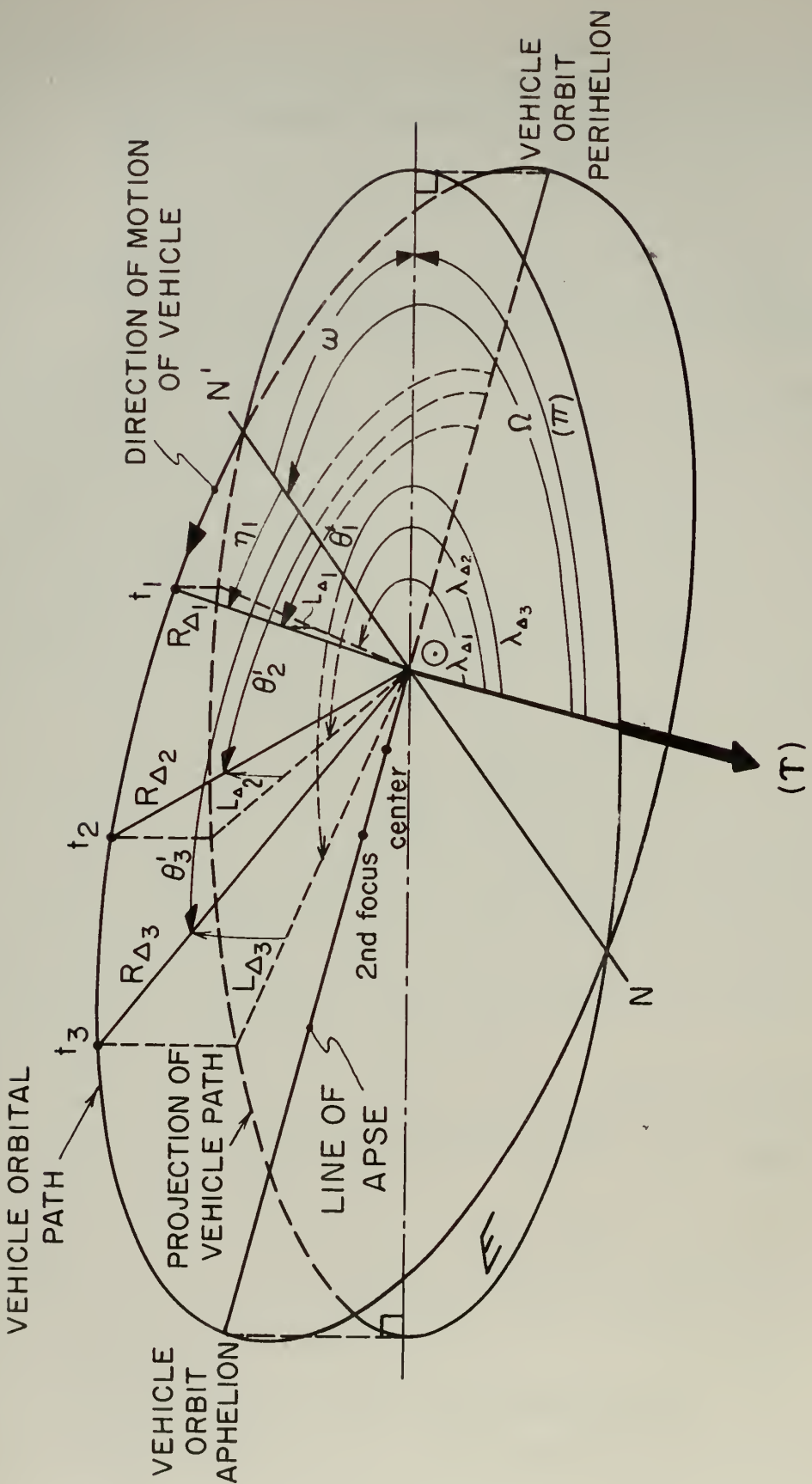


Fig. 7.5 The rocket ellipse in space

$$\begin{aligned}
 R_{\Delta_3} - R_{\Delta_1} &= e (R_{\Delta_1} \cos \theta_1' - R_{\Delta_3} \cos \theta_3') \\
 e &= \frac{R_{\Delta_3} - R_{\Delta_1}}{R_{\Delta_1} \cos \theta_1' - R_{\Delta_3} \cos \theta_3'} = \frac{R_{\Delta_2} - R_{\Delta_1}}{R_{\Delta_1} \cos \theta_1' - R_{\Delta_2} \cos \theta_2'}
 \end{aligned} \tag{11}$$

From (11) we obtain

$$\begin{aligned}
 R_{\Delta_1} (R_{\Delta_2} - R_{\Delta_3}) \cos \theta_1' - R_{\Delta_2} (R_{\Delta_1} - R_{\Delta_3}) \cos \theta_2' \\
 + R_{\Delta_3} (R_{\Delta_1} - R_{\Delta_2}) \cos \theta_3' = 0
 \end{aligned} \tag{12}$$

$$\theta_2' = \theta_1' + (\theta_2' - \theta_1') \tag{13}$$

$$\theta_3' = \theta_1' + (\theta_3' - \theta_1') \tag{14}$$

$(\theta_2' - \theta_1')$ and $(\theta_3' - \theta_1')$ have been determined along with R_{Δ_1} ,

R_{Δ_2} , R_{Δ_3} by establishing the three instantaneous positions of the vehicle. We can now substitute (13) and (14) into (12)

$$\begin{aligned}
 R_{\Delta_1} (R_{\Delta_2} - R_{\Delta_3}) \cos \theta_1' - R_{\Delta_2} (R_{\Delta_1} - R_{\Delta_3}) \cos [\theta_1' + (\theta_2' - \theta_1')] \\
 + R_{\Delta_3} (R_{\Delta_1} - R_{\Delta_2}) \cos [\theta_1' + (\theta_3' - \theta_1')] = 0
 \end{aligned} \tag{15}$$

Expanding the summed angle terms in (15) leads to

$$\begin{aligned}
 R_{\Delta_1} (R_{\Delta_2} - R_{\Delta_3}) \cos \theta_1' - R_{\Delta_2} (R_{\Delta_1} - R_{\Delta_3}) [\cos \theta_1' \cos (\theta_2' - \theta_1') - \\
 - \sin \theta_1' \sin (\theta_2' - \theta_1')] + R_{\Delta_3} (R_{\Delta_1} - R_{\Delta_2}) [\cos \theta_1' \cos (\theta_3' - \theta_1') - \\
 - \sin \theta_1' \sin (\theta_3' - \theta_1')] = 0
 \end{aligned} \tag{16}$$

DERIVATION SUMMARY 7.1

(Page 2 of 3)

Solving (16) for θ'_1 we get

$$\theta'_1 = \tan^{-1} \left[\frac{R_{\Delta_1}(R_{\Delta_2} - R_{\Delta_3}) - R_{\Delta_2}(R_{\Delta_1} - R_{\Delta_3}) \cos(\theta'_2 - \theta'_1) + R_{\Delta_3}(R_{\Delta_1} - R_{\Delta_2}) \cos(\theta'_3 - \theta'_1)}{-R_{\Delta_2}(R_{\Delta_1} - R_{\Delta_3}) \sin(\theta'_2 - \theta'_1) + R_{\Delta_3}(R_{\Delta_1} - R_{\Delta_2}) \sin(\theta'_3 - \theta'_1)} \right] \quad (17)$$

From (11), substituting the value obtained in (17) we obtain

$$e = \frac{R_{\Delta_3} - R_{\Delta_1}}{R_{\Delta_1} \cos \theta'_1 - R_{\Delta_2} \cos \theta'_3} \quad (18)$$

Substituting the value obtained in (18) into (7) and rearranging leads to

$$a = \frac{R_{\Delta_3} (1 + e \cos \theta'_3)}{1 - e^2} \quad (19)$$

DERIVATION SUMMARY 7.1

(Page 3 of 3)

$$\theta'_1 = \tan^{-1} \left[\frac{R_{\Delta_1}(R_{\Delta_2} - R_{\Delta_3}) - R_{\Delta_2}(R_{\Delta_1} - R_{\Delta_3}) \cos(\theta'_2 - \theta'_1) + R_{\Delta_3}(R_{\Delta_1} - R_{\Delta_2}) \cos(\theta'_3 - \theta'_1)}{-R_{\Delta_2}(R_{\Delta_1} - R_{\Delta_3}) \sin(\theta'_2 - \theta'_1) + R_{\Delta_3}(R_{\Delta_1} - R_{\Delta_2}) \sin(\theta'_3 - \theta'_1)} \right]$$

(7-5)

$$e = \frac{R_{\Delta_3} - R_{\Delta_1}}{R_{\Delta_1} \cos \theta'_1 - R_{\Delta_2} \cos \theta'_3}$$

(7-6)

$$a = \frac{R_{\Delta_3} (1 - e \cos \theta'_3)}{1 - e^2}$$

(7-7)

7.9 Determination of Orientation of Actual Transfer Ellipse

Two additional elements of the transfer ellipse, Ω and i , are required for determining the orientation of the vehicle trajectory with respect to the reference plane. These can be obtained by applying the method suggested in reference⁶⁷ using two positions of the vehicle. A rather obvious observation can be made that the further these two positions are from each other the more accurate will be the values of Ω and i obtained. However, since corrective action is more economical if performed early in the flight, it is apparent that Ω and i should be determined as early as possible. If the trajectory is satisfactory at this time more accurate values can be obtained at the next determination.

From the first vehicle position, as illustrated in Fig. 7.6 we can obtain the following:

S_1 is to NN'

$$A(R_{\Delta_1} - S_1) \odot = 90^\circ - \eta_1$$

$$Z_i = R_{\Delta_1} \sin L_{\Delta_1}$$

$$S_1 = R_{\Delta_1} \cos A(R_{\Delta_1} - S_1) \odot = R_{\Delta_1} \cos (90^\circ - \eta_1) = R_{\Delta_1} \sin \eta_1$$

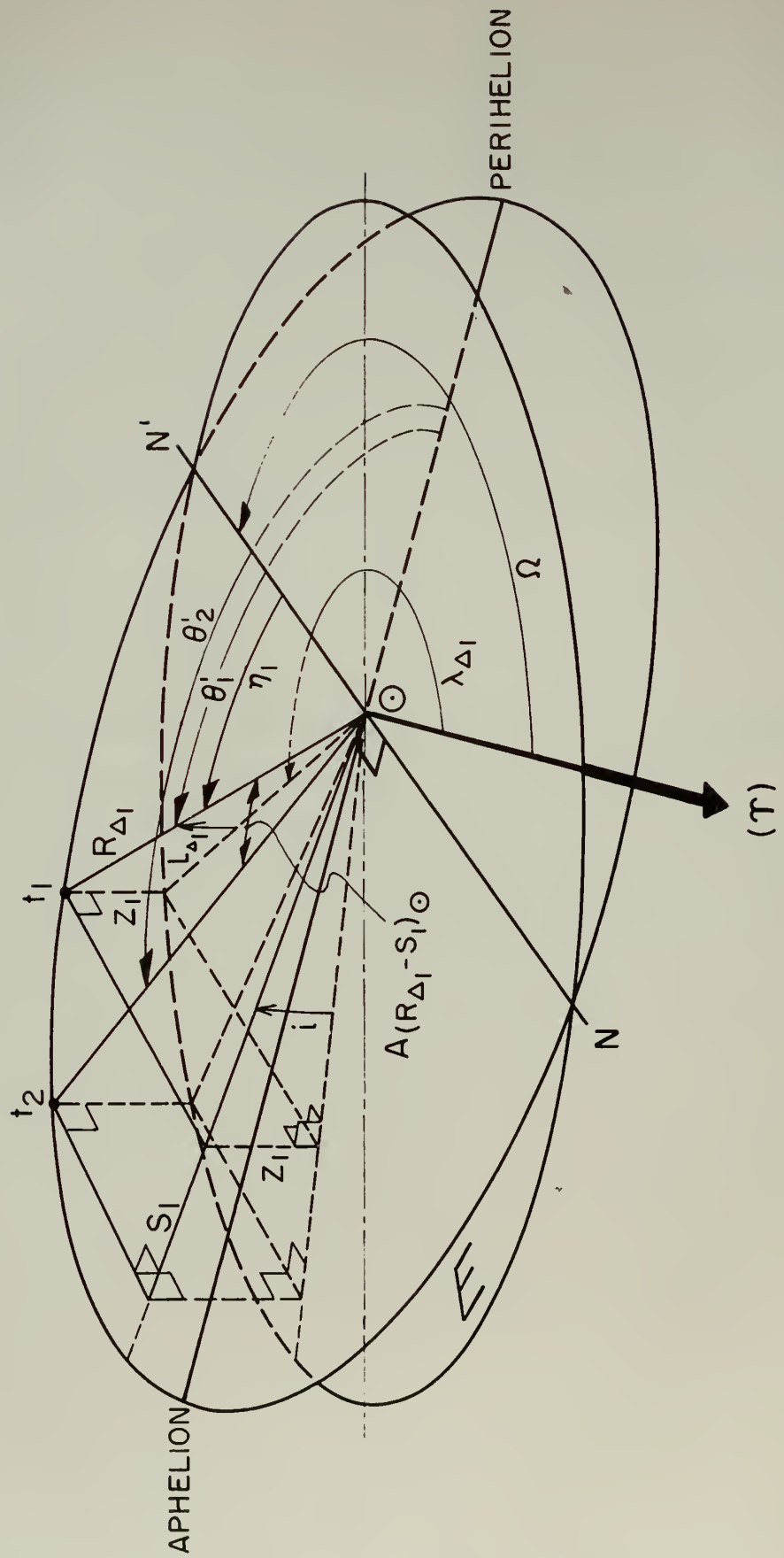


Fig. 7.6 Orientation of transfer ellipse

therefore

$$\sin i = \frac{\sin L_{\Delta_1}}{\sin \eta_1} \quad (7-8)$$

For the second position we can likewise determine that

$$\sin i = \frac{\sin L_{\Delta_2}}{\sin[\eta_1 + (\theta_2' - \theta_1')]} \quad$$

Combining the above

$$\frac{\sin L_{\Delta_1}}{\sin \eta_1} = \frac{\sin L_{\Delta_2}}{\sin[\eta_1 + (\theta_2' - \theta_1')]} = \frac{\sin L_{\Delta_2}}{\sin \eta_1 \cos(\theta_2' - \theta_1') + \cos \eta_1 \sin(\theta_2' - \theta_1')}$$

Multiplying by $\sin \eta_1$ and regrouping leads to

$$\eta_1 = \tan^{-1} \left[\frac{\sin L_{\Delta_1} \sin(\theta_2' - \theta_1')}{\sin L_{\Delta_2} - \sin L_{\Delta_1} \cos(\theta_2' - \theta_1')} \right] \quad (7-9)$$

η_1 can now be converted to the plane of the ecliptic. If we then subtract it from λ_{Δ_2} we have Ω

After determining η_1 we can then solve for the inclination of the orbit of the vehicle using equation (7-8)

$$i = \sin^{-1} \left[\frac{\sin L_{\Delta_1}}{\sin \eta_1} \right] \quad (7-10)$$

B. IN-FLIGHT CORRECTIONS

7.10 Introduction

It is considered inevitable that the rocket may fail to follow its prescribed path in space. Errors in initial conditions or unknown gravitational influences will cause deviations from the predicted trajectory.

As soon as differences between actual position (as described in Part A above and predicted position become known, a new situation arises. The decision must be made to either return to the previously calculated orbit by means of corrective thrust, or to recompute a new path which will be within the capabilities of the rocket. Time is an important consideration in this discussion since corrective action must place the rocket on a path which will result in almost simultaneous coincidence of Mars and rocket. This is discussed further below.

It is presumed that almost continuous position finding data will be available so that comparisons can, in fact, be made between actual and predicted position. It is also reasonable to assume that deviations, hence corrections, will be incremental in nature. For the sake of simplicity, let us also assume that computation of a new trajectory, when required, can take place instantaneously. Under actual conditions, solution time can be allowed for with no great difficulty.

The desirability of placing the rocket on a new path rather than forcing it to adhere to a previously defined path has been mentioned. The latter method implies, in effect, the application of continuous corrective thrust. Reference 26 has indicated an

analytical approach to the thrust requirements necessary to fly a prescribed path. Until such time as fuel supply poses no problem, however, continuous corrective thrust is prohibitive. As little application of corrective thrust as possible is desired, since there is little available for expenditure.

The objective of corrective action is not necessarily to achieve a pinpoint interception of Mars, but rather to reach a position favorable for entry into orbit about Mars. This might conceivably be a position at some distance thousands of miles from the planet as well as on the planet itself, since the gravitational influence of the arrival planet and decelerating thrust will combine to make entry into orbit a less significant consideration. Therefore, some error can be tolerated. However, when and if deviations occur which are outside tolerance limit, corrective thrust becomes necessary. Obviously, the tolerable deviation is smaller at the early stages of flight.

For purposes of analysis let us assume that the allowable tolerance has been exceeded and that corrective action is called for. The rocket is moving primarily under the attraction of a single body, the sun, which is justifiable in accordance with the calculations of section 3.6. We will also consider Mars as a massless point to be "intercepted" (in the sense defined above) at a specified time.

The subsequent analysis parallels that of Lawden²⁸ although different in many respects.

7.11 Analytical Development

Let r_o , θ_o' define present position in space at time t_o . Let r_1 , θ_1' define the position the rocket would occupy at time t_o had flown the correct path. r_2 , θ_2' define the position of Mars at time

t_2 , the planned time of interception. It is desired to intercept Mars at time t_2 via a route which obviates the necessity of returning to the original trajectory. Figure 7.7 is helpful in the interpretation to follow. The route is a conic passing through P and J.

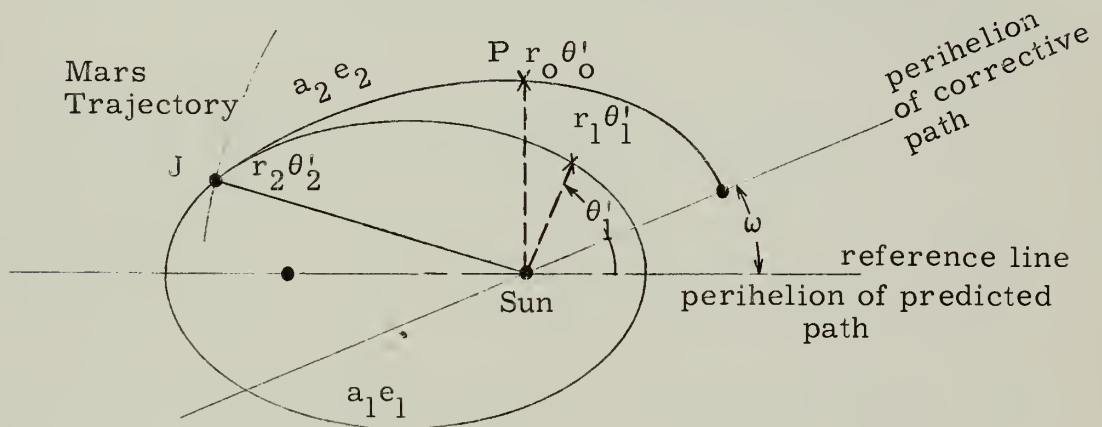


Fig. 7.7 Interception at Originally Predicted Time, t_2

Clearly, it is a restriction to be forced to intercept the planet at time, t_2 , but results in a great simplification in the computer requirements. Let us pursue this analysis first.

The conic path to be flown is presumed to be a segment of an ellipse (because of velocity requirements) with sun as focus. The line of apsides of this new ellipse, whose elements are designated (a_2, e_2) is aligned at an angle ω with the reference line of the originally prescribed ellipse (elements a_1, e_1).

From the fundamental elliptical equation 4-1

$$r_o = \frac{a_2 (1 - e_2^2)}{1 + e_2 \cos (\theta_o - \omega)} \quad (7-11)$$

$$r_2 = \frac{a_2 (1 - e_2^2)}{1 + e_2 (\theta_2' - \omega)} \quad (7-12)$$

where r_0 , r_2 , θ_0' , and θ_2' are known.

Position in an elliptical orbit at any time t can be found from the relationship ⁴⁷

$$\frac{2\pi t}{T} = \frac{e \sqrt{1 - e^2} \sin \theta_1'}{1 + e \cos \theta_1'} - \sin^{-1} \frac{e_1 + \cos \theta_1'}{1 + e \cos \theta_1'} + \frac{\pi}{2}$$

where t is measured from $t = 0$ which occurs at perihelion passage of ellipse being considered..

T , the period of the ellipse, can be expressed⁴⁴ as a function of a , and is usually known.

$$T_2 = \frac{2\pi a_2^{3/2}}{\sqrt{GM}} \quad (7-13)$$

From these relationships,

$$\frac{2\pi t_2}{T_2} = \frac{e_2 \sqrt{1 - e_2^2} \sin (\theta_2' - \omega)}{1 + e_2 \cos (\theta_2' - \omega)} - \sin^{-1} \frac{e_2 + \cos (\theta_2' - \omega)}{1 + e_2 \cos (\theta_2' - \omega)} + \frac{\pi}{2}$$

and

$$\frac{2\pi t_0}{T_2} = \frac{e_2 \sqrt{1 - e_2^2} \sin (\theta_0' - \omega)}{1 + e_2 \cos (\theta_0' - \omega)} - \sin^{-1} \frac{e_2 + \cos (\theta_0' - \omega)}{1 + e_2 \cos (\theta_0' - \omega)} + \frac{\pi}{2}$$

where t_2 and t_0 are unknowns, measured from the reference line inclined at an unknown angle ω to a known reference line.

If the time of travel from r_0 to r_2 is constrained to be the originally planned interval of time from r_1 to r_2 , the interval $t_2 - t_0$ becomes a known quantity, and t_2 and t_0 need not be known individually.

$$t_2 - t_o = \Delta t = \frac{T_2}{2\pi} \left[\frac{e_2 \sqrt{1 - e_2^2} \sin(\theta_2' - \omega)}{1 + e_2 \cos(\theta_2' - \omega)} - \frac{e_2 \sqrt{1 - e_2^2} (\theta_o' - \omega)}{1 + e_2 \cos(\theta_o' - \omega)} \right]$$

$$- \sin \frac{-1 e_2 + \cos(\theta_2' - \omega)}{1 + e_2 \cos(\theta_2' - \omega)} + \sin^{-1} \frac{e_2 + \cos(\theta_o' - \omega)}{1 + e_2 \cos(\theta_o' - \omega)} \quad (7-14)$$

In summary, position finding data will provide r_o , θ_o . The quantities r_1 , θ_1' and r_2 , θ_2' are known in advance as functions of time. Thus, Δt , the time till interception, is known for any r_1 , θ_1' . Equations 7-11 - 7-14 involve four unknowns a_2 , e_2 , ω , and T_2 , and are solvable by iterative methods.

Since corrections are assumed to be incremental in nature when compared with the elements of the path being flown (a_o , e_o , ω_o), a_2 , e_2 and ω , may be replaced by $a + \delta a$, $e + \delta e$, and $\omega + \delta \omega$. It is assumed T_2 has been replaced by its value in terms of a_2 .

If these substitutions are made and small angle assumptions are valid ($\sin \delta \omega = \delta \omega$, $\cos \delta \omega = 1$) equations in the three unknown δa , δe , and $\delta \omega$ result. a_o , e_o and ω_o (assumed zero, initially) can be found as described in the navigational section and are good first approximations to a , e and ω .

Successive improvements of the accuracy of δa , δe , and $\delta \omega$ can be made if desired.

7.12 Corrective Action

Since changes must inevitably be reflected in an alteration of velocity and angle of fire, we may again write two basic relationships

$$(v_o + \Delta v)^2 = GM \left(\frac{2}{r_2} - \frac{1}{a_2} \right)$$

$$\tan(\phi_o + \Delta\phi_o) = \frac{e_2 \sin(\theta_2^i - \omega_2)}{1 - e_2 \cos(\theta_2^i - \omega_2)}$$

Replacing a_2 , e_2 and ω_2 by $a + \delta a$, $e_2 + \delta e$ and $\omega + \delta \omega$, we arrive at

$$(v_o + \Delta v)^2 = GM \left[\frac{2}{r_2} - \frac{1}{a + \delta a} \right]$$

$$\Delta v = \left[GM \left[\frac{2}{r_2} - \frac{1}{a + \delta a} \right] \right]^{\frac{1}{2}} - v_o$$

where v_o is the velocity at the time corrective action is deemed necessary, and ϕ_o is the corresponding angle of orientation as defined earlier. Similarly, direction must be altered to effect $\Delta\phi_o$ which can be written

$$\Delta\phi_o = \tan^{-1} \frac{(e + \delta e) \sin(\theta_2^i - \omega - \delta \omega)}{1 - (e + \delta e) \cos(\theta_2^i - \omega - \delta \omega)} - \phi_o$$

$a + \delta a$, $e + \delta e$, and $\omega + \delta \omega$ are presumed to be known accurately as described in the preceding paragraphs.

Corrective thrust must be actuated to produce the changes required.

7.13 Interception at Newly Calculated Time

Let us now consider the prospect of intercepting Mars at some time other than the originally planned time.

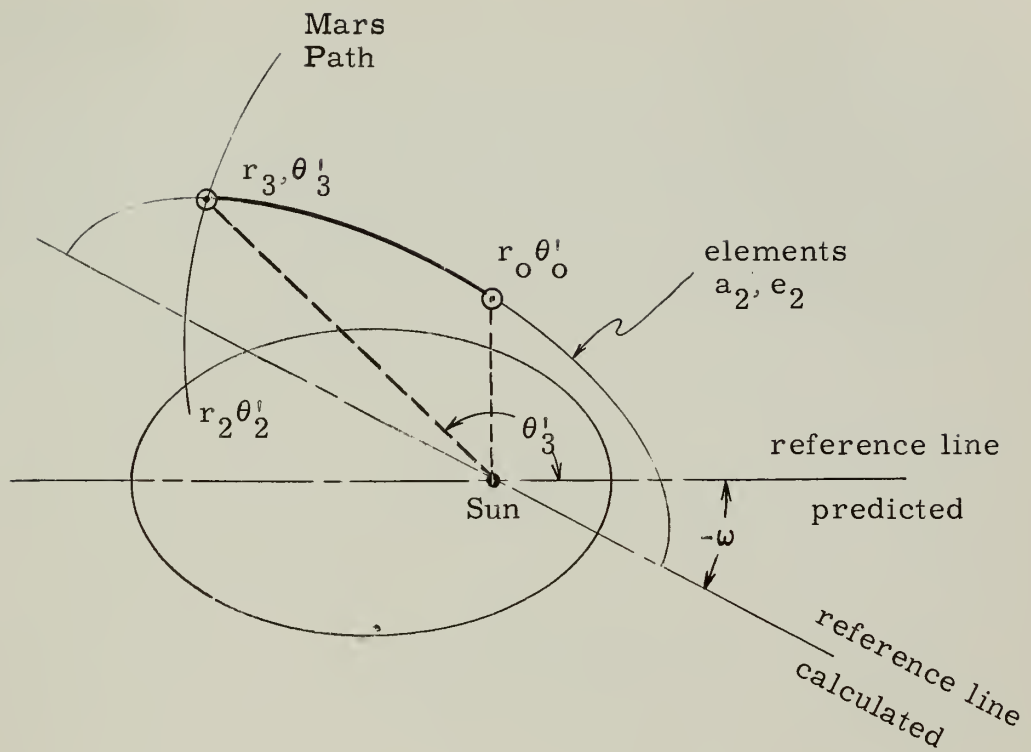


Fig. 7.8 Interception at Newly Calculated Time

It is recognized at t_0 that present position, r_0, θ_0' is unsatisfactory, i.e. a continuation along present track will not achieve interception. Moreover, assume that rocket corrective thrust capabilities will not permit an interception at r_2, θ_2' , the originally planned arrival point. We desire a conic (elliptical) path from r_0, θ_0' to some arbitrarily selected Mars position, r_3, θ_3' which has been chosen because it is within the rocket's thrust capabilities. This new position may also, in fact, represent the position of Mars which can be most economically reached. The choice of this position does present a formidable problem, since the optimization process is necessarily involved. The selection of a Mars position is not discussed here although its importance is emphasized.

Presumably, there is on board a means of establishing Mars position as a function of some base time - a Mars Ephemeris of sorts. Fixing the desired interception point will fix the time, t_3 , of interception. t_0 is known from an accurate time piece. Thus, the interval of corrective travel becomes $t_3 - t_0$. These times are both based upon a common reference. The time interval is therefore determinable.

Employing the previously developed reasoning procedures,

$$r_0 = \frac{a_2(1 - e_2^2)}{1 + e_2 \cos(\theta_0 + \omega)}$$

$$r_3 = \frac{a_2(1 - e_2^2)}{1 + e_2 \cos(\theta_3 + \omega)}$$

$$\Delta t = t_3 - t_0 = \frac{T_2}{2\pi} \left[\frac{e_2 \sqrt{1 - e_2^2} \sin(\theta_3 + \omega)}{1 + e_2 \cos(\theta_3 + \omega)} - \frac{e_2 \sqrt{1 - e_2^2} \sin(\theta_0 + \omega)}{1 + e_2 \cos(\theta_0 + \omega)} \right. \\ \left. - \sin^{-1} \frac{e_2 + \cos(\theta_3 + \omega)}{1 + e_2 \cos(\theta_3 + \omega)} + \sin^{-1} \frac{e_2 + \cos(\theta_0 + \omega)}{1 + e_2 \cos(\theta_0 + \omega)} \right]$$

and

$$T_2 = \frac{2\pi a_2^{3/2}}{\sqrt{GM}}$$

By the methods previously described, the elements of the new path a_2 , e_2 , ω_2 can be found and corresponding δa , δe , and $\delta \omega$'s determined. It is now a relatively simple matter to calculate the velocity and angular changes necessary to fly the corrected path.

7.14 Summary

It is seen that both approaches are essentially the same. From the standpoint of instrumentation, however, interception at time other than planned requires on board a knowledge of Mars position at all times and necessitates the selection of a new interception point. The choice of this point is essentially an optimization process.

CHAPTER 8

GUIDANCE AND CONTROL

8.1 General

The instrumentation of any guidance and control system for interplanetary travel is extremely complex. As stated previously, this paper studies the so-called "combination" trajectory (i.e. - an initial thrust period followed by unpowered free-fall flight; modified, if necessary, by corrective thrusts). Primary emphasis has been placed upon what has been defined as the "mid-course" of this type trajectory. Although considerable thought has been devoted to the use of departure and arrival orbits, the applicability of this paper is not limited solely to interorbital trajectories. Whether the vehicle orbits prior to commencing mid-course travel or simply continues directly from the ascent from the surface of the Earth does not affect requirements of the vehicle velocity vector orientation and magnitude and other parameters for the actual transfer period.

This Chapter outlines in simple form a suggested Mid-course Guidance and Control system based upon the material developed in previous portions of this paper. The major problem of reducing the system to the least possible weight and size has been ignored except to the extent that simplification has been attempted where it will not detrimentally affect the overall accomplishment of the mission (i.e. - the arrival of the rocket at Mars within certain limits).

Time-sharing of a miniaturized low-power digital computer, a common ephemeris memory, and one basic time generating mechanism have been assumed. This appears justifiable since

the elasped time between computations need not be of the order of fractions of a second, but can be several minutes or possibly hours. Digital computation is necessary due to the extremely low rates of change of rocket position, velocity, and acceleration; and the need for a high degree of accuracy.

The problems of instrumentation have been divided into several sections as follows:

- (1) The Basic System
- (2) The Tracking Section
- (3) The Computing Section
 - (a) Tracking Line Computation
 - (b) Prediction Computation
 - (c) Comparing Function
 - (d) Correction Computation
- (4) Thrust and Stabilization Section
- (5) Errors and Effects

These sections are treated below.

8.2 The Basic System

The functional responsibilities of Guidance and Control have been segmented into three basic categories, as shown in Fig. 8-1. A brief general description follows:

The Tracking Section - Maintains Lines-of-Sight upon prescribed bodies and provides Tracking Line data therefrom to the Computing Section.

The Computing Section - Performs the necessary computations to the Tracking Lines to obtain signals proportional to the corrections required to the rocket velocity vector to insure accomplishment of the mission.

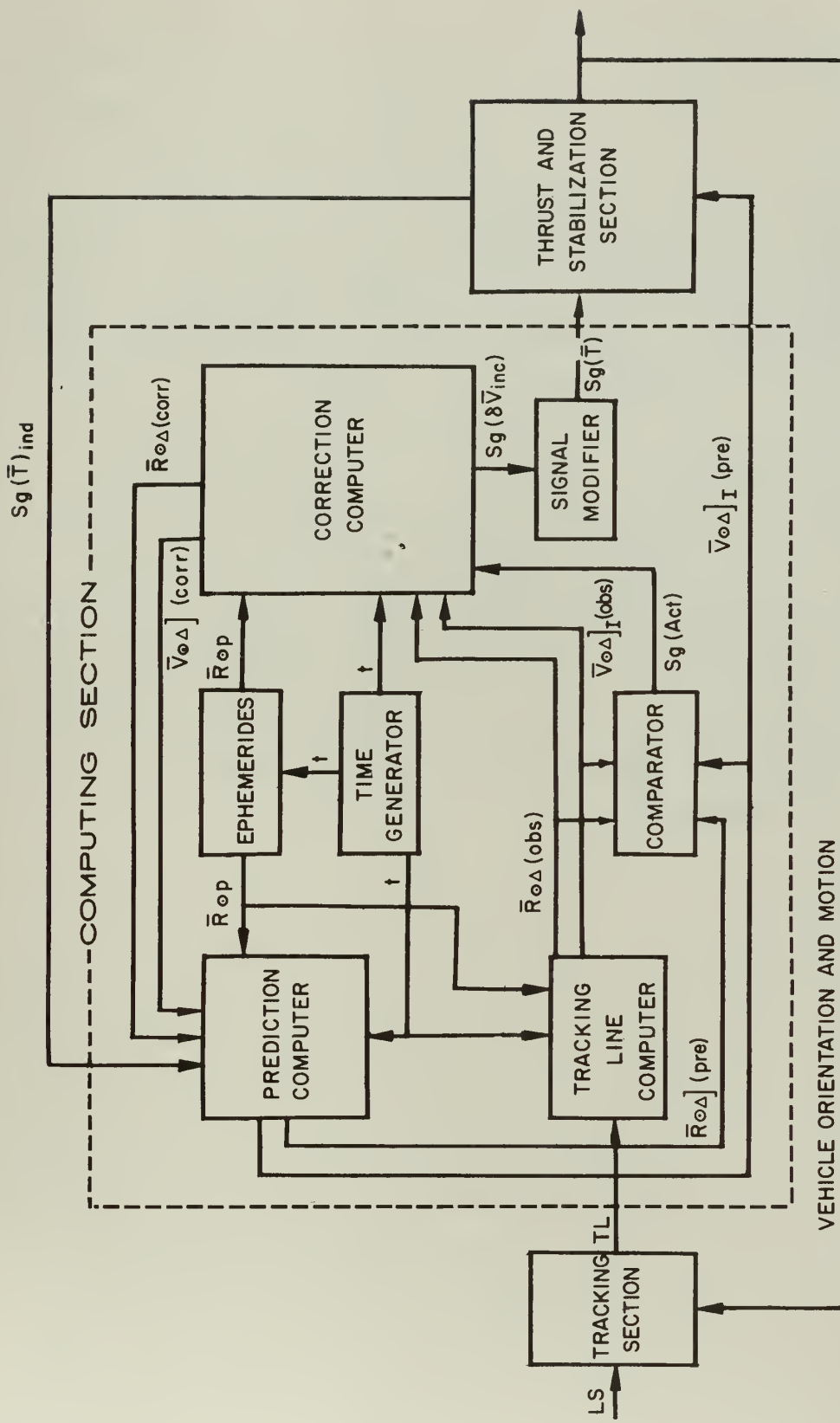


Fig. 8.1 Line functional information flow diagram of a proposed guidance and control system

The Thrust and Stabi-
lization Section

- Provides vehicle orientation and corrective thrust in accordance with the received signals.

The aforementioned system sections will be examined in more detail in the following sections of this paper. The Computing Section of the rocket involves such a complex problem that it has been subdivided into four parts, each of which will be discussed in its own Section of this Chapter.

8.3 The Tracking Section

The tracking section envisioned determines tracking lines from the vehicle to the Sun and planets measured in an helio-centric ecliptic coordinate system. These angular measurements are then sent as electrical signals (TL_i) to the tracking line computer in the tracking section. Two systems are presented which differ in method of space reference frame determination, number of star and planet trackers required, and in probable degrees of accuracy and reliability.

8.31 System One

The first system obtains space reference from star trackers rigidly mounted to a control member platform isolated from vehicular motion by gimbals. This platform is "fixed" in space and is maintained in this attitude by tracking error signals generated in the fixed star tracking units, which are used to actuate the gimbal drive motors. A gyro package is mounted on the controlled member solely to assist in holding track during periods of radical maneuver and to aid in initial lock on. Three additional star trackers are mounted on the controlled member, each with its own tracking member drive system, as illustrated in Fig. 8.2 and 8.3. One tracking head determines the rocket-sun tracking line while the others determine two different rocket-planet tracking lines.

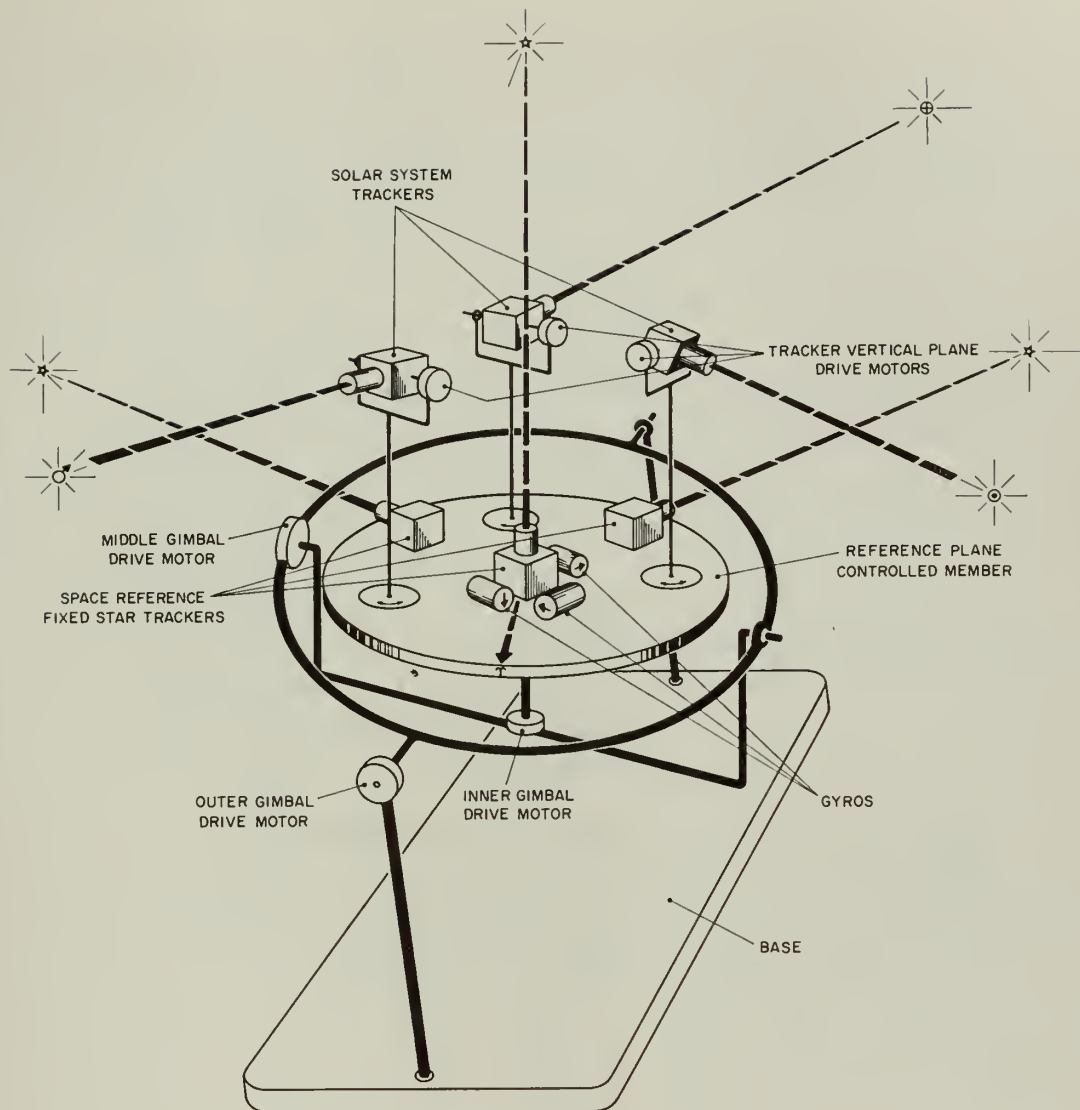


Fig. 8.2 Illustrative schematic of tracking system
with gyro assist

COMPUTING SECTION

TRACKING SECTION

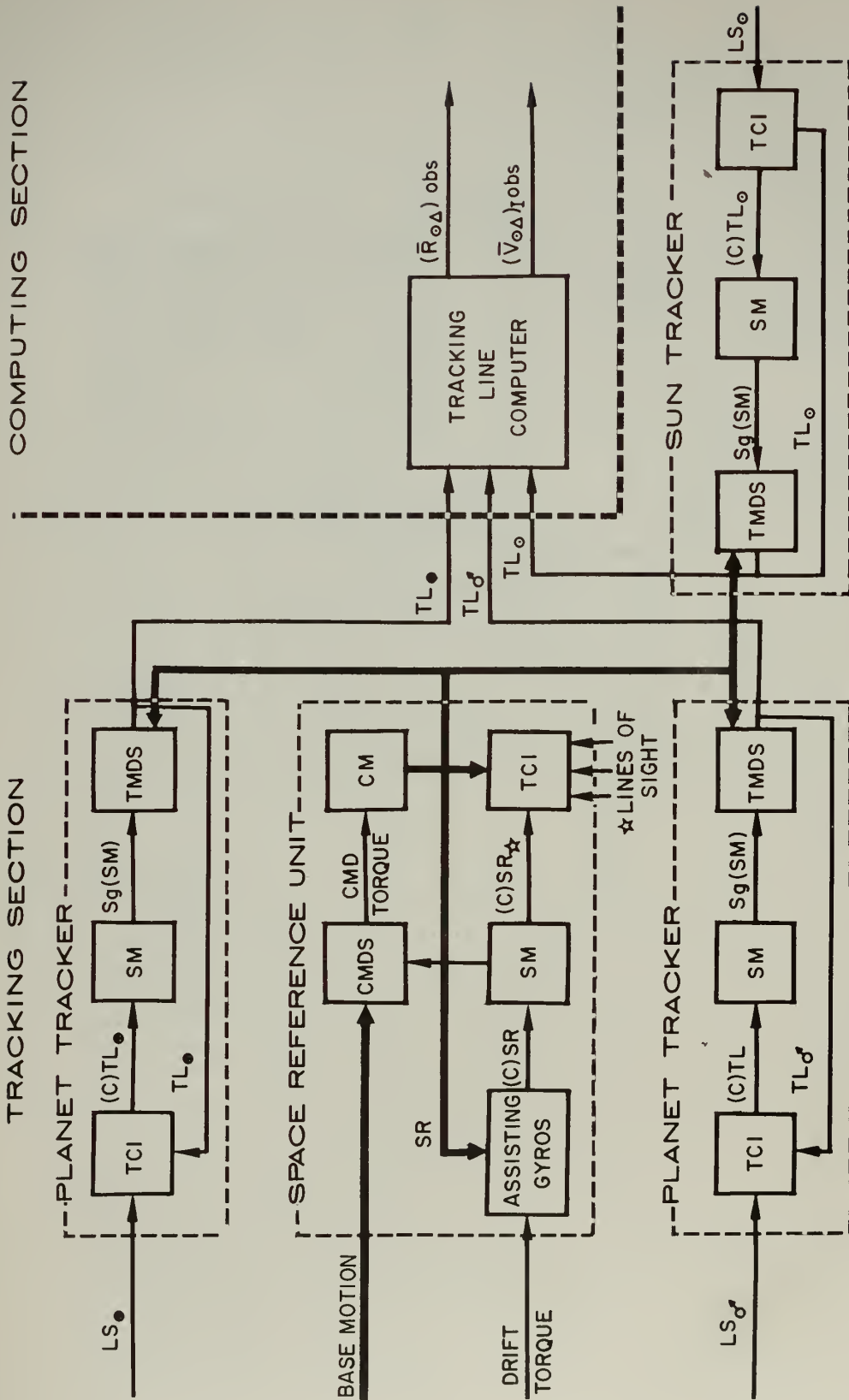


Fig. 8.3 Line functional information flow diagram of Tracking System I

Angular measurements of these lines are made in heliocentric ecliptic coordinates, (see Fig. 7.1) and transmitted to two separate range computers within the tracking line computer of the computing section.

8.32 System Two

The second tracking system (Figs. 8.4 and 8.5) consists of a space reference gyro package, and only three star trackers. The reduction in the number of trackers used is made solely to simplify construction at the expense of system accuracy. Three orthogonally positioned single degree of freedom gyros are assisted by a single "fixed star" tracker rigidly mounted to the controlled member. Smoothed error signals from this tracker are combined with the signals from the gyros. This resultant signal is then used to actuate the gimbal drive motors maintaining the controlled member reference plane in proper orientation. Two star trackers are then mounted on the controlled member, each with its own tracking member drive system. As in the first system, one tracker determines the rocket-sun line, while the second tracker determines a rocket-planet line. Angular measurements of these lines feed into a range computation section of the tracking line computer.

8.33 Comparison of Systems One and Two

It is obvious from comparing Figs. 8.2, 8.3, 8.4 and 8.5, that the second method discussed in 8.32 is much simpler to design and construct since only three stellar tracking heads are needed while the system discussed in 8.31 requires six tracking heads. (Possibly this could be reduced to five if only two heads were used for space reference determination). The main draw back to system two is the dependence upon gyros for space reference. These units are not, at present, stable enough nor predictable to the degree required, for a time of flight of the length required for an Earth-Mars transit. Section 8.64 discusses this

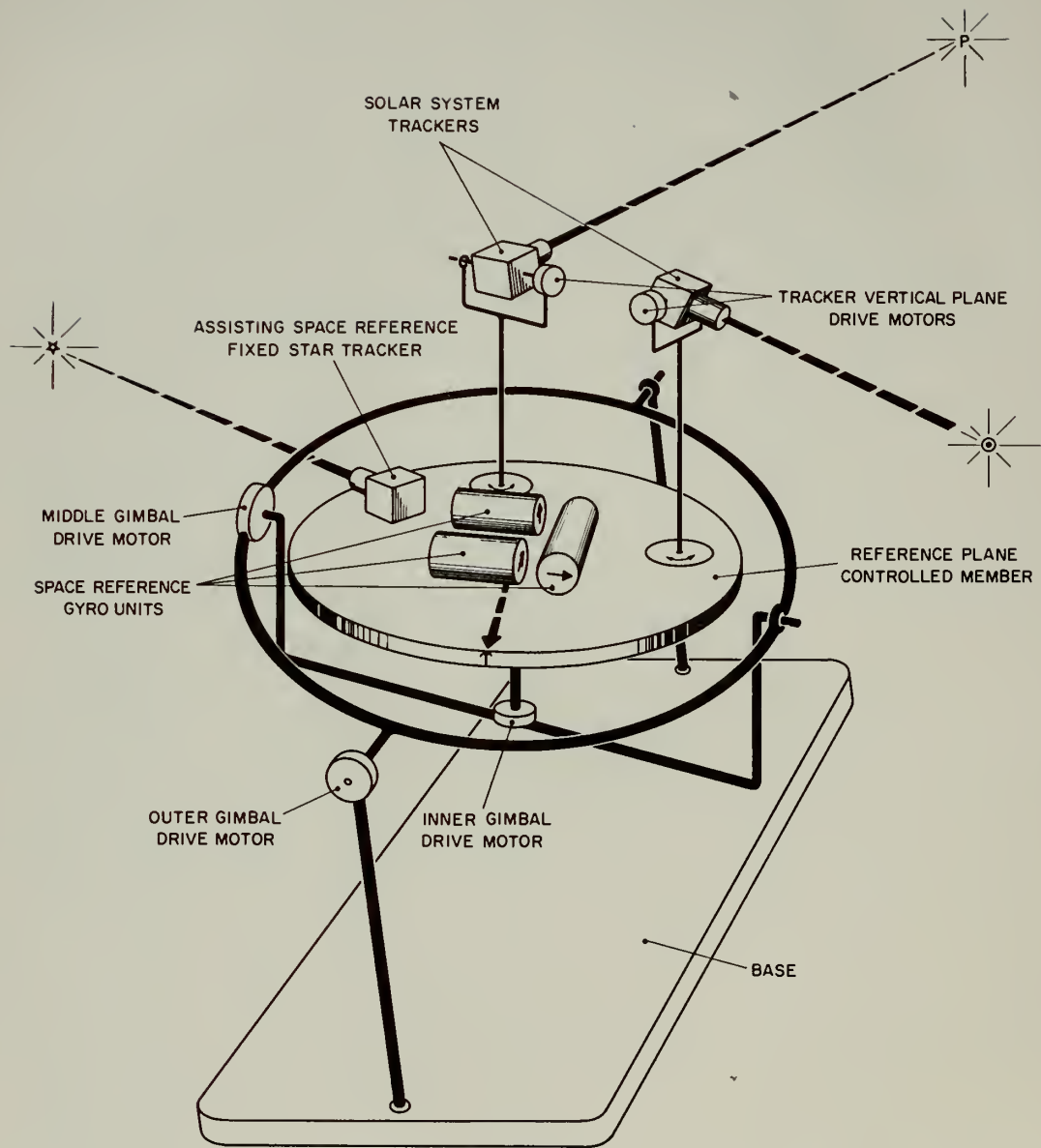


Fig. 8.4 Illustrative schematic diagram of tracking system with stellar assisted gyro space reference

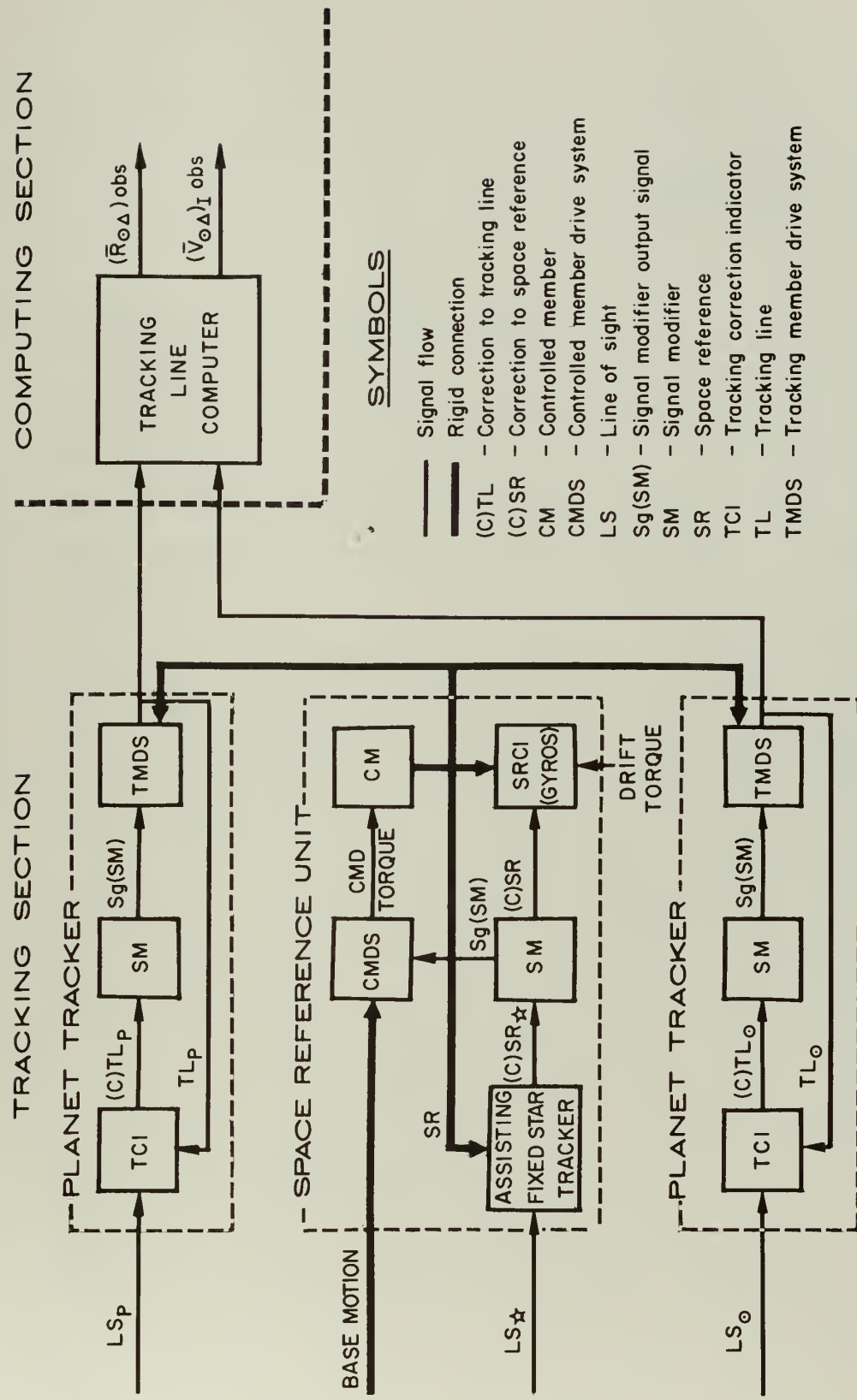


Fig. 8.5 Line functional information flow diagram, Tracking Section II

particular aspect.

A second drawback to the simplified system of section 8.32 is the use of only one planet. The effect of this is felt in computation of $(\bar{R}_{\odot\Delta})_{\text{obs}}$, and will be treated in section 8.41.

8.4 The Computing Section

8.41 Tracking Line Computation

The tracking line computation section of the Guidance System receives the angular measurements of the tracking lines determined in the tracking section. Using these measurements and data from the Ephemeris Storage and Time Generator within the computing section, $(\bar{R}_{\odot\Delta})_{\text{obs}}$ and $(\bar{V}_{\odot\Delta})_{\text{obs}}$ are determined. In addition the various separate elements of the ellipse are computed for complete identification of the actual trajectory being followed by the vehicle.

The method of computation is geometric using discrete measurements, and not the integration of velocities and accelerations experienced by the vehicle.^{71, 72} The reasons for this are shown in section 8.6. Chapter 7 developed the equations necessary for the solution of this problem and illustrated the various geometric relations in Figs. 7.2 through 7.6.

The first tracking system discussed in section 8.31 has as outputs TL_{\odot} , TL_{\oplus} and TL_{\ominus} . These are inputs to two separate range computers which determine two values of $R_{\odot\Delta}$ using the equation of section 7.6. These two values are then averaged and smoothed for greater accuracy and then combined with the vehicular heliocentric latitude and longitude $(L_{\Delta}, \lambda_{\Delta})$ as presented by TL_{\odot} . Since a series of $\bar{R}_{\odot\Delta}$ must be used in computation of the elements of the elliptical trajectory, these must be held in a memory storage unit, and fed to the trajectory elements computer upon demand. The determination of $(\bar{V}_{\odot\Delta})_{\text{obs}}$ is made by a simple integration process and along with $(\bar{R}_{\odot\Delta})_{\text{obs}}$ is a direct output of the tracking line computer. The output of the trajectory elements computer are θ , a , e , and i observed. The simplified information flow

diagram of the above system is shown in Fig. 8.6.

The second system is the same as that described above but uses only one range computer with the resultant loss of a degree of accuracy in the solution, although a system simplification is achieved which may be permissible. A simplified information flow diagram of this is illustrated in Fig. 8.7

8.42 The Prediction Computation Section

The Prediction Computation Section consists primarily of a number of components collectively termed the Prediction Computer, (see Fig. 8.8). The purpose of the Prediction Computer is to continuously establish, as a function of time after t_0 , the position and velocity of the rocket relative to the reference body. The position and velocity so established may be termed "predicted" in the sense that they do not stem directly from observations, but rather are values which should actually occur if no uncompensated events transpire to alter the rocket motion. The computer must establish these values without reference to any source of information from outside the rocket itself. This in no way prohibits the computer from sharing storage data, power supply, time generation, and the like, with other components. If no corrections to the trajectory were envisaged all the outputs could be computed prior to launch, stored in a memory, and sampled as needed. Since corrections are envisaged the computer must possess the capability of solving values for the rocket position and velocity during the entire time of flight.

Selecting the Sun as the center of our inertial reference frame we may write Equation 3-11.

$$\ddot{\overline{R}}_{\odot\Delta} \Big|_I = \overline{f}_{nf} + \overline{G}_{\odot\Delta} + (\overline{G}_{\oplus\Delta} - \overline{G}_{\oplus\odot}) + (\overline{G}_{\odot\Delta} - \overline{G}_{\odot\odot}) + (\overline{G}_{O\Delta} - \overline{G}_{O\odot}) \quad (8-1)$$

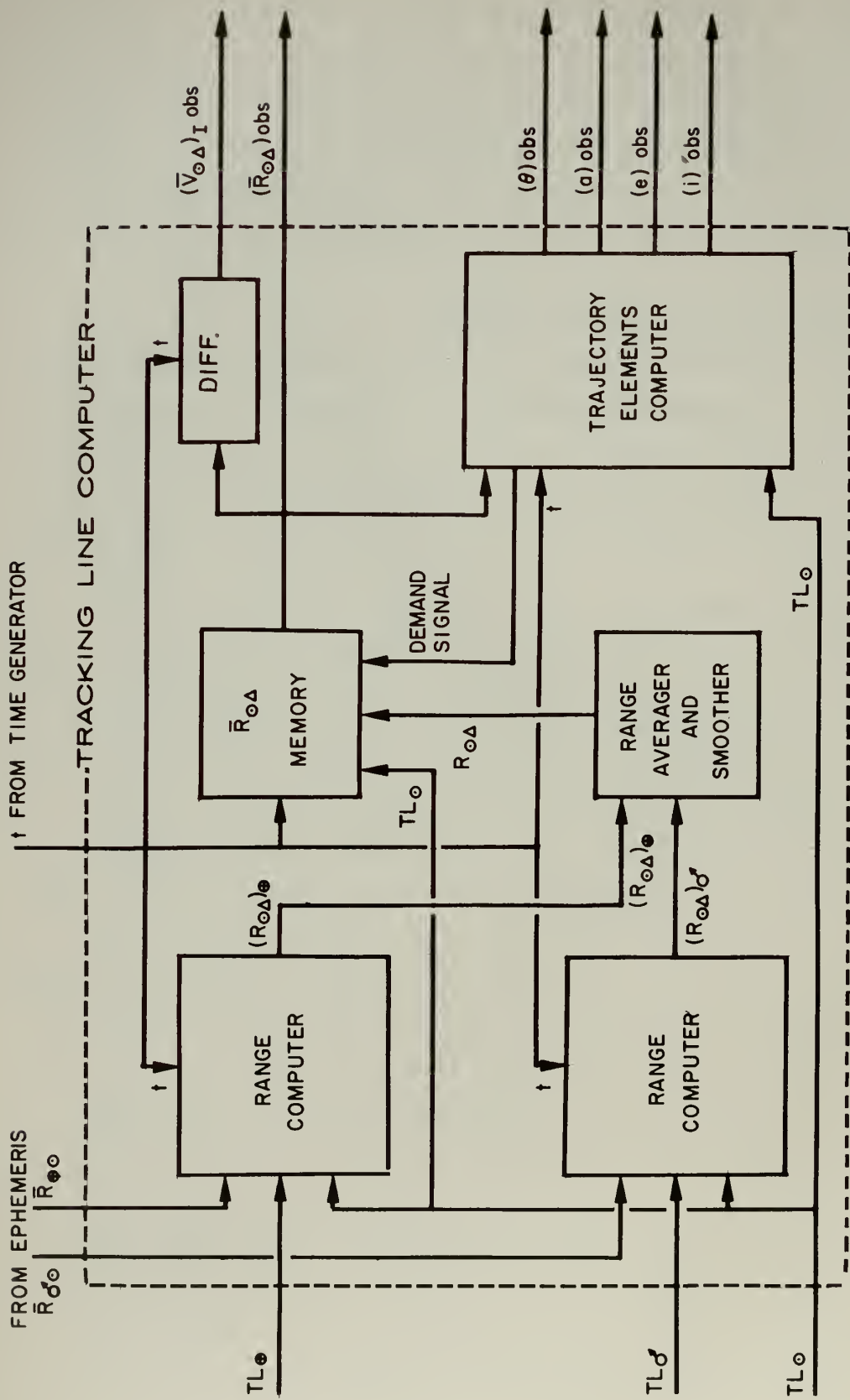


Fig. 8.6 Line functional information flow diagram for tracking line computer (System One)

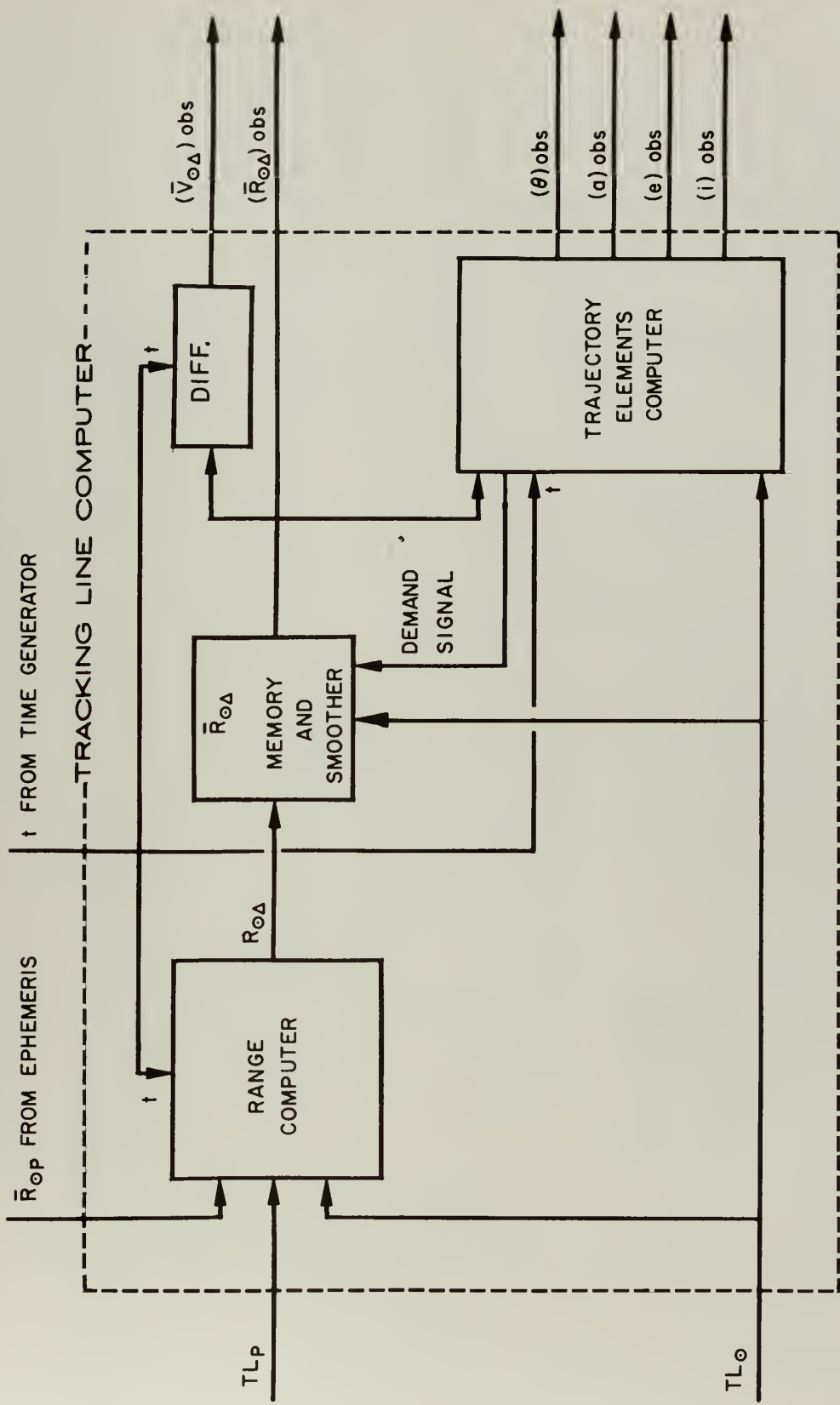


Fig. 8.7 Line functional information flow diagram for tracking line computer (System Two)

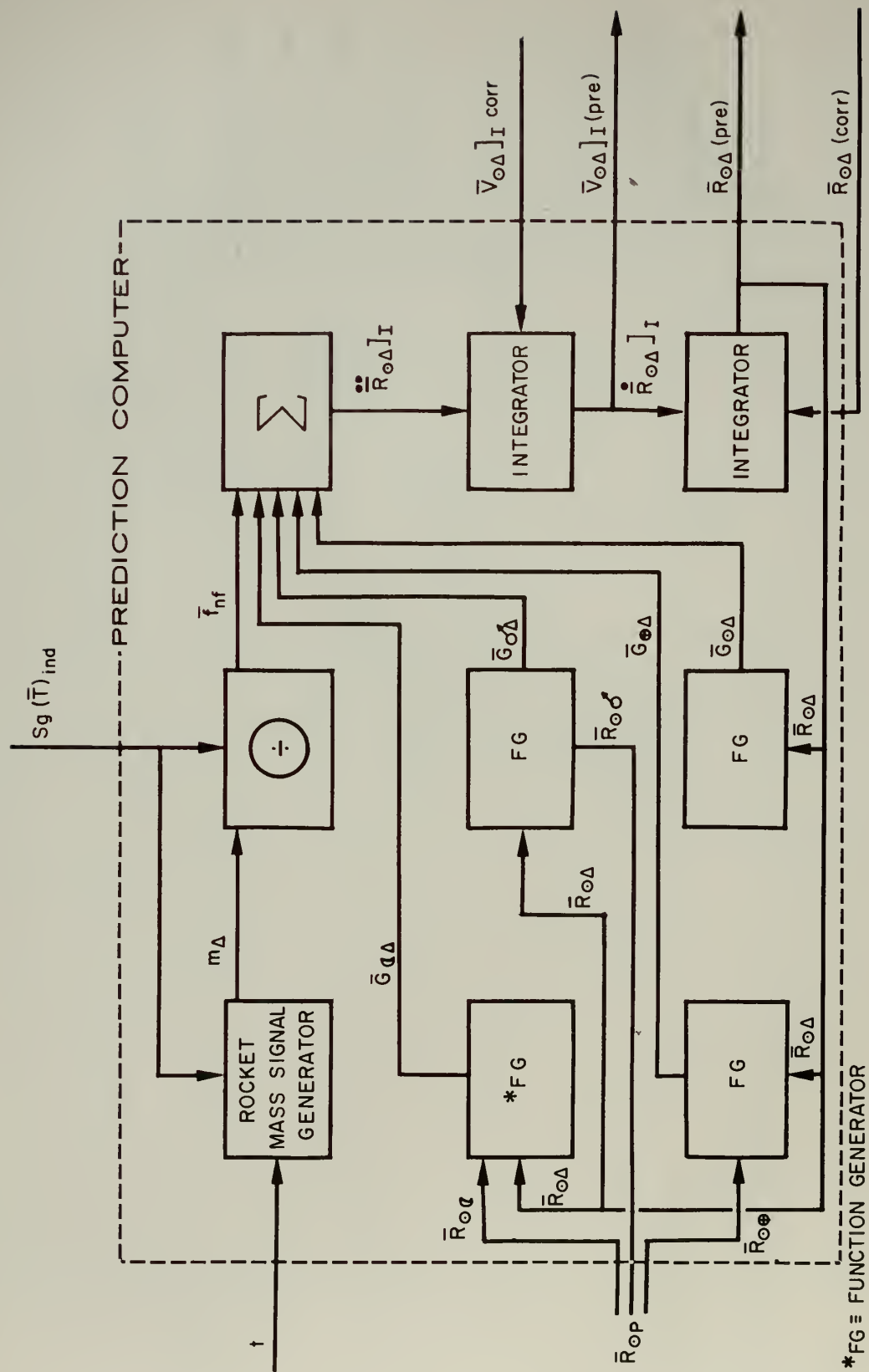


Fig. 8.8 Line functional information flow diagram for prediction computer

From Fig 2.8 we determine

$$\left. \begin{aligned} G_{\oplus\odot} &< 10^{-7} \text{ ft/sec}^2 \\ G_{\odot\odot} &< 10^{-9} \text{ ft/sec}^2 \\ G_{\odot\odot} &< 10^{-8} \text{ ft/sec}^2 \end{aligned} \right\} \doteq 0 \quad (8-2)$$

Hence the equation of motion to be solved continuously by the Prediction Computer is

$$\ddot{\bar{R}}_{\odot\Delta} \Big|_I = \bar{f}_{nf} + \bar{G}_{\odot\Delta} + \bar{G}_{\oplus\Delta} + \bar{G}_{\odot\Delta} + \bar{G}_{\odot\Delta} \quad (8-3)$$

The threshold sensitivities of the components will determine the Phases referred to in Section 3.6. Below these thresholds a particular component will be inactive and the problem will be reduced to the appropriate one of Equations 3-14, 3-15, or 3-16.

Referring to Fig 8.8 the functions of the sub-components are almost self-explanatory when examined with regard to Equation 8-3. The Summer forms the quantity representing the acceleration of the rocket with respect to the Sun. The acceleration is integrated twice to form the rocket position vector, which is fed-back to obtain values for those gravity fields considered in the equation. Thrust and rocket mass form the remaining inputs to the Summer.

8.43 Comparator Section

The comparator section may be considered an integral part of the main computer. Its function is to compare observed position in space, $(\bar{R}_{\odot\Delta})_{obs}$, emanating from the tracking computer, with predicted position in space, $(\bar{R}_{\odot\Delta})_{PRE}$, derived from the prediction computer. Deviations of observed position from predicted position are determined and, if of sufficient

magnitude, form the basis for corrective action. The test of "sufficient magnitude" is a function of the position of the vehicle with respect to Mars. Obviously, the permissible deviations would be small during the early stages of flight, when the position of the rocket relative to Mars is quite large. Similarly, as this relative position becomes less, tolerances become larger and errors assume a lesser importance. A deviation computer weighs or assesses the rocket position relative to Mars and creates this standard of measurement. Fig. 8.9 is a functional representation of this section.

If actual deviations in position, $(D_A) R_{\odot\Delta}$, exceed those permissible deviations, $(D_p) R_{\odot\Delta}$, the correction comparator is assumed to emit a signal actuating the corrector section. This will automatically cause initiation of the computation of the new trajectory.

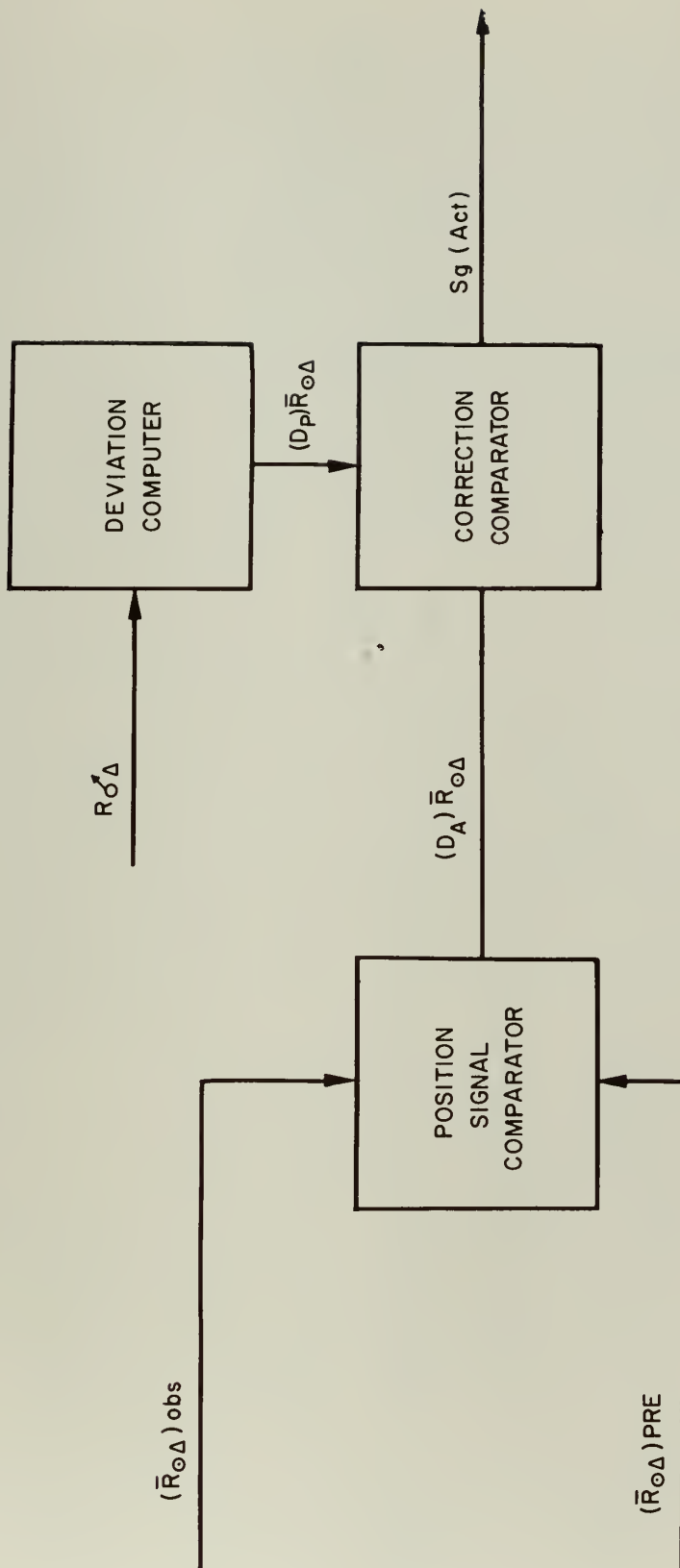
8.44 The Corrector Section

The corrector section can properly be considered a most complex and critical part of the computer. Upon its proper performance will depend an accurate approach to the objective planet or the alternative, a body in free orbit in space forever.

The corrector section is continually supplied with observed rocket position, $(\bar{R}_{\odot\Delta})_{\text{obs}}$, and the elements of the observed trajectory, as well as the position of Mars with respect to the Sun as a function of time, $R_{\odot\odot}(t)$. These quantities form the basis for the computation of a new path to the sought-after planet. A discussion of this general problem has appeared in Chapter 7.

The initiation of operations within this section will be dependent upon receipt of the comparator section actuating signal, $S_g(\text{Act})$.

The modified trajectory is assumed chosen through an optimization process which minimizes fuel expenditure, time,



$(\bar{R}_{\Omega\Delta})_{\text{obs}}$: Observed rocket position with respect to the sun.
 $(\bar{R}_{\Omega\Delta})_{\text{PRE}}$: Predicted rocket position with respect to the sun.
 $(D_A) R_{\Omega\Delta}$: Deviations of observed rocket position from predicted position

$(D_P) \bar{R}_{\Omega\Delta}$: Permissible deviations of observed rocket position from predicted position
 $Sg (\text{Act})$: Corrector section actuating signal

Fig. 8.9 Line functional information flow diagram for comparator section

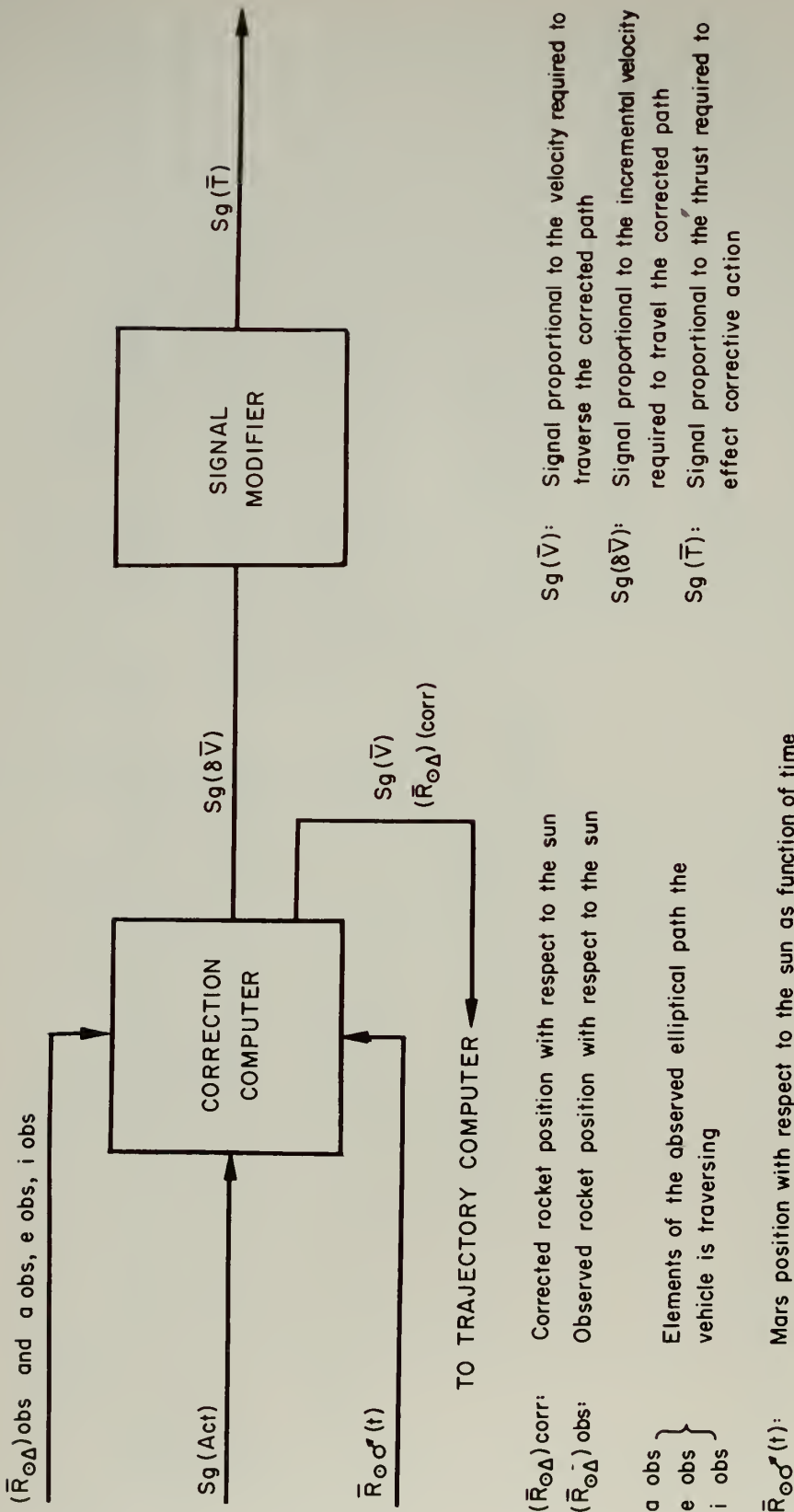


Fig. 8.10 Line functional information flow diagram for corrector section

or some predesigned parameter. Once this selection process is completed, signals proportional to the required velocity changes can be converted into control system commands, $(S_g)T$, which will eventually translate the changes into corrective action. (See Fig. 8.10.)

From a practical viewpoint, however, the selection of an alternate path in flight can be expected to pose a difficult problem. Size and weight considerations will necessitate an absolute economy in functional employment of components. Even then, the optimization problem is complex and may well represent a major obstacle.

8.5 Thrust and Stabilization

The thrust and stabilization unit is essentially a modification of the familiar control loop, altered because of operating environment to include rocket thrust device rather than control surfaces. A signal proportional to the required velocity actuates the thrust device which is positioned prior to firing. Several means of directional control are available for corrective thrust requirements:

- (1) Movable vanes in the jet stream
- (2) Small, individual variable thrust jets
- (3) Universally mounted main jet engine
- (4) Gimbal mounted rocket thrust chamber

Positioning of the thrust device would be in response to the correct or section output signal, as would the controlled metering of propellant to insure a velocity change of proper magnitude.

The accelerated motion of the rocket produced by the thrust device would then be sensed by an accelerometer which compares, in effect, commanded thrust, with resulting thrust.

The stabilization of the rocket in space is another problem

of no little difficulty. Some of the proposals for rocket orientation have included micro-jet control, gyroscopic torque stabilization, and flywheels. Many authors combine vehicle motion and the stabilization although they distinctly differ and require functional separation.

Fig. 8.11 is a line functional information flow diagram of a proposed thrust and stabilization sections.

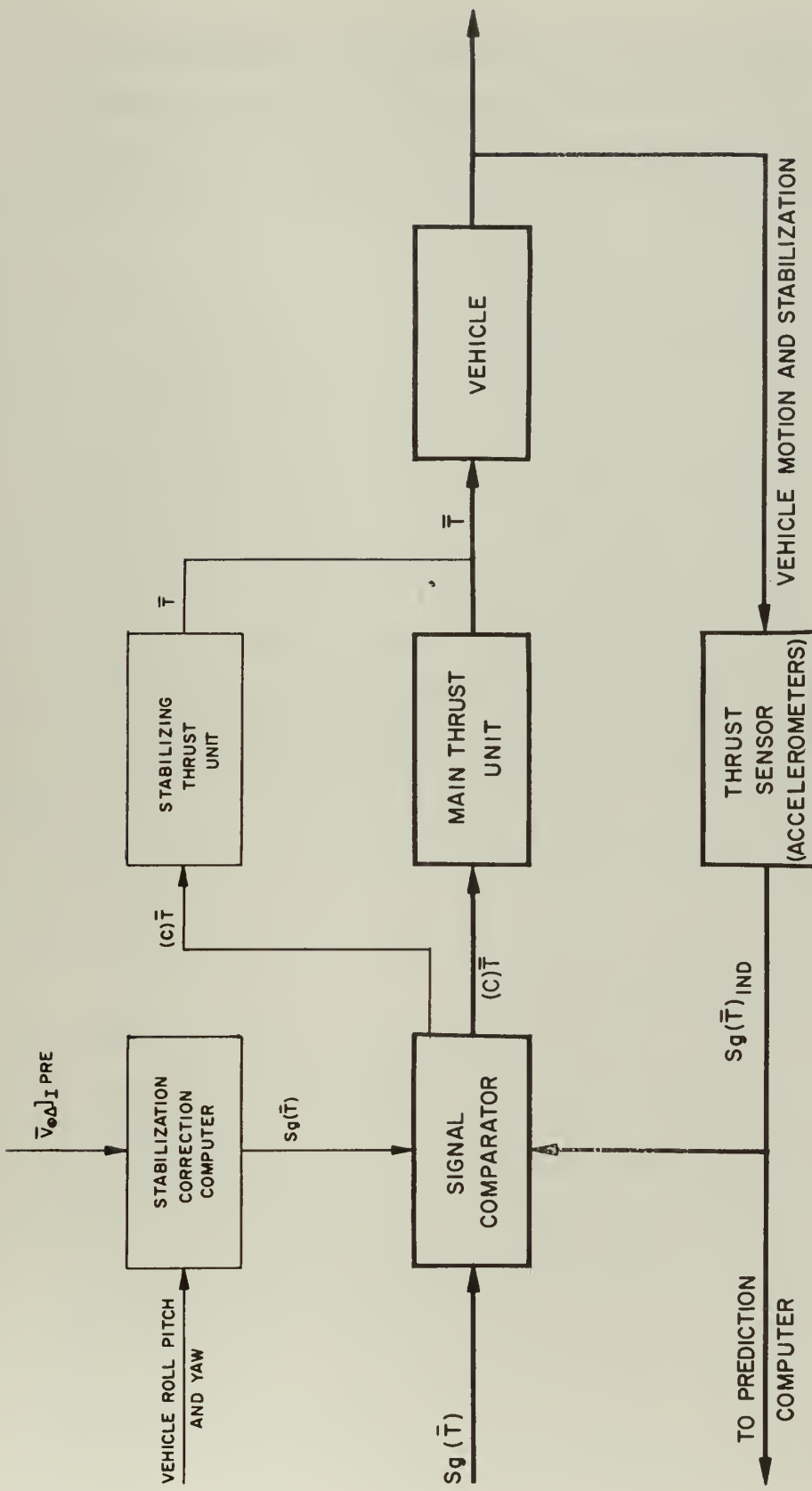
8.6 Errors and Effects

It has been stated previously that the unpowered elliptical orbit trajectory for transfer between planets is subject to large errors in terminal position caused by very small perturbing forces during transit and also very slight errors in velocity vector orientation at the end of the initial thrust period. If, as has been assumed in this paper, corrective action must be taken during mid-course, the reduction in terminal error will be a function of time remaining till intercept, accuracy in determining the actual trajectory being traveled and the accuracy of determination and orientation of the corrective velocity vector. We will now show the magnitude of some of the terminal errors caused by various assumptions and inaccuracies.

8.61 The Assumption of Circular Coplanar Orbits

The assumption of coplanar circular orbits has been made by numerous authors for the sake of simplicity in presenting basic ideas. 22, 30, 31, 40, 62, 68 and others. If we compare the orbits of Earth and Mars and transfer between these orbits we find the following to be true for the worst possible cases.

At "favorable opposition" (once every 16 years) Mars is 35×10^6 miles from Earth. At "unfavorable opposition" Mars is 63×10^6 miles from Earth. This gives a maximum actual variation in distance between orbits of 28×10^6 miles (.3 AU), while the so called average distance is only 49×10^6 miles (.523 AU).



NOTES :
 (C) \bar{T} correction to thrust vector
 Heavy line indicates Main Thrust System. Light line indicates Stabilization System.

Line functional information flow diagram for thrust and stabilization section

This is a 57% variation which is ignored with the assumption of circular orbits. Using the coplanar assumption (not taking the actual orbital inclination of $1^{\circ} 51''$ into account) we introduce a terminal vertical error of 4.57×10^6 miles for the worst possible case.

8.62 Errors in Astronomical Distance

The basic unit of astronomical distance is the Astronomical Unit (AU). This is determined by the mean range of the sun from the Earth and by international agreement (Paris, 1911) has been established to be 93×10^6 miles. However, this distance is based on angular measurements of the diameter of the sun. Due to limits of resolution, limited base lengths for triangulation and other effects, this basic unit is thought to have a probable error of 10,000 miles.^{54, 69} This uncertainty is therefore carried over to the measurement of positions of solar bodies and hence to vehicular orientation in solar space. Until more accurate astronomical measurements are available a rather large residual error in spatial position will have to be accepted and worked with.

8.63 Errors in Initial Velocity Vector

If we now take a typical trajectory from Earth to Mars, we can see the effects of errors in initial velocity vector on terminal positions. Assume a trajectory of arc length 354×10^6 miles such as used in section 4.14. This trajectory has a time of flight of 172 days, and an orbital inclination of 2.51° . An initial velocity error of 1 foot per second for this trajectory will give an error in arc length alone of 2820 miles. This is neglecting the effects on the actual elliptical properties of the orbit which increase the actual miss distance even more. Using an average orbital velocity of 23.8 miles per second, this would be equivalent to an error in arrival of 118.5 seconds, at which time Mars

(traveling approximately 15 miles per second) would be 1780 miles behind the initially proposed intercept point.

An error in inclination or angular orientation of the initial velocity vector of .01 degrees gives a terminal error normal to the trajectory of 18,600 miles. We can also approach initial angular error from the standpoint of what will be the requirement for insuring a terminal error of not more than 1,000 miles. This will necessitate an accuracy within 1.94 second of arc.

J. G. Porter⁴⁹ discusses the effects of small initial velocity vector errors on the shape of a simple Earth-Mars elliptical trajectory. This trajectory starts at its perihelion and arrives at Mars at aphelion and has a basic time of flight of 281 days. Porter concludes that in order for this trajectory to arrive at Mars within a distance of 50,000 miles, the velocity must be controlled to .001 miles per second or one part in 18,000. This would mean that to get within 1,000 miles of the desired terminal position the initial error would have to be less than .106 feet per second.

For this same trajectory Porter concludes that an error of 12 seconds of arc in initial velocity vector orientation will lead to a 50,000 mile error at termination. This means that for a 1,000 mile error we would have to be within .4 of a second of arc at burn out.

The major conclusion which can be drawn from a look at errors in initial velocity vector orientation is that a simple unpowered trajectory with no corrective thrust applied during mid-course will not suffice for interplanetary travel. This was previously stated in section 4.4. However, of the two errors considered, velocity and angular, the errors in angular orientation are the more critical.

8.64 Mid-Course Errors

We can now look at errors in some instruments which might

be used within the vehicle for guidance purposes such as star trackers, accelerometers, gyro packages, and associated equipment.

If we presume the need for a maximum star tracker error equal to or less than 1,000 miles in determining the positions of solar bodies 1 AU distant, we obtain a limit of 2.22 seconds or .0382 minutes of arc. This is a maximum allowable closed loop error composed of errors in reference plane, tracking head, and all associated equipment.

Another approach to this problem of star tracker error is to assume that each sighting is a random event with Gaussian distribution of the error in angular measurement. If we now postulate that we have a "maximum" error of -5 seconds of arc in the values obtained from a star tracker and that 99.7% of the measurements will lie within these values, 95% will be in error less than 3.33 seconds while 68% will be in error less than 1.67 seconds. Since an error of 1 second of arc is equivalent to 450 miles at a distance of 1 AU, we can assume that 68% of the measurements would have an error less than 750 miles, and 95% would have an error less than 1,500 miles when sighting bodies 1 AU distant. It appears, then, if a number of readings are taken over a short period of time with proper smoothing and averaging, suitably accurate values can be obtained from tracker systems which may by themselves have a considerable possible error.

To determine an upper limit of the threshold of sensitivity to acceleration required for the trajectory of Section 4.14 of this paper we can again use a maximum error of 1,000 miles at termination. This corresponds to 4.75×10^{-8} feet per second for a time of flight of 172 days. For this same trajectory the maximum allowable drift of a purely "inertial"⁷¹ guidance system to insure vertical displacement error of not more than 1,000 miles would be 1.64×10^{-5} mr per day. This is determined using the

trajectory arc length of 354×10^6 miles and time of flight of 172 days.

The primary conclusion that can be drawn from the above simplified mid-course guidance system errors is that although completely self contained inertial guidance systems are highly desirable, the required accuracies are rather high; particularly if return trips are contemplated without rezeroing the system. However, with the addition of star tracking units, suitably accurate guidance can be obtained which is not limited by or dependent upon time of flight.

CHAPTER 9

CONCLUSIONS AND RECOMMENDATIONS FOR FURTHER STUDY

9.1 Introduction

The contents of this paper lead to several conclusions and recommendations of interest to those pursuing the problem of interplanetary travel. Many areas included in this thesis are presented with a view toward future use by students of the field and lead to a better definition of the problem. The bibliography represents a comprehensive literature search of available unclassified related material.

9.2 Conclusions

- (1) During the time of flight of a rocket from Earth to Mars the center of the Sun may be considered an inertial point.
- (2) During a major portion of the trajectory the problem may be considered one of two bodies, with some perturbations.
- (3) Threshold sensitivities and drift uncertainties of current gyroscopic mechanisms preclude the use of a pure inertial navigation system¹¹ at this time, particularly when a return trip is contemplated.
- (4) During the time of flight of the rocket the motion of the "fixed" stars is so small that they provide a means of establishing a space reference frame.
- (5) Determination of rocket present position in space within the limits proposed in this paper lies within the capa-

bilities of the current "state of the art".

- (6) Within the limits of the assumptions made, the "combination" trajectory (i.e., an initial thrust period followed by free fall flight; modified, if necessary, by corrective thrust) appears to offer the most immediately feasible method of travel to Mars.
- (7) Rocket velocity vector orientation appears to be more critical than magnitude.
- (8) The Hohmann ellipse²² provides the minimum required velocities to get to Mars but if rocket capabilities include V_{inc} (as defined within this paper) of 10,000 ft/sec or more a wide range of trajectories is available.
- (9) The Rocket Plane Concept provides a means of reducing the trajectory to a two-dimensional problem, thereby greatly simplifying rocket construction requirements. It is emphasized that certain assumptions often made in the literature to reduce the problem to two-dimensions are unrealistic when viewed in the light of actual condition. The Rocket plane concept does not assume two-dimensions but selects the reference plane such that deviations from this reference plane are negligibly small.
- (10) On a kinetic energy basis a certain optimum departure orbit exists for any given trajectory to Mars. Similarly an optimum arrival orbit exists about Mars. Additionally these optimum orbit radii are characterized by the property that for a relatively small increase in available velocity a satisfactory departure orbit radius may be used which is much nearer to the Earth surface than the optimum orbit radius.
- (11) Instrumentation for travel between planets appears to lie within the capabilities of the present "state of the art".

9.3 Recommendations for Further Study

- (1) Digital computer trajectory analysis should be instituted covering:
 - (a) Required parameters for all trajectories whose initial rocket velocity lies within reasonable limits.
 - (b) The effect of variations in initial conditions on linear miss distance at Mars.
 - (c) Perturbative effects of solar system masses which were ignored in this paper due to their small magnitude.
- (2) Additional study should be instituted on the design and construction of free-fall space reference stabilization systems suitable for interplanetary travel.
- (3) Studies should be commenced which would lead to the establishment of optimization standards for trajectories to Mars on the basis of both fuel expenditure and kinetic energy.
- (4) A study of permissible deviations from prescribed path during flight allowing terminal accuracy within prescribed limits should be instituted.

SYMBOLS
DEFINITION SUMMARY 1

Symbol	Definition
⊕	Sun
☾	Moon
⊕	Earth
♂	Mars
♃	Jupiter
♄	Saturn
♅	Uranus
♆	Neptune
♇	Pluto
☿	Mercury
♀	Venus
☆	Star
a	Semi major axis of any ellipse
b	Semi minor axis of any ellipse
c	The magnitude of the effective exhaust velocity vector measured with respect to the walls of the rocket nozzle
e	Eccentricity of any ellipse: defined by the relation $e = 1 - \frac{b^2}{a^2}; \quad a > b$
\bar{f}_f	Unit field forces - forces per unit mass whose existence is due to the presence of a field

Symbol	Definition
\overline{f}_{nf}	Unit non field force - forces per unit mass whose existence is due to all causes other than fields
i	Inclination of orbit - the angle measured from reference plane to plane of orbit, in a plane perpendicular to the line of nodes; generally positive where measured in a direction "above" the reference plane
j	A variable indicator which may take on identities as propounded within the text
m_{Δ}	Instantaneous mass of rocket
p	An arbitrary planet
r_j	Magnitude of radius vector from the reference focus of an ellipse to the indicated point on that ellipse. Subscript j refers to indicated quantity
r_{js}	Radius of the circular orbit about the indicated body
t	The independent variable time
t_b	Burning time - that period of time wherein a given amount of propellant is consumed
t_c	The time at which an imaginary rocket would have arrived at Mars future position if it had departed aphelion of its ellipse at $t = t_o$ Note: $t_f = t_c - t_d$

Symbol	Definition
t_d	The time at which an imaginary rocket would have arrived at Earth present position if it had departed aphelion of its ellipse at $t = t_o$
t_f	Time of flight
t_j	Time at "j" instant; subscript "j" refers to indicated quantity
t_o	The instant of time at which a given operation commences.
A	Angle
AU	Astronomical Unit - the distance associated with the mean parallax of the sun. By international agreement (Paris 1911), this was set as 8.80" of arc and corresponds to about 93,000,000 miles. In this text the numerical value of the AU will be taken as 93,000,000 miles.
\overline{D}	Drag - as conventionally defined
E	The ecliptic plane - the plane defined by the loci of points representing the instantaneous position of the earth throughout the year measured with respect to the sun
\mathcal{E}	Eccentric Anomaly
\overline{F}	Force - as conventionally defined

Symbol	Definition
G	Gaussian gravitational constant approximately equal to: $6.67 \times 10^{-8} \text{ cm}^3/\text{gram (m)} \text{ sec}^2$
\bar{G}_j	Directed acceleration due to gravity field of the indicated body. A second subscript refers to that body experiencing this directed acceleration. Subscript "j" refers to indicated body
GM_j	The product of the Gaussian gravitational constant and the mass of the indicated body. Subscript "j" refers to indicated body
Imp	Impulse - the integral of the magnitude of thrust over the time of its duration
KE	Kinetic Energy - as conventionally defined
L_j	Celestial heliocentric latitude - angle measured in a plane perpendicular to the ecliptic plane from the ecliptic plane to the line drawn from the sun to the indicated point; measured positively toward celestial north
\bar{L}	Lift - as conventionally defined
M_p	Total mass of propellant
M_o	Gross mass of rocket at instant of firing

Symbol	Definition
NN'	Line of nodes - line drawn through the ascending and descending nodes
PE	Potential Energy - as conventionally defined
PR	Payload Ratio - $PR = 1 - \zeta$
\bar{R}	Vector from the reference point to the indicated point
R	Magnitude of \bar{R}
\bar{T}	Thrust - reaction force on the rocket or vehicle unit structure
TE	Total Energy - as conventionally defined
$\bar{v}_{\odot j}$	Velocity vector of the indicated body with respect to a heliocentric non rotating coordinate system.
$\bar{v}_{j\Delta}$	Velocity vector of the rocket relative to the indicated body, and measured in a heliocentric non rotating coordinate system
\bar{v}_{js}	Velocity vector of the rocket in circular orbit about the indicated body measured in a body centered non rotating coordinate system
\bar{v}_{je}	Velocity vector of "escape" from the gravity field of the indicated body, equal to $\sqrt{2} \times \bar{v}_{js}$ measured in a body centered non rotating coordinate system

Symbol	Definition
$\bar{V}_{(j\Delta)g}$	Velocity vector of the rocket with respect to the indicated body taking into account the kinetic energy required to overcome the effect of the gravity field of the indicated body, measured in heliocentric non rotating coordinate system
\bar{V}_{inc}	That increment of $\bar{V}_{(j\Delta)g}$ which must be provided by the rocket
α	Angle measured from the x-axis to the thrust vector
β	Angle measured from the y-axis to the thrust vector
γ	Angle measured from the z-axis to the thrust vector
ζ	x, y, and z axes represent an orthogonal coordinate set. The thrust vector has its origin at the origin of this coordinate set
η_j	Propellant loading factor = $\frac{M_p}{M_O}$ $\theta' - \omega$ for the orbit of indicated body
θ	The angle, measured in the rocket plane of motion, between a body-sun line and rocket ellipse aphelion-sun line; positive angles when direction of measurement is opposite to rotation of planets about the sun.

Symbol	Definition
θ (contd)	Prime ('') indicates measurement from perihelion vice aphelion with direction of measurement positive when same as rotation of planets about sun
θ_j	θ at any time j
θ_d	θ at $t = t_d$
θ_c	θ at $t = t_c$
θ_s	θ of Mars at $t = t_d$
λ_j	Celestial heliocentric longitude - angle measured in the ecliptic plane from the reference direction Aries (Υ), in the direction of rotation of planets about the sun, to the projection on the ecliptic plane of the line drawn from the sun to the indicated point.
π_j	Longitude of perihelion of indicated orbit
ϕ	The angle, measured in the rocket plane of motion included between the velocity vector of the rocket or vehicle and a line perpendicular to the radius vector from the sun to the vehicle
ϕ_d	ϕ at $t = t_d$
ϕ_c	ϕ at $t = t_c$
$\psi_{\oplus\Delta}$	The angle measured in the rocket plane of motion included between

Symbol	Definition
$\psi_{\oplus\Delta}$ (contd)	$\bar{v}_{\oplus\Delta}$ and the projection of $\bar{v}_{\odot\oplus}$ on the rocket plane.
$\psi_{\odot\Delta}$	The angle measured in the rocket plane of motion, included between $\bar{v}_{\odot\Delta}$ and the projection of $\bar{v}_{\odot\odot}$ on the rocket plane.
ω_j	The angle included between perihelion and the line of nodes measured in direction of rotation of planets for indicated orbit.
Δ	Rocket or vehicle
τ	The period - elapsed time between repetitive events
Υ	The vernal Equinox (the first point of Aries) defined as the direction indicated when projection of the line of intersection of the earth equatorial plane and the earth ecliptic plane passes through the center of the sun; this action occurring as the sun apparently passes from south to north of the equator
Ω_j	Longitude of ascending node of indicated plane
ν_j	Longitude of descending node of indicated plane
	Ascending node - celestial heliocentric longitude occupied by a

Symbol	Definition
	body passing from "below" to "above" the ecliptic plane.
	Descending node - Ascending node plus 180° "Above" ecliptic defined as that part of space wherein an observer would note counter-clockwise rotation of planet.

BIBLIOGRAPHY

1. AFOSR-TR-57-14 AD 120-430, Summary Session Astronautics Symposium (San Diego, February 20, 1957)
2. American Ephemeris and Nautical Almanac for the Year 1955, U. S. Government Printing Office, Washington: 1952.
3. Atkinson, R. d'E., "II-Some Problems of Interplanetary Navigation", Journal of Institute of Navigation, Vol. 3 pp 365-73, October 1953.
4. Bernard, H. J.; Bennett, D. A.; and Rice, H. S., New Hand Book of the Heavens, New York: McGraw Hill, June 1954.
5. Clarke, A. C., Interplanetary Flight, New York: Harpers, 1951
6. Clarke, A. C., "I — The Dynamics of Space Flight", Institute of Navigational Journal, London, Vol. 3 No. 4: pp 365-75, October 1954.
7. Clarke, A. C., "Stationary Orbits", Journal of the British Astronomical Association, 1957.
8. Clarke, A. C., "The Dynamics of Space Flight," Journal of British Interplanetary Society, "Vol. 8: pp 71-84, March 1949.
9. Dutton, Benjamen, Navigation and Nautical Astronomy, Annapolis: U.S. Naval Institute, 1948.
10. Ehricke, Krafft A., "Free and Powered Orbits in Cislunar Space", Summary Session Astronautics Symposium, (U.S. Air Force Office Scientific Research, February 20, 1957).
11. Ehricke, Krafft A., "Instrumental Satellites and Instrumental Comets", Interavia, Vol. 11 No. 12: pp 960-967, December 1956.
12. Ehricke, Krafft A., "Satellite Orbits for Interplanetary Flight", Journal of American Rocket Society, Vol. 24: pp 381-82, 1954.

13. Forbes, George F., "Application of General Trajectory Equation", Journal of British Interplanetary Society, Vol. 10 No. 5, September 1951.
14. Forbes, George F., "Equations of Motion of a Rocket in Central Force Space" (M.I.T. thesis, 1948).
15. Forbes, George, R., "Powered Orbits in Space", Journal of British Interplanetary Society, Vol. 14 No. 2, March 1955.
16. Forbes, George, F., "The Trajectory of a Powered Rocket in Space", Journal of British Interplanetary Society, Vol. 9 No. 2, March 1950.
17. Golay, M. J., "The Application of Radio Interferometry to the Guidance of Interplanetary Rockets", Space Flight Problems, pp 71-74, 1953.
18. Herrick, Samuel, "Accurate Navigation of Intercontinental and Satellite Vehicles in Earth's Gravitational Field", Summary Session Astronautics Symposium (U.S. Air Force Office Scientific Research, February 20, 1957).
19. Herrick, Samuel, "Rocket Navigation", Navigation, Vol. 2, December 1950.
20. Herrick, Samuel, "Space Rocket Trajectories", Journal of British Interplanetary Society, Vol. 9, September 1950.
21. Herrick, Samuel, Tables for Rocket and Comet Orbits (National Bureau of Standards, Applied Math Series, No. 20, U. S. Government Printing Office, 1953).
22. Hohmann, W., Erreichbarkeit der Himmelskörper, München: Oldenbourg, 1925.
23. Ketchum, H. B., "Navigational Calculations in Space Flight", Journal of Space Flight, ("Planetary Orbital Distances", Vol. 5 No. 4: pp 1-8, April 1953), ("Planetary Orbital Velocities and Gravitational Fields; and the Gravitation of the Sun", Vol. 5 No. 7: pp 1-5, September 1953), ("Satellite Gravitational Fields,

Orbital Velocities and Elements of Orbits" Vol. 5 No. 10: p. 1-9, December 1953), and ("The Aspects of Atmospheric Friction", Vol. 6: pp 1-8, June 1954).

24. Kölle, H. H., "Fliegen durch den Weltemarun", Die Weltluftfahrt, Vol. 1 No. 1-2, January-February 1949.
25. Kölle, H. H. and Kaeppler, H. J., Literature Index of Astronautics, Germany, 1954.
26. Kooy, J. M. J. and Uytenbogaart, J. W. H., Ballistics of the Future, New York: McGraw Hill, 1946.
27. Kooy, J. M. J., "On Plotting Small Thrust Space Ship Orbits. Space-Flight Problems", Collection of Lectures at Fourth Astronautical Congress in Zurich, 1953, Cie-Biel-Bienne: Laubscher, 1953, pp 108-111.
28. Lawden, D. F., "Correction of Interplanetary Orbits", Journal of British Interplanetary Society, Vol. 13: pp 215-223, 1954.
29. Lawden, D. F., "Dynamic Problems of Interplanetary Flight", Aeronautics Quarterly, Vol. 6: pp.165-180, August 1955.
30. Lawden D. F., "Entry into Circular Orbits - 1", Journal of British Interplanetary Society, Vol. 10 No. 1: pp.5-17, January 1951.
31. Lawden, D. F., "Entry into Circular Orbits - 2", Journal of Biritish Interplanetary Society, Vol. 13: pp. 27, January 1954.
32. Lawden, D. F., "Escape to Infinity from Circular Orbits", Journal of British Interplanetary Scoiety, Vol. 12: pp. 68, March 1953.
33. Lawden, D. F., "Fundamentals of Space Navigation", Journal of British Interplanetary Society, Vol. 13: pp 87-101, March 1954.
34. Lawden, D. F., "Optimal Programming of Rocket Thrust Direction", Astronautica Acta, Vol. 1 No. 1: pp 41-56, 1955.

35. Lawden, D. F., "Optimal Transfer Between Circular Orbits about Two Planets", Astronautica Acta, Vol. 1 No. 1: pp 89-99, 1955.
36. Lawden, D. F., "Minimal Rocket Trajectories", Journal of American Rocket Society, Vol. 23, November-December 1953.
37. Lawden, D. F., "Minimal Trajectories", Journal of British Interplanetary Society, Vol. 9 No. 4: pp 179-186, July 1950.
38. Lawden, D. F., "Perturbation Manoeuvres", Journal of British Interplanetary Society, Vol. 13: pp 329-334, 1954.
39. Lawden, D. F., "Satellite Orbits for Interplanetary Flight", Journal of American Rocket Society, Vol. 24 No. 6: pp 382, November-December 1954. (Comments on the article by Ehricke).
40. Lawden, D. F., "The Calculation of Orbits", Journal of British Interplanetary Society, Vol. 14 No. 4: pp 204, July 1955.
41. Lawden, D. F., "Transfer Between Circular Orbits", Journal of American Rocket Society, Vol. 26: pp 555, July 1956.
42. Ley, Willy, Rockets, Missiles and Space Travel, New York: Viking Press, 1952.
43. Locke, A. S., (et al), Guidance, Princeton: Van Nostrand, 1955.
44. Moulton, F. R., Introduction to Celestial Mechanics, New York: Mac Millan, 1902.
45. Oberth, Herman J., "A Satellite Attitude Control System", Summary Session Astronautics Symposium, (U. S. Air Force Office Scientific Research, February 20, 1957).
46. Oberth, Herman J., Wege zur Raumschiffart, Munich: R. Oldenbourg, 1925.
47. Orbital and Satellite Vehicles (M. I. T. Department of Aeronautical Engineering Vol. I and II, Published Notes for Undergraduate Course in Orbital Vehicles, Spring 1958).

48. Porter, J. G., "Interplanetary Navigation", Journal of Institute of Navigation, Vol. 8 No. 1: pp 35-38, January 1955.
49. Porter, J. G., "Navigation Without Gravity", Journal of British Interplanetary Society, Vol. 13: 1954.
50. Porter, J. G., "Some Problems in Space Travel", Journal of Institute of Navigation, Vol. 8 No. 3: pp 224-230, July 1955.
51. Preston-Thomas, H., "Inter-orbital Transport Techniques", Journal of British Interplanetary Society, Vol. 11 No. 4: pp 173-193.
52. Preston-Thomas, H., "Two Aspects of the Time Element in Interplanetary Flight", Proceedings of 5th International Astronautical Congress, Innsbruck, Vienna: Springer-Verlag, 1954.
53. Payne-Gaposchkin, Cecilia, Introduction to Astronomy, New York; Prentice-Hall, Inc., 1954.
54. Russell, H. N.; Dugan, R. S.; and Stewart, J. Q.; Astronomy, I- The Solar System, Astronomy, II- Astrophysics and Stellar Astronomy, Boston: Ginn and Company, 1945.
55. Saenger, E., "The Laws of Motion in Space Travel", Interavia, Vol. IV, July 1949.
56. Schaub, Werner, "Der innere Marsmond Phobos-ein Mond in Anflösung" Weltraumfahrt, Vol. 4 No. 3: pp 65-67, July 1953.
57. Shepherd, L. R., "Basic Principles of Astronautics, Part I", Journal of British Interplanetary Society, Vol. 14: January 1955.
58. Shostak, Arnold, "Radio Astronomy", Summary Session Astronautics Symposium (U. S. Air Force Office Scientific Research, February 20, 1957).
59. Skilling, W. T.; and Richardson, R. S., Astronomy, New York: Henry Holt, 1941.

60. Smart, W. M., Celestial Mechanics, London: Longmans, Green and Co., 1953.
61. Spitzer, L., Jr., "Interplanetary Travel between Satellite Orbits", Journal of American Rocket Society, Vol. 22 No. 2; March 1952.
62. Stuhlinger, Ernst, "The Flight Path of an Electrically Propelled Space Ship", Journal of American Rocket Society, Vol. 27 No. 4, April 1957.
63. Sutton, George P., Rocket Propulsion Elements, New York: John Wiley & Sons, 1956.
64. Thompson, L. N., "Fundamental Dynamics of Reaction-Powered Space Vehicles" Proceedings of Institute of Mechanical Engineers, Vol. 164 No. 3: 1951.
65. Thuring, B., "Compensation for Path Deviations by Continuous Rocket Thrust", Weltraumfahrt, Vol. 5, October 1954.
66. Tsien, H. S., "Take-off from Satellite Orbit", Journal of American Rocket Society, Vol. 23 No. 4: pp 233-236, July-August 1953.
67. Vertregt, M., "Orientation in Space", Journal of British Interplanetary Society, Vol. 15 No. 6: pp 324-328, November-December 1956.
68. Von Braun, Wernher, The Mars Project, Urbana: University of Illinois Press, 1953.
69. Whipple, Fred J., "Orbital Accuracy and Ranges from Ground Based Optical Tracking", Summer Session Astronautics Symposium (U. S. Air Force Office Scientific Research, February 20, 1957).
70. Wintner, A., The Analytical Foundations of Celestial Mechanics, Princeton, 1941.
71. Wrigley, Walter, Inertial Guidance, Institute of Aeronautical Science, 1957.

72. Wrigley, Walter and Hovorka, John, Encyclopedia of Fire Control Vol. 1, Cambridge, Mass. M.I.T. Instrumentation Laboratory, June 1957.

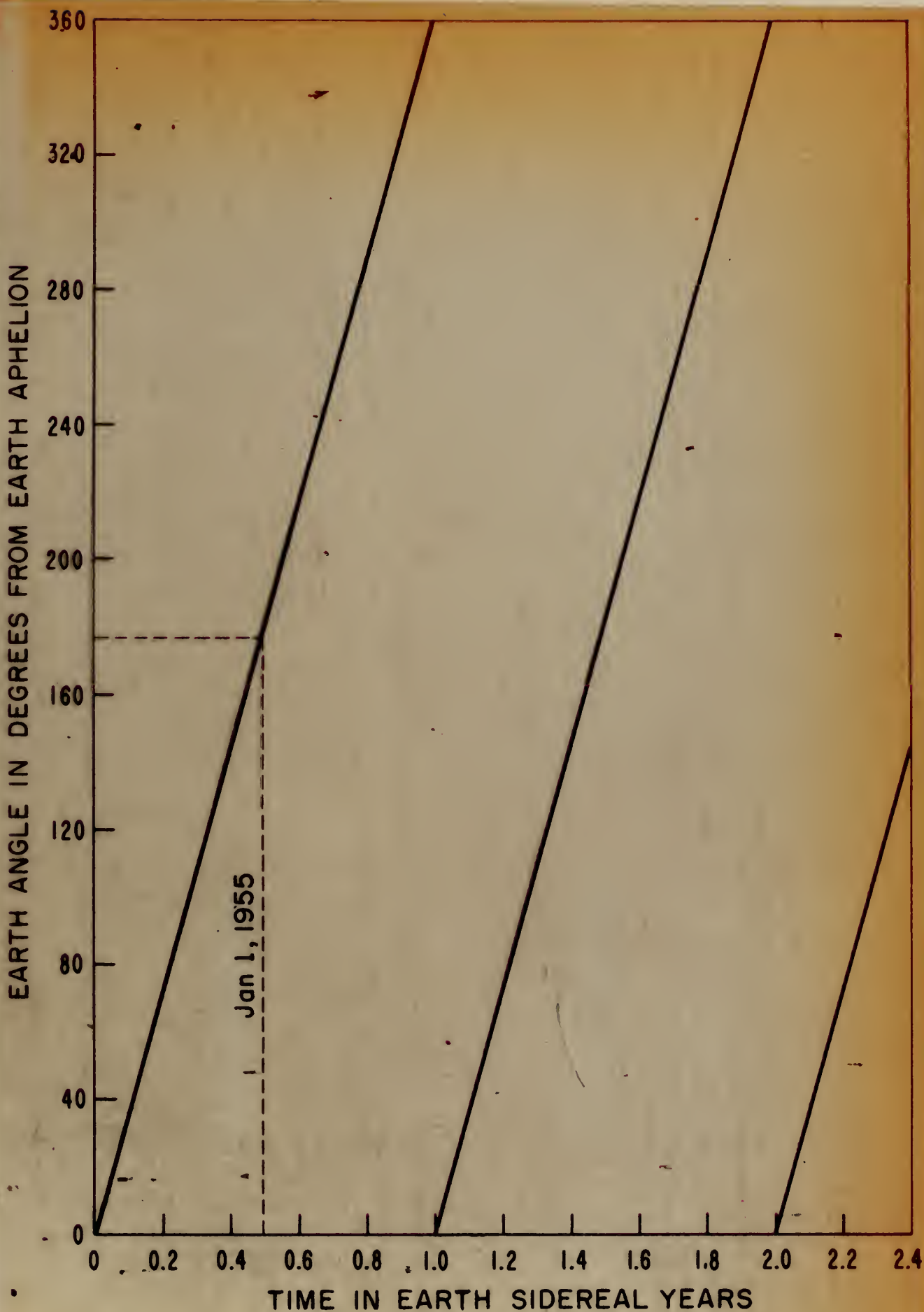


Fig. 4.12 Earth angular position measured from Earth aphelion as a function of time (Overlay #1)



